NASA Contractor Report 4016

Temperature Dependent Nonlinear Metal Matrix Laminate Behavior

David J. Barrett and Kent W. Buesking

CONTRACT NAS1-17822
SEPTEMBER 1986

NASA

NASA Contractor Report 4016

Temperature Dependent Nonlinear Metal Matrix Laminate Behavior

David J. Barrett and Kent W. Buesking
Materials Sciences Corporation
Spring House, Pennsylvania

Prepared for
Langley Research Center
under Contract NAS1-17822

National Aeronautics
and Space Administration

**Scientific and Technical
Information Branch**

1986

PREFACE

This report describes the work performed by Materials Sciences Corporation (MSC) under NASA Contract NAS1-17822 during the period from December 4, 1984 to November 30, 1985. Dr. David Barrett served as principal investigator for this program and developed the incremental laminate analysis procedure. Mr. Kent Buesking served as program manager for MSC and developed the unidirectional material model. Dr. Stephen Tompkins served as the technical contract monitor for NASA-Langley.

APPROVED BY:

Kent W. Buesking

Kent W. Buesking
Director of Advanced Materials

TABLE OF CONTENTS

INTRODUCTION

Graphite reinforced metals are especially attractive for structures which require a high degree of dimensional stability. These composites possess high axial moduli and near zero axial thermal expansion coefficients. They are currently being developed for satellite components such as antenna supports and wave guides. Since these materials will be employed on satellites, they will be subjected to temperature extremes caused by solar radiation. However, experiments over typical orbital temperature cycles by several investigators, references 1 and 2, have found that the composites exhibit nonlinear thermal expansions. The data typically show a response such as that plotted in Figure 1.

The figure shows that as the material is cooled from room temperature it initally contracts with the expected thermal expansion coefficient. However, near 0°F the thermal response changes drastically and the material actually expands as it cools. Once it reaches the minimum temperature (-225°F), and is then heated it continues to expand but again it responds with the expected thermal expansion coefficient. As the temperature rises to near 50°F, the expansion coefficient again changes and the material begins to contract slightly. This continues to the maximum temperature of 275°F. Then as the material is cooled it contracts as expected. The data also show that the material does not return to its original starting strain but contains a permanent set. Further thermal cycles appear to cause additional residual strain but less per cycle. The nonlinear thermal expansions and the permanent set exhibited by these materials can be potentially very damaging to components that are designed on the basis of dimensional stability.

A major cause of the nonlinear thermal expansions is the yielding and subsequent plastic behavior of the matrix material. Metal matrix materials are fabricated by combining the constituents at high temperatures where the matrix is nearly molten. As the composite cools, the matrix begins to solidify and stresses are generated because of the difference in thermal

expansions of the constituents. In the case of a graphite/ aluminum composite (e.g. P100/6061), the matrix contracts and the fibers expand as the material cools. This generates tensile stresses in the matrix as shown schematically in Figure 2. Figure 2 shows qualitatively the composite thermal expansion, the stress-strain behavior of the matrix and the motion of the matrix yield surface as the composite cools from its stress-free temperature. At the stress free temperature (point 1 in Figure 2) the matrix stress is initially zero and the composite thermal strain is zero. As the material cools, the composite contracts and tensile stresses build up in the matrix. At some temperature, the stresses in the matrix will reach the yield point of the material (point 2 in Figure 2). Further cooling causes the matrix to deform plastically with a reduced stiffness which results in a nonlinear composite thermal expansion. The plastic deformation also causes the matrix yield surface to move in stress space. (The motion of the yield surface assumes that aluminum hardens kinematically). When the temperature reaches its minimum value (point 3 in Figure 2) the composite thermal expansion will be nonlinear, the matrix will be in a plastic state and the matrix yield surface will have shifted due to the large tensile stresses.

If the composite is now heated, the material will behave as shown in Figure 3. During heating the matrix will expand and the fibers will contract. In this case the stresses in the matrix will be compressive. The compressive stresses cause the matrix to unload elastically which results in the initial linear composite thermal strains shown in Figure 3. During the first portion of the heating cycle the composite expands linearly, the matrix unloads with an elastic stiffness and the stress point moves back across the center of the yield surface. Further heating, however, will generate compressive stresses in the matrix large enough to reach the yield point (point 4 in Figure 3). Notice that the yield point in this state is not the same as the initial compressive yield stress of the matrix. The compressive yield point has shifted because of the high tensile stresses generated during the cooling cycle. This is referred to as the Bauschinger effect and is characteristic of

aluminums. Heating above the compressive yield temperature will cause the matrix to deform plastically, the composite thermal expansion to be nonlinear and the matrix yield surface to shift in the direction of the compressive stresses. When the composite reaches its maximum temperature the thermal expansion will be nonlinear, the matrix will be plastic and the matrix yield surface will have shifted because of the high compressive stresses.

Clearly, if the temperature is now varied through subsequent cooling and heating cycles, the process will repeat and qualitatively follow the same pattern as shown by the experimental data in Figure 1. The actual process will be more complex than that outlined in Figures 2 and 3 because the constituent properties will vary with temperature, the matrix will be in a multiaxial stress state and local failures (e.g. matrix microcracks and interface debonding) may occur. However, Figures 2 and 3 represent a simple, qualitative description of the process and provide a starting point for the investigation of nonlinear metal matrix composite behavior.

The experimental data shown in Figure 1 and the qualitative explanations described in Figures 2 and 3 focus upon the behavior of unidirectional graphite reinforced composites. Although most of the applications for graphite/metal composite investigated to date have involved unidirectional materials, research work is beginning to shift to laminates. Clearly, it will be necessary to fabricate and design graphite/metal laminates if these materials are ever going to be used in more demanding two-dimensional structures such as plates and shells. The behavior of the laminated materials, however, will be strongly influenced by the behavior of the unidirectional composites. The nonlinear response of the lamina will cause nonlinear behavior of the laminate. Thus, in order to fabricate, test, design and understand graphite/metal laminates it is necessary to develop a laminate analysis method that accounts for the nonlinear behavior of the individual laminae.

The technical study detailed in this report describes the development of a nonlinear, temperature-dependent, incremental laminate analysis. The following sections detail the background, objectives, approach and results of this study.

BACKGROUND

Nonlinear composite laminate response includes the study of two related problems. The first is the nonlinear response of the unidirectional material which defines the layer properties to be utilized in the laminate. The second problem is the proper combination of the layer properties to determine the effective laminate response. Several investigators have analyzed both the nonlinear response of the unidirectional material and the nonlinear response of a composite laminate. In order to study the nonlinear metal matrix response, the previous analyses have been reviewed to understand alternate approaches to the problem. The discussion of the previous work is separated into sections on unidirectional response and laminate response.

NONLINEAR UNIDIRECTIONAL MATERIAL BEHAVIOR

The previous studies of nonlinear unidirectional behavior can be divided into two general categories which are designated finite element analysis and approximate stress fields. Each of these categories is discussed below.

Finite Element Analyses

Several authors have used finite element or numerical approaches to study nonlinear behavior of unidirectional composites, references 3 to 7.

Lin, et al., reference 3, analyzed a unidirectional composite under an axial mechanical load. The results showed that the fibers and matrix carry equal strain and that the matrix yields uniformly when the matrix stress equals the yield stress.

Adams, reference 4, investigated a rectangular array of fibers in a plastic matrix under a transverse load. He allowed the matrix elements to yield sequentially and computed nonlinear transverse stress-strain curves of Boron/Aluminum composites. Comparisons with experimental data showed excellent agreement to the point where the matrix stress in an element was equal to the ultimate matrix stress. At this point, the analysis was terminated although the experimental data showed further

composite load carrying capability. Adams postulated that at this load the matrix began to develop microcracks. Although these cracks reduced the stiffness of the composite, they grew in a stable fashion allowing the composite to contain several cracks before finally failing.

Foye, reference 5, adopted a similar approach to Adams although he included the effects of axial shear and interactions between transverse tension and shear stresses. He also analyzed B/Aℓ along with Gr/Epoxy and B/Epoxy. His analytical results for B/Aℓ were similar to Adams although he made no comparisons (other than qualitatively) to experimental data. He found that there is a significant interaction between shear and transverse stresses. For example, his results show that the computed transverse stress-strain curve depends upon the magnitude of the axial shear stress.

Dvorak et. al., reference 6, utilized a hexagonal array finite element model to investigate yield surfaces of unidirectional composites. This paper includes a good description of the boundary conditions required to analyze loads due to a general stress state and temperature change. The composite yield surfaces are computed by finding the applied composite stress which causes yielding in any matrix element. His results show that a unidirectional composite yield surface can be described in four dimensional stress space (σ_a, σ_t, τ_a, τ_t). He found that because the fibers remain elastic, uniform temperature increases or hydrostatic stresses can cause yielding in the composite. Dvorak also computed that a temperature change of between 50°F and 100°F was large enough to cause significant yielding in several metal matrix composites.

Hashin and Humphreys, reference 7, used a temperature dependent hexagonal array finite element model to compute certain composite stress-strain curves, specifically axial shear and transverse shear. It was then postulated that the remaining three dimensional stress-strain relations could be generalized from this information. Using assumptions of negligible strain in the fiber direction, and transverse isotropy during plastic flow, explicit relations were developed that allowed one to

compute nonlinear composite behavior from the computed shear response. Although the relations were derived in reference 7, they were not compared with experimental data or other results to test the theory.

In general, the finite element analyses are all based upon assumed regular geometries and detailed calculations of the local micromechanical stress. Since the analysis involves matrix plasticity, the calculations are nonlinear and require iterative solutions. Typically this generates considerable computer costs which limits these methods, although they are very accurate, from becoming useful engineering design tools.

Approximate Stress Fields

An alternate approach that has been applied to the problem of nonlinear metal matrix composite behavior can be categorized as approximate stress fields. These models have typically been analytical as opposed to numerical. They are based upon simplifying assumptions of the stress field within the material which allows the calculation of composite level stress-strain behavior. Several different authors, references 10 and 12 to 17, have utilized this approach. A description of their studies and a comparison of their results is outlined in the following paragraphs. The phase average stress model which was employed in this study and described in detail in the appendix to this report also assumes an approximate stress field in the constituents. The major difference between the phase average model and the approaches described in this section is in the method utilized to compute effective unidirectional composite properties. The phase average model utilizes the composite cylinders assemblage, reference 8, whereas the methods described here use rule of mixtures models, reference 9.

Huang, reference 10, treats the composite as rigid inclusions within a rigid plastic matrix. He uses relatively simple assumptions of stress and strain within the composite. For example, he assumes that because the inclusions are rigid the strains are zero in the fiber direction and in the transverse directions:

$$\sigma_1 = v_f \sigma_1^f + v_m \sigma_1^m$$

$$\sigma_2 = v_f \sigma_2^f + v_m \sigma_2^m$$

$$\tau_{12} = v_f \tau_{12}^f + v_m \tau_{12}^m$$

and,

$$\varepsilon_1 = v_m \varepsilon_1^m$$

$$\varepsilon_2 = v_m \varepsilon_2^m$$

$$\gamma_{12} = v_m \gamma_{12}^m$$

These assumptions are consistent with rigid fibers and a rigid-plastic matrix. Then, by treating the matrix as a power-law work hardening material, he is able to develop composite stress-strain relations. He compares his results to finite element calculations of transverse stress-strain curves and shows relatively good agreement at large strains (i.e.ε_2>3%). He further modified the model to include the elastic strains by adding the strains computed from a self-consistent method, reference 11. The approach appears valid for large strains but has limited applicability in typical metal matrix composites where transverse fracture generally occurs at strains lower than 1%.

Dvorak and Bahei-El-Din, references 12 through 15, have together and separately published several papers on nonlinear unidirectional composite behavior. Their approximate stress field analysis is termed the vanishing fiber diameter model. They assume that the fibers have vanishingly small diameters so that the presence of the fibers does not perturb the transverse and shear stress fields. This leads to assumed stress and strain fields such that:

$$\bar{\sigma}_{ij} = \sigma^f_{ij} = \sigma^m_{ij} \qquad i, j \neq 3$$

$$\bar{\sigma}_{33} = v_f \sigma^f_{33} + v_m \sigma^m_{33} \qquad 3 \text{ - fiber direction}$$

and,

$$\bar{\varepsilon}_{ij} = v_f \varepsilon^f_{ij} + v_m \varepsilon^m_{ij} \qquad i, j \neq 3$$

$$\bar{\varepsilon}_{33} = \varepsilon^f_{33} = \varepsilon^m_{33}$$

By further assuming that the fibers are elastic and the matrix is elastic plastic with a Mises yield condition, they have developed closed form expressions for the elastic constants and yield surface of the composite. Furthermore, by treating the matrix as a kinematic hardening material, they are able to develop a hardening law and a flow rule for the composite. They exercise the model and compare it to experimental data and previous finite element analyses, (i.e. reference 6). It was found that it was necessary to modify the matrix material properties in order to predict accurate elastic properties. However, this was not unexpected since the transverse stress field was assumed to be uniform. Their model was found to work quite well for materials subjected to mechanical loading to induce a plane stress state. This implies that the model will be an excellent tool for nonlinear analysis of laminated composites under mechanical loads. The model appears to be limited in its ability to analyze the effects of high hydrostatic stresses or thermal loadings. The authors point out that the model may give erroneous results if it is utilized to study the case of cyclic thermal loadings. It was also found that the yield criterion for a unidirectional composite will be significantly different than that assumed by Hill in his anisotropic yield criterion. Therefore, Hill's yield criterion may be applicable to homogeneous, anisotropic materials but is not valid for unidirectional composites.

Min, reference 16, and Min and Crossman, reference 17, describe a model very similar to Dvorak's outlined above. They include further assumptions that the material is in a state of plane stress, the matrix is perfectly plastic and that the fiber has a zero Poisson's ratio. They compare the model to experimental data to investigate the effects of cyclic thermal loading and cyclic mechanical loading at various temperatures. They utilize typical graphite fiber properties and choose matrix properties to match the measured unidirectional transverse stress-strain curves. The model shows good agreement with the experimental data although the calculated results appear to be sensitive to the assumed residual matrix stress state.

In general, the approximate stress field models appear to be fairly similar. All assume that the fibers and matrix have equal strain in the axial direction. For transverse and shear stresses, the models either assume that the stress field is uniform (Min and Dvorak) or the composite response is based upon self-consistent scheme (Huang). The approximate models are also limited to the study of temperature independent constituent properties. For the particular problem of thermal cycling, only Min's model has been compared to data.

NONLINEAR LAMINATE BEHAVIOR

Several authors have published analyses of nonlinear temperature independent laminate behavior. The approach used by most authors is fairly similar so only a few are included in this review, references 18 thru 20. The laminate is analyzed in a incremental, piecewise linear fashion. That is, incremental stresses or loads are applied to the laminate. Then laminated plate theory is employed to compute the incremental stress state in each layer. The layer stress state is then utilized to determine the instantaneous stiffness for each layer. The layer response is either determined from tests on unidirectional materials, reference 19, or from a unidirectional material model, reference 18. The layer

stiffnesses are then integrated to give the new composite stiffness and the process can be repeated for the next stress increment.

Of particular interest is a nonlinear laminate analysis, NOLIN, developed at MSC, reference 20. The theory employed in NOLIN assumed that the individual plies were nonlinear in axial shear and transverse stress. Ramberg-Osgood relations, reference 21, were used to describe the uniaxial response of the plies. Then by postulating an interaction criterion between the stresses, it was possible to define a nonlinear, inelastic problem which described the behavior of the laminate. This led to a system of nonlinear equations that was solved using a Newton-Raphson technique. The code proved useful for the analysis of the room temperature behavior of organic matrix and metal matrix laminated composites. The limitations of NOLIN with respect to the problem under consideration include inability to handle plastic strains in the fiber direction and the assumption of temperature independent properties. Furthermore, the feature which makes NOLIN most attractive is the use of Ramberg-Osgood relations for the description of the layer response. In other words, the layer strains are explicit functions of the layer stresses. In the more general problem outlined in this report the layer behavior is path dependent and must be solved micromechanically and therefore cannot be written in explicit form. Thus, it appears that although NOLIN will provide useful background information for this program, it is not directly applicable to the general solution under consideration.

OBJECTIVES

The primary goal of this program was to develop a laminate analysis code which could be utilized to study the thermal hysteresis behavior of laminated metal matrix composites. The specific objectives of the laminate study were to create an incremental analysis which incorporates the temperature dependent nonlinear unidirectional material model capable of describing the behavior of metal matrix composites. The laminate analysis can be utilized to study the behavior of various metal matrix structures as potential satellite components. For example, $\pm\theta$ continuous graphite fiber reinforced aluminum tubes are being considered for space trusses. The laminate analysis can be employed to study the materials to define methods for reducing or eliminating the thermal hysteresis. Alternatively, if the nonlinear behavior cannot be prevented, the laminate analysis will serve as a tool to design materials that are capable of performing their function in spite of the inelastic behavior. The analytical results will provide an understanding of the composite behavior and define directions for improved materials and structures.

It should be emphasized that although the proposed laminate analysis depends upon the theory which is used to describe the unidirectional ply behavior, the laminate model will be constructed in a modular fashion. The unidirectional analysis will be contained in a subroutine that can be replaced or modified as the understanding of the material is improved. Thus, the laminate analysis will provide a fairly standard framework which can be easily improved by replacing or modifying the unidirectional material model. For example, based upon the available results of research programs which exist today, the best choice of the unidirectional model is the phase average stress theory described in the appendix. However, if improvements are made to that model they can be easily incorporated in the laminate analysis code.

APPROACH

The technical approach utilized in developing the metal matrix laminate analysis includes the theory utilized for the temperature dependent layer model and the theory utilized for the incremental laminate analysis. The layer model is described in detail in the appendix to this report. The following section outlines the incremental laminate analysis.

NONLINEAR LAMINATE MODEL

The nonlinear laminate analysis is relatively straightforward once the unidirectional problem has been solved. The laminate analysis is an incremental, piecewise linear model. In order to describe the laminated plate analysis, consider a single layer (ply) located in the x-y plane. Following standard laminated plate theory, reference 9, assume that the significant displacements are u and v which are linear through the thickness of the plate. In incremental fashion, these can be written as:

$$\dot{u} = \dot{u}_o - z \frac{\partial \dot{w}}{\partial x}$$

$$\dot{v} = \dot{v}_o - z \frac{\partial \dot{w}}{\partial y} \qquad (1)$$

Assuming the ply is in a state of plane stress the only stress components are $\dot{\sigma}_x$, $\dot{\sigma}_y$ and $\dot{\tau}_{xy}$. The corresponding strains, derived from the above displacement fields are:

$$\dot{\varepsilon}_x = \frac{\partial \dot{u}_o}{\partial x} - z \frac{\partial^2 \dot{w}}{\partial x^2} = \dot{\varepsilon}^o_x + z \dot{\kappa}_x$$

$$\dot{\varepsilon}_y = \frac{\partial \dot{v}_o}{\partial y} - z \frac{\partial^2 \dot{w}}{\partial y^2} = \dot{\varepsilon}^o_y + z \dot{\kappa}_y \qquad (2)$$

$$\dot{\gamma}_{xy} = \frac{\partial \dot{u}_o}{\partial y} + \frac{\partial \dot{v}_o}{\partial x} - 2z \frac{\partial^2 \dot{w}}{\partial x \partial y} = \dot{\gamma}^o_{xy} + z \dot{\kappa}_{xy}$$

Each layer can be described in terms of a stress-strain relation in principle material coordinates such that:

$$\left\{\dot{\sigma}_1\right\} = [Q] \left\{\dot{\varepsilon}_1\right\} + \left\{\Gamma\right\} \Delta T \qquad (3)$$

where Q represents the local layer stiffness matrix and Γ represents the local layer thermal stress vector. The stresses and strains can be transformed into the global plate coordinate system which results in the following global stress-strain relation:

$$\left\{\dot{\sigma}_x\right\} = [\theta_s] \left\{\dot{\sigma}_1\right\}$$

$$\left\{\dot{\varepsilon}_x\right\} = [\theta_e] \left\{\dot{\varepsilon}_1\right\} \qquad (4)$$

$$\left\{\dot{\sigma}_x\right\} = [\bar{Q}] \left\{\dot{\varepsilon}_x\right\} + \left\{\bar{\Gamma}\right\} \Delta T \qquad (5)$$

In equation (5) $\bar{Q}$ and $\bar{\Gamma}$ represent the global stiffness matrix and global thermal stress vector, respectively. It should be pointed out that since this is a nonlinear problem $\bar{Q}$ and $\bar{\Gamma}$ will be functions of the stress and temperature state and therefore represent instantaneous quantities.

The equations discussed so far have described the behavior of each individual ply that are part of the laminated plate. It is now necessary to combine the properties of the plies in order to describe the behavior of the laminated plate. In order to do this it is first necessary to define the forces and moments that act on the boundary of the plate.

$$\left\{\dot{N}\right\} = \int_{-h}^{h} \left\{\dot{\sigma}_x\right\} dz \qquad \left\{\dot{M}\right\} = \int_{-h}^{h} \left\{\dot{\sigma}_x\right\} z \, dz \qquad (6)$$

Substituting the global stress-strain relations for each ply

$$\left\{\dot{N}\right\} = \int_{-h}^{h} [\bar{Q}] \left\{\dot{\varepsilon}\right\} dz + \int_{-h}^{h} [\bar{Q}] \left\{\dot{\kappa}\right\} z dz + \int_{-h}^{h} \left\{\bar{\Gamma}\right\} \Delta T \, dz \qquad (7)$$

$$\left\{\dot{M}\right\} = \int_{-h}^{h} [\bar{Q}] \left\{\dot{\varepsilon}\right\} z dz + \int_{-h}^{h} [\bar{Q}] \left\{\dot{\kappa}\right\} z^2 dz + \int_{-h}^{h} \left\{\bar{\Gamma}\right\} \Delta T z dz$$

Rewriting these equations in the more familiar laminated plate notation.

$$\begin{Bmatrix} \dot{N} \\ \dot{M} \end{Bmatrix} = \left[\begin{array}{c|c} A & B \\ \hline B & D \end{array}\right] \begin{Bmatrix} \dot{\varepsilon}_x \\ \dot{\kappa}_x \end{Bmatrix} + \begin{Bmatrix} \dot{N}_T \\ \dot{M}_T \end{Bmatrix} \qquad (8)$$

Equation (8) can be easily inverted to compute laminated plate strain increments which are caused by increments in plate forces, moments and temperatures.

The solution then follows a straightforward process for each load increment as detailed in Figures 4 and 5. Assuming that at some initial step the laminate stresses and strains are defined, the load increment in terms of stresses or temperatures is applied to the laminate. Standard laminated plate theory is utilized to compute the layer stresses in global coordinates. Stress transformations are employed in each layer to calculate the layer stress state in principal material coordinates. These layer coordinate stresses are then applied to the unidirectional material model to compute stress and strain increments within each layer. If necessary, the layer properties are modified to reflect changes in the constituents due to plastic flow or temperature. The layer properties are transformed into global coordinates and integrated to give new laminated plate stiffnesses. The incremental stresses and strains within the material are added to the initial values to give total stresses and strains. This completely defines the laminated plate at the end of the load step so that the process can be continued for the next load increment.

Once the laminate analysis is developed, it can be employed parametrically to study materials and structures of interest. The analytical tool can be utilized to understand experimental data, define improved materials or design metal matrix structures.

MODEL VERIFICATION AND RESULTS

Once the layer stiffnesses of a laminate are known, either through the elastic or the elastic-plastic incremental stress-strain laws, the complete structural stiffness can be assembled. For any given increment in the nonlinear laminate analysis, this assembly process and the subsequent layer stress analysis (based on the proper incremental stress-strain law) are identical to those steps of a conventional elastic laminate analysis. That is, the basic laminate procedures are the same. Therefore, once the individual layer stiffnesses are known and once the load step has been verified (legitimate stiffness, legal load path, etc.) the results of an increment in the nonlinear laminate analysis can be compared against an equivalent increment in an elastic analysis. Such comparisons were made in order to verify the correctness of the nonlinear laminate procedures.

The nonlinear laminate analysis was used to examine a number of practical problems. These problems considered both thermally and mechanically loaded laminates. For ease of interpretation and to gain insight into more complex thermal responses, the example problems considered here have material properties which are temperature independent (the next section will release this restriction).

The laminates that are studied consist of P100/6061 composite material layers with a 45% fiber volume fraction. The thermophysical and mechanical properties of the constituent materials are shown in Table 1 (see the appendix for the reference sources). The temperature independent solutions of this section assume that the material properties retain their room temperature values. The stress free state of a P100/6061 composite layer is also assumed to exist at room temperature. Because the constituent materials respond differently to thermal loads (the carbon fiber tries to contract axially while the aluminum matrix seeks to expand during heating) very large stress levels are reached through relatively small temperature changes. The matrix material is soon stressed beyond its

elastic limit. This plus the fact that P100/6061 is a leading candidate material for satellite systems, make the laminates of this material ideal for study by the nonlinear laminate analysis.

THERMAL LOADS

The first problem determines the effect of a single complete temperature cycle on a set of three different laminates. The temperature cycle, whose extreme values are characteristic of orbital temperatures, starts by cooling from an arbitrary stress free temperature of 75°F to a temperature of -225°F. The temperature path is then reversed, heating to a temperature of 275°F. The laminate is then recooled to a temperature of 75°F. The stress free temperature was chosen arbitrarily since the purpose of these analyses are to examine the sensitivity of the model to angle ply orientation. It will be seen that this thermal cycle induces sequential phases of mechanical response.

The laminates that are examined are a [+15/-15]s, a [+30/-30]s, and a [+45/-45]s (which under a thermal load is equivalent to a cross ply). The normal strain in the longitudinal direction of these balanced plates, due to the loading of the thermal cycle, is shown in Figures 6, 7, and 8. Though each of these plots show a distinctly different response, there is an underlying similarity in the mechanical state history of the laminates.

All of the laminates show an initial elastic response where the fibers are growing axially and the matrix is contracting under the falling temperature. Note that the angle ply laminates have a total growth response opposite to that of the cross ply laminate. The [±15]s laminate initially has almost a zero coefficient of thermal expansion. These initial elastic responses are corroborated by the axial thermal expansions shown in Figure 9 which is based on a purely elastic laminated plate theory.

During the initial elastic response of the composites shown in Figures 6, 7, and 8, high levels of stress are quickly generated.

In stress space the load path of the matrix material soon reaches the yield surface. Table 2 is a compilation of the temperature points at which initial yielding occurs for each of the subject laminates, as well as for a unidirectional laminate. The table also includes the longitudinal laminate strain at these temperatures. It is seen in Table 2 that the temperature at which initial yielding occurs is nearly independent of angle ply orientation while the deformational responses are radically different.

Returning to Figures 6, 7, and 8 it can be seen that after the matrix yields at approximately -70°F the fibers have a greater role in determining the overall laminate response. Thus, in the angle ply laminates, Figures 6 and 7, the expansion proceeds at a greater rate while in the cross ply, Figure 8, the matrix dominated contraction is severely curtailed.

Upon subsequent heating of each laminate it can be seen in each figure that the stresses due to the mismatch in responses of the constituent materials are relieved. The laminate thermal response is again elastic as the load path moves away from the yield surface. Further heating causes the stresses to build up once again with the load path reaching another point on the yield surface. During this elastic response, the angle ply laminates, Figures 6 and 7, are contracting while the cross ply laminate, Figure 8, is expanding. Yielding again affects the rate at which these responses occur, speeding up the shrinking in the angle ply laminates, Figures 6 and 7, while diminishing the growth rate of the cross ply laminate, Figure 8.

Subsequent cooling to room temperature elicits another elastic response. It is seen that at the end of the thermal cycle each of the laminates possesses a different residual strain state.

The [+15/-15]s laminate is now examined under a second thermal cycle which repeats the path of the first cycle. The second cycle results are shown in Figure 10. Comparing Figure 10 with Figure 6, it is seen that the longitudinal strain of the second cycle is coincident with that of the first cycle. This occurs because during the first thermal cycle the yield surface is centered with respect to the subsequent thermal load path, i.e. temperature range.

Successive thermal cycles will, therefore, retrace the original laminate response. Note that this is a consequence of temperature independent material properties. By introducing temperature dependency, thermally induced hysteresis will occur (see results of the next section

The obvious conclusion of these test problems is that laminates which are designed to provide dimensional stability for elastic thermal loading, will undergo significant deformation when the thermal load causes the matrix material to respond plastically.

The next problem examines the effect of the orbital thermal cycle on an unsymmetric [+45/-45] laminate. In Figure 11 it is seen that the laminate response is qualitatively similar to that of the previous problems (compared with Figure 8), with the laminate undergoing successively different mechanical phases or response. However, since the new laminate is unsymmetric, it will experience changes of curvature under this loading. Figure 12 is a plot of the twisting curvature that occurs during the thermal cycle. This plot shows that the plate will possess a residual twisting curvature upon completion of the cycle.

MECHANICAL LOADS

The final problem set of this section studies the response of a [+22.5/-22.5]s laminate under various mechanical load histories. These load histories are (see Figure 13):

1. The load history, AT, where the laminate is loaded incrementally in the axial direction by 1 ksi load steps to a level of 7 ksi. The axial load increments are followed by 1 ksi load increments in the transverse direction also to a level of 7 ksi.

2. The load history, TA, where the sequence of axial then transverse load increments of history AT are reversed.

3. The load history EQ where the axial and transverse load increments of history AT are applied simultaneously.

Prior to the application of load, the laminate is assumed to be stress free. Note that each load history leads to the same level of final loading.

The laminate strains resulting from load history AT are shown in Figures 14 and 15. These plots show that under this loading the laminate undergoes four phases of response. The nature and cause of these responses are best explained through the aid of Figure 16 which shows a schematic representation of the yield surface and its sequential position in stress space. Prior to the application of load, the load point is at the origin of stress space (no initial stresses). As the axial load increments are applied, the load path moves away from the origin and out towards the yield surface. Therefore, during the first phase, the laminate is responding elastically. Eventually the level of loading is such that the load path reaches the yield surface and initiates plastic flow. That the matrix material is responding plastically is indicated by the increased rate of deformation in Figures 14 and 15. After the last axial load increment, the first transverse load increment is applied. Though this added load increases the level of loading on the laminate, in stress space it actually corresponds to an unloading with respect to the yield surface. Thus, this third phase of response is purely elastic. Eventually, however, the transverse load increments cause the load path to reach the yield surface again. This results in plastic flow for the final phase of response.

Figures 17, 18, 19, and 20 show the laminate response under the TA and EQ load histories. The development of these plots can be explained in a manner similar to that of the AT load history. Note that the total number of phases and the history of response are quite different for all of the load histories.

As a final consideration, an additional load history is examined. Prior to the application of the load steps of history EQ let it be postulated that the laminate has been cooled 100°F from a stress free temperature of 175°F. The load steps are then applied, resulting in the deformational responses shown in Figures 21, and 22. In these figures it is seen that the drop in temperature has resulted in a minor amount of elastic pre-strain (this laminate has a small coefficient of thermal expansion as per Figure 9). As compared to Figures 19 and 20, these figures show a shift in the initial yield point due to the presence of the substantial residual stresses that exist prior to the mechanical loading.

The mechanical load problem clearly illustrates the path dependent nature of laminate plasticity. In Tables 3 and 4 it is seen that although the load histories terminate at an equal level of loading, the final stress and strain fields can show quite distinct differences. Also, the rough accounting of residual processing stresses shows the importance of these stresses. In the problem examined here the presence of these stresses lead to significant differences in the final laminate state. The existence of these stresses imply that the load point at the beginning of the load history is no longer at the origin in stress space. Depending upon the nature of the subsequent loading such a condition can lead to very surprising behavior (for instance, in the Appendix A see the Figure A-15 and its associated discussion).

THERMAL HYSTERESIS OF ANGLE PLY LAMINATES

Unlike the last section the problems to be studied here will deal with materials whose thermphysical and mechanical properties are temperature dependent. The approach of the temperature dependent analysis is presented in the appendix and the basic considerations developed in that part of the report will not be repeated here. Instead, this section will undertake a study of thermal hysteresis of both unidirectional and angle ply laminates since dimensional stability is a critical factor in satellite design. It will be

seen that when the temperature dependent matrix properties are taken into account the changes in the thermal hysteresis of laminates can arise solely from the behavior of the unidirectional layer and that no other mechanism, such as system degradation, need be postulated to account for such behavior.

The composite layer to be studied is the P100/6061 material of the previous section with a 45% fiber volume fraction and with constituent material properties as specified in Table 1. A stress free state is assumed to exist at room temperature. Once again the stress free state is chosen arbitrarily since the purpose is to examine the computed response of metal matrix laminates with different angle ply orientations.

The temperature cycle is the orbital thermal cycle previously described. That is, the laminate is cooled from room temperature to -255°F, heated to 275°F and then recooled. The temperature history repeats this cycle as required.

Figure 23 shows the response of a unidirectional laminate subjected to four cycles of the thermal loading. At the scale of this plot the shift in the residual strain is barely visible. Figure 24 is an enlargement of the left hand edge of Figure 23. It shows the shift in residual strain more clearly with the sequence of successive cycles proceeding in the negative strain direction. That is, under the thermal loading the laminate is changing, albeit minutely. The underlying cause for this growth, the reasons for which will be explained in detail, is the successive increase in the matrix plastic strains (Figure 25). The matrix stress also experiences corresponding small residual shifts as illustrated in Figure 26.

The causes of plastic strain growth can be found by studying the effects of temperature on the load path and on the yield surface as the load path moves through stress-temperature space. Figure 27 is a schematic representation of the yield surface as it sits in stress-temperature space, where for the purposes of illustration, the multi-dimensional stress space has been reduced to a plane and the ellipsoidal yield surface is represented as an ellipse. The figure shows the yield surface as it would appear at

room temperature and at the extremes of the orbital cycle. The size of the yield surface varies since the strength parameter is related to the uniaxial matrix yield stress which is affected by temperature. During the thermal cycle the load path moves out along the stress and temperature directions. After the load path reaches the yield surface,plastic flow will occur under further loading.

Consider the sequence of events in Figure 28 which depicts the load path as it develops under the thermal loadings. At room temperature the laminate is stress free so that the load point is at the origin of stress space. The yield surface is centered on this origin. The thermal cycle begins with a cooling phase where the matrix contracts and the fibers extend axially, thus, generating stresses in the constituents. The load path moves away from the origin and out towards the yield surface while descending in the temperature direction. The yield surface grows since the uniaxial yield stress increases at lowered temperatures. The rate at which the load path moves along the stress coordinates is constantly varying since the stiffness properties and the coefficient of thermal expansion change with temperature. The load path eventually reaches the yield surface. It does so at a higher level of loading than that which would have been found from an analysis based on room temperature properties (Figure 29). The load path then displaces the yield surface, shifting it with respect to the origin of stress space, and producing plastic flow. The rate of flow is affected by the temperature, once again through the temperature dependence of the material properties. Upon heating, the load path moves away from the yield surface and the resulting deformational response is elastic. The yield surface shrinks but does not translate in the stress directions. As the temperature continues to increase the load path again reaches the yield surface, this time at a temperature higher than that predicted by a temperature independent analysis (Figure 29). The resulting plastic flow continues until the maximum temperature is reached. Note that the yield surface is displaced first towards and then past its original position in the stress coordinates. The temperature increase,

therefore, works out the positive plastic strains and produces negative plastic strains (refer to Figure 25). The rate of flow during this heating phase is in general different than that which occurred during the cooling phase. The final leg of the cycle cools the laminate back down to room temperature. During this cooling the laminate responds elastically so that the yield surface remains in the position established at the maximum temperature. Therefore, upon returning to the starting temperature there is a residual shift of the yield surface with respect to its original position. With further cooling the load path will reach the yield surface again, this time at a temperature higher than that of the temperature independent problem. This second cycle of loading will follow a sequence of events comparable to that of the preceeding cycle.

The residual shift of the yield surface means that the first cycle of thermal loading produced a residual plastic (and total) strain state. This was also found to be true in the temperature independent problem where for successive load cycles no higher levels of residual strain were achieved. The yield surface had centered itself with respect to the load path. This centering does not occur in the temperature dependent problem; Table 5 shows that the yield surface is continually shifted by successive load cycles resulting in plastic strain growth and changes in laminate hysteresis.

As stated before, the cause for the plastic strain growth can be found in the events that occur as the load path moves through the temperature-stress space. A study of the history reveals two basic sources for this growth. The first is the disparate extent to which the laminate is subjected to plastic straining over the thermal cycle. In Figure 29 it is seen that plastic flow occurs over a larger range of temperature upon cooling (approximately 225°) then upon heating (approximately 175°). The second mechanism is the temperature dependence of the rate of flow, since for the same travel of temperature, different total plastic strains will occur upon heating than upon cooling. The principal explanation then is as follows. During cooling, plastic flow results in positive plastic strains. During heating, the flow results in negative plastic strains. Since, due to the aforementioned mechanisms,

these flows do not balance one another each successive thermal cycle leads to additional growth. (Note that for the temperature independent problem the two zones of plastic flow occur over equal temperature transits. Also, since the material properties are constant the flow rates will be the same. Therefore, the negative strain flow is balanced by the positive strain flow and no net laminate growth occurs).

An additional problem considers the effects of the thermal cycle on a [+15/-15]s and a [+30/-30]s laminate. The results of these analyses are shown in Figures 30 and 31. These plots show that the shifts in residual strain can be quite pronounced for angle ply laminates. This is true in spite of the fact that the subject laminates are close to a design that would lead to zero coefficients of thermal expansion for purely elastic responses (Figure 9). The cause for this behavior is found in the shear stresses which induce and drive plasticity. By their very nature angle ply laminates contain large in-plane shear stresses under loading. During the thermal cycle these in-plane shear stresses lead to extensive plastic flow. This magnifies the imbalance in plastic straining that exists during the heating and cooling phases. Thus, the resulting shifts in the hysteresis loops are large. These results imply that the present method of selecting metal matrix composite designs to result in near zero axial thermal expansion coefficients may lead to unwanted material behavior. The results shown in Figures 23 and 30 illustrate the problem. The response of the unidirectional material, presented in Figure 23, shows that although the material has an initial nonzero thermal expansion, the subsequent hysteresis loops are relatively stable and repeatable. On the other hand, the results for the ±15° laminate presented in Figure 30, show that this angle ply composite initially has a near zero axial thermal expansion coefficient yet produces a large shift in residual axial strain after each thermal cycle. These results must be validated experimentally; however, from a design point of view it may be more beneficial to develop a zero thermal expansion material by increasing either the fiber modulus or fiber volume

fraction in a unidirectional material than by utilizing angle ply laminate orientations.

Figure 32 plots the thermal response of a [+45/-45]s laminate. Under this loading the laminate is equivalent to a cross ply so that no in-plane plate shear stresses are developed. Because of this the thermal hysteresis is seen to be substantially smaller than that of the angle plys, Figures 30 and 31.

The analysis has shown that the use of angle-ply laminates to provide dimensional stability may be a problem when the thermal loads are such as to induce plastic deformation in the matrix. The results suggest that low layer angle designs will produce near zero thermal expansion but large residual shifts in the hysteresis loops. The hysteresis study suggests several courses of action for material and component development.

An obvious effort is to seek to extend the range of elastic behavior through matrix selection and metallurgical advances. Besides this effort another area of study would be the control of secondary properties such as temperature resistance and post-yielding stiffness. In this way favorable design approaches may be achieved.

Another area of component improvement may be found in altering the balance between fiber and matrix effects. For instance a unidirectional laminate can theoretically achieve elastic dimensional stability when provided with a high enough fiber content. Such a design would require fiber contents approaching 60% (at least for P100 fibers and aluminum matrices), a density level not readily achievable by current processing procedures. Improving the processing procedures would prove to be a worthwhile effort since a fiber dominated system with the correct matrix may lessen the effect of matrix plastic deformation on the overall laminate response. The same result may also be achieved by resorting to high modulus fibers.

As a last comment, any design procedure that would reduce shear stresses would lead to improvements in component performance. This secondary consideration (such as stacking sequence, processing methods, etc.) should be reviewed for the possible cause of extraneous shear stressing.

MODEL LIMITATIONS

The approximations used in the temperature dependent phase average stress model discussed in detail in the appendix impose certain limitations upon the accuracy of the laminated composite material model. There appear to be three areas in which the approximations may cause concern. These include the computation of initial yielding, the anisotropic plastic behavior of the matrix and the assumption that the matrix plastic modulus, h, is temperature independent. Each of these limitations is discussed in the following paragraphs.

The layer model does not compute the actual heterogeneous stress field within the fiber and matrix but approximates these stresses with uniform field based upon average values. Under a general loading condition, the actual distributed stresses in the matrix will cause yielding at some points in the material before yielding will be predicted by the phase average model. This will result in the phase average model overpredicting the composite yield surface. This effect will be most noticeable in transverse loading where the actual stress field in the matrix is far from uniform. In axial, thermal, or shear loadings, however, the matrix stress state is more nearly homogeneous and the phase average model provides an excellent approximation.

An additional limitation of the phase average model is that the matrix must be treated in the composite as if it is transversely isotropic during plastic flow. Be examining the matrix flow rule, equation (12) in the appendix, it can be seen that in general the matrix plastic compliance may be fully populated so that during yielding the matrix may behave as if it is completely anisotropic. Therefore, under a general loading condition (i.e. not uniaxial) the matrix may be deforming anisotropically while the composite model at best must treat the matrix as transversely isotropic. The quantitative effects of this assumption are discussed in the appendix. Once again this effect will be strongest for transverse loads where the matrix is in a general state of loading. For axial, thermal, or shear loads the stresses in the matrix can be divided

between a hydrostatic and a uniaxial component. In these cases the assumed isctropy in the matrix is exact and the phase average model is an accurate approximation of the matrix behavior.

The other limitation of the layer model is the assumption that the plastic modulus is temperature independent. Based upon 6061 stress-strain data from MIL-HDBK-5, appendix reference A-7, the plastic modulus is seen to vary by approximately 15% over the range of room temperature to 300°F. This assumption may be improved in the future, however, it significantly complicates the computations of plastic strain and motion of the yield surface.

CONCLUSIONS AND RECOMMENDATIONS

The results of this study have led to several important conclusions regarding the structural behavior of metal matrix composites. This program has developed an analytical model that can be used to study the temperature dependent nonlinear behavior of unidirectional metal matrix composite layers. The layer model has been incorporated in a nonlinear laminate analysis which can be employed to study the temperature dependent nonlinear response of laminated metal matrix composites. The results of the analytical studies have shown that if a unidirectional graphite/aluminum material is heat treated to eliminate thermal hysteresis then an angle ply laminate made of the same constituents, heat treated in the same manner, should also exhibit no thermal hysteresis. In other words, if the stresses thermally induced between the fiber and matrix remain below the matrix yield strength in a unidirectional material, then the additional stresses generated in an angle ply laminate will not cause yielding. On the other hand, the analysis has shown that if an angle ply laminate does yield, it hysteresis loop will experience more motion than the loop related to a unidirectional composite. This effect is predicted to be strongest in a $\pm 22.5°$ angle ply laminate in which the layer shear stresses reach a maximum. These results imply that if an angle ply laminate is used to give a zero coefficient of thermal expansion, it must be properly heat treated to prevent any hysteresis because the hysteresis theoretically exhibited by an angle ply will be much stronger than the hysteresis exhibited by a unidirectional. This result implies that it may be more beneficial to construct zero coefficient of thermal expansion materials by utilizing higher modulus fibers or by increasing the fiber volume fraction in the unidirectional materials.

It should be emphasized that the results described here are based upon a theoretical model. Although the model has shown good correlation with experimental data on unidirectional

materials, it has not been tested specifically against laminated composite data. Therefore, the effects predicted here should be corroborated by experimental data.

SYMBOLS

A - Laminate Membrane Stiffness Matrix

B - Laminate Membrane-Bending Coupling Stiffness Matrix

D - Laminate Bending Stiffness Matrix

h - Plate Half Thickness

M - Bending Moment (mechanical)

M_T - Bending Moment (thermal)

N - Membrane Force (mechanical)

N_T - Membrane Force (thermal)

Q - Local Plane Stress Stress-Strain Matrix

$\bar{Q}$ - Global Plane Stress Stress-Strain Matrix

U - Plate Displacement in x Direction

U_o - Midplane Plate Displacement in x Direction

V - Plate Displacement in y Direction

V_o - Midplane Plate Displacement in y Direction

v_f - Fiber Volume Fraction

v_m - Matrix Volume Fraction

x - In-Plane Plate Coordinate

y - In-Plane Plate Coordinate

z - Through Thickness Plate Coordinate

γ - Shear Strain

Γ - Local Thermal Stress Vector

$\bar{\Gamma}$ - Global Thermal Stress Vector

ΔT - Temperature Change

ε - Extensional Strain

θ_e - Strain Transformation Matrix

θ_s - Stress Transformation Matrix

κ - Plate Bending or Twisting Curvatures

σ - Extensional Stress

τ - Shear Stress

SUBSCRIPTS

a - Axial
t - Transverse

SUPERSCRIPTS

f - Fiber
m - Matrix
- - (overbar) Average
. - (dot) Increment

REFERENCES

1. Tompkins, S. S.; and Dries, G. A.: "Thermal Expansion Measurements of Metal-Matrix Composites." ASTM Symposium on Testing Technology of Metal Matrix Composites, Nashville, TN, November 18-20, 1985.

2. Wolff, E. G.: "Review of Thermal Expansion Characteristics of Metal Matrix Composites." Presentation at 1983 TMS/AIME Fall Meeting, Philadelphia, PA, October, 1983.

3. Lin, T. H.; Salinas, D.; and Ito, Y. M.: "Elastic-Plastic Analysis of Unidirectional Composites." Journal of Composite Materials, Vol. 6, January, 1972.

4. Adams, D. F.: "Inelastic Analysis of a Unidirectional Composite Subjected to Transverse Normal Loading." Journal of Composite Materials, Vol. 4, July, 1970.

5. Foye, R. L.: "Theoretical Post-Yielding Behavior of Composite Laminates. Part I - Inelastic Micromechanics." Journal of Composite Materials, Vol. 7, April, 1973.

6. Dvorak, G. J.; Rao, M. A. M.; and Tarn, J. W.: "Yielding in Unidirectional Composites Under External Loads and Temperature Changes." Journal of Composite Materials, Vol. 7, April, 1973.

7. Hashin, Z.; and Humphreys, E. A.: "Elevated Temperature Behavior of Metal Matrix Composites." MSC Final Report on AFOSR Contract F49620-79-C-0059, November, 1981.

8. Hashin, Z.: "Analysis of Properties of Fiber Composites With Anisotropic Constituents.", JAM, Vol. 46, no. 3, pp. 543-550, September, 1979.

REFERENCES (CONT'D)

9. Jones, R. M.: Mechanics of Composite Materials, McGraw-Hill, New York, 1975.

10. Huang, W. C.: "Plastic Behavior of Some Composite Materials." Journal of Composite Materials, Vol. 5, July, 1971.

11. Hill, R.: "Theory of Mechanical Properties of Fibre-Strengthened Materials.", J. Mech. Phys. Solids, Vol. 12, p. 199f, 1964.

12. Bahei-El-Din, Y. A.; and Dvorak, G. J.: "Plastic Yielding at a Circular Hole in a Laminated FP-Aℓ Plate." Modern Developments in Composite Materials, ASME Winter Annual Meeting, December, 1979.

13. Dvorak, G. J.; and Bahei-El-Din, Y. A.: "Plasticity Analysis of Fibrous Composites." Journal of Applied Mechanics, Vol. 49, June, 1982.

14. Bahei-El-Din, Y. A.; and Dvorak, G. J.: "Plasticity Analysis of Laminated Composite Plates." Journal of Applied Mechanics, Vol. 49, December, 1982.

15. Dvorak, G. J.: "Metal Matrix Composite: Plasticity and Fatigue. Mechanics of Composite Materials: Recent Advances, Proceedings of IUTAM Symposium on Mechanics of Composite Materials, Pergamon, NY, 1982.

16. Min, B. K.: "A Plane Stress Formulation for Elastic-Plastic Deformation of Unidirectional Composites." Journal of the Mechanics and Physics of Solids, Vol. 29, 1981.

17. Min, B. K.; and Crossman, F. W.: "History-Dependent Thermo-mechanical Properties of Graphite/Aluminum Unidirectional Composites." Composite Materials: Testing and Design (Sixth Conference), ASTM STP 787, American Society for Testing and Materials, 1982.

REFERENCES (CONT'D)

18. Craddock, J. N.; Zak, A. R.; and Majerus, J. N.: "Nonlinear Response of Composite Material Structures," Journal of Composite Materials, Vol. 11, April, 1977.

19. Petit, P. H.; and Waddoups, M. E.: "A Method of Predicting the Nonlinear Behavior of Laminated Composites." Journal of Composite Materials, Vol. 3, January, 1969.

20. Hashin, Z.; Bagchi, D.; and Rosen, B. W.: "Nonlinear Behavior of Fiber Composite Laminates." NASA CR-2313, April, 1974.

21. Mendelson, A.: Plasticity: Theory and Application. Macmillan, New York, 1968.

Table 1 Constituent Properties Used in Nonlinear Metal Matrix Laminate Analysis

Table 1a. P100 Fiber Properties

E_a		E_t		G_a		ν_a	ν_t	α_a		α_t	
GPa	Msi	GPa	Msi	GPa	Msi	–	–	$10^{-6}/°C$	$10^{-6}/°F$	$10^{-6}/°C$	$10^{-6}/°F$
690	100	3.45	0.50	17.2	2.50	0.41	0.45	-1.62	-0.90	20.3	11.3

Table 1b. 6061 Aluminum Matrix Properties

Temperature		E		ν	α		σ_y		E_{tan}*	
°C	°F	GPa	Msi	–	$10^{-6}/°C$	$10^{-6}/°F$	MPa	Ksi	GPa	Msi
-184	-300	75.9	11.0	0.33	18.7	10.4	140	20.3	13.9	2.020
-129	-200	73.8	10.7	0.33	20.3	11.3	130	18.9	13.9	2.010
- 73	-100	71.0	10.3	0.33	21.6	12.0	128	18.6	13.8	1.995
- 18	0	69.6	10.1	0.33	22.3	12.4	124	18.0	13.7	1.983
24	75	68.3	9.9	0.33	22.9	12.7	121	17.5	13.7	1.980
38	100	67.6	9.8	0.33	23.0	12.8	119	17.3	13.6	1.976
93	200	66.9	9.7	0.33	23.4	13.0	111	16.1	13.6	1.973
149	300	64.9	9.4	0.33	23.9	13.3	101	14.7	13.5	1.960

* Tangent modulus when $\sigma \geq \sigma_y$

Table 2. Computed Temperature and Axial Strain at Initial Thermal Yield Point for Various P100/6061 Balanced Symmetric Laminates [V_f= 45%, To = 24C (75°F)]

Laminate —	Axial Strain at Yield 10^{-6}	Temperature at Yield °C	°F
0°	-82.6	-57.8	-72.1
[±15]s	3.80	-56.7	-70.0
[±30]s	67.3	-57.1	-70.7
[±45]s	-287.3	-58.8	-73.9

Table 3. Final Computed Laminate Strain States after Various Load Histories Showing Path Dependence of Metal Matrix Laminate Response

(P100/6061, V_f = 45%, [±22.5]s)

Load History	ε_{xx} %	ε_{yy} %
AT - Axial, Transverse	-0.335	3.12
TA - Transverse, Axial	-0.417	3.55
EQ - Equal	-0.314	3.06
ΔT, EQ - Cool Down, Equal	-0.333	3.10

Table 4. Computed Final Matrix Stress States for First Layer in Layer Coordinates for [±22.5]s P100/6061 Laminates after Various Load Histories (V_f =45%)

Load History —	σ_{11}		σ_{22}		σ_{12}		σ_{33}	
	MPa	Ksi	MPa	Ksi	MPa	Ksi	MPa	Ksi
AT - Axial, Transverse	247	35.8	388	56.3	174	25.2	-2.07	-0.30
TA - Transverse, Axial	279	40.0	378	54.8	158	22.9	-1.72	-0.25
EQ - Equal	206	29.9	379	55.0	183	26.6	-1.72	-0.25
ΔT, EQ - Cool down, Equal	290	42.1	402	58.3	163	23.6	0.76	0.11

Table 5. *Computed* Yield Surface Center and Temperature at Subsequent Yielding for a 0° P100/6061 Laminate After Several Thermal Cycles (V_f = 45%)

State of Material	Yield Surface Center at Room Temperature ε_{11}^{mp}, με	Yield Temperature on Subsequent Cooling °C	°F
Initial State	0.0	-63.6263	-82.5273
End of 1st Cycle	-782.24	-17.8663	- 0.1594
End of 2nd Cycle	-769.16	-17.8444	- 0.1200
End of 3rd Cycle	-756.10	-17.8225	- 0.0805
End of 4th Cycle	-743.04	—	—

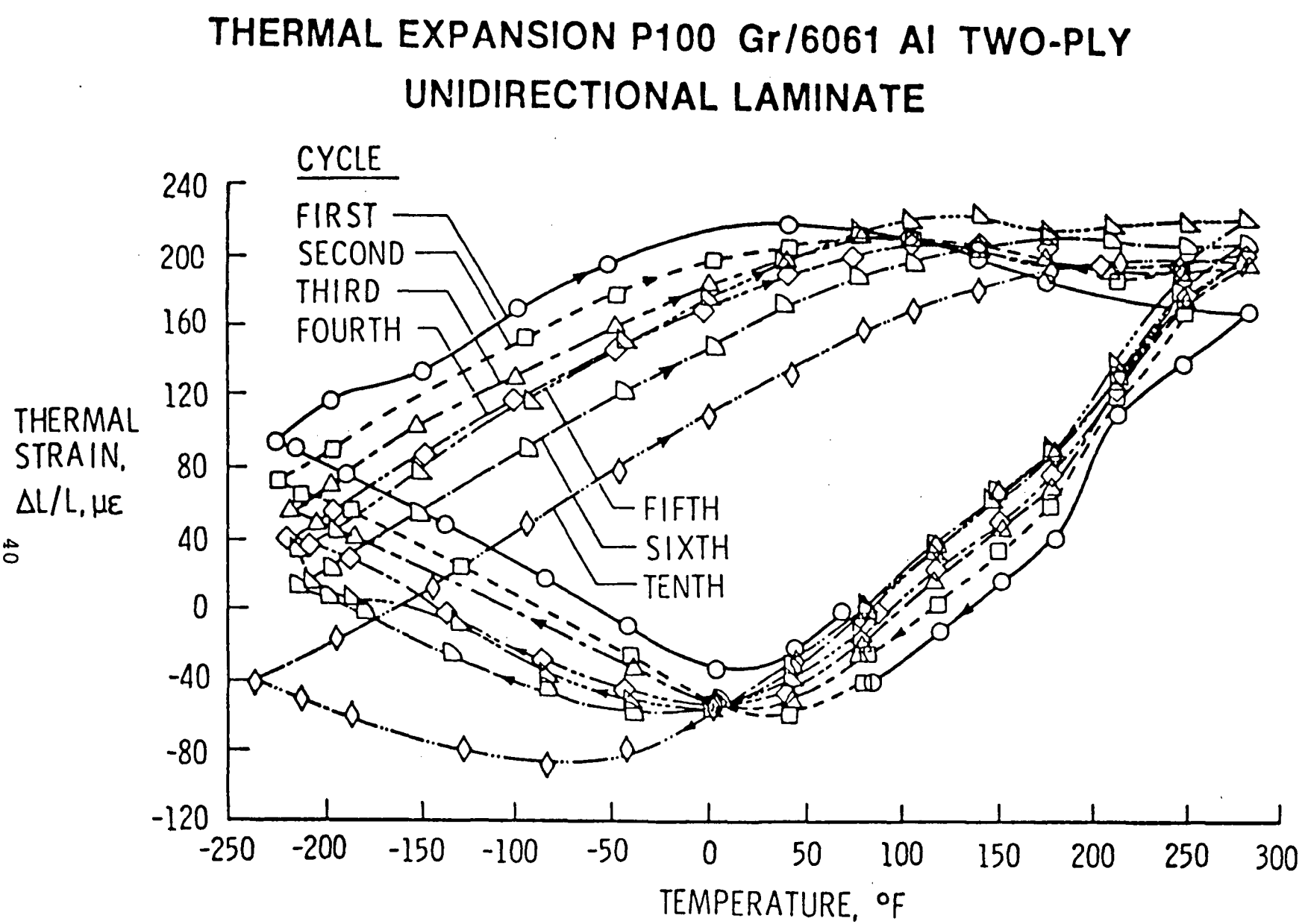

Figure 1. Thermal Cycling Hysteresis Seen in P100/6061 Unidirectional Composites. Data obtained from reference 1.

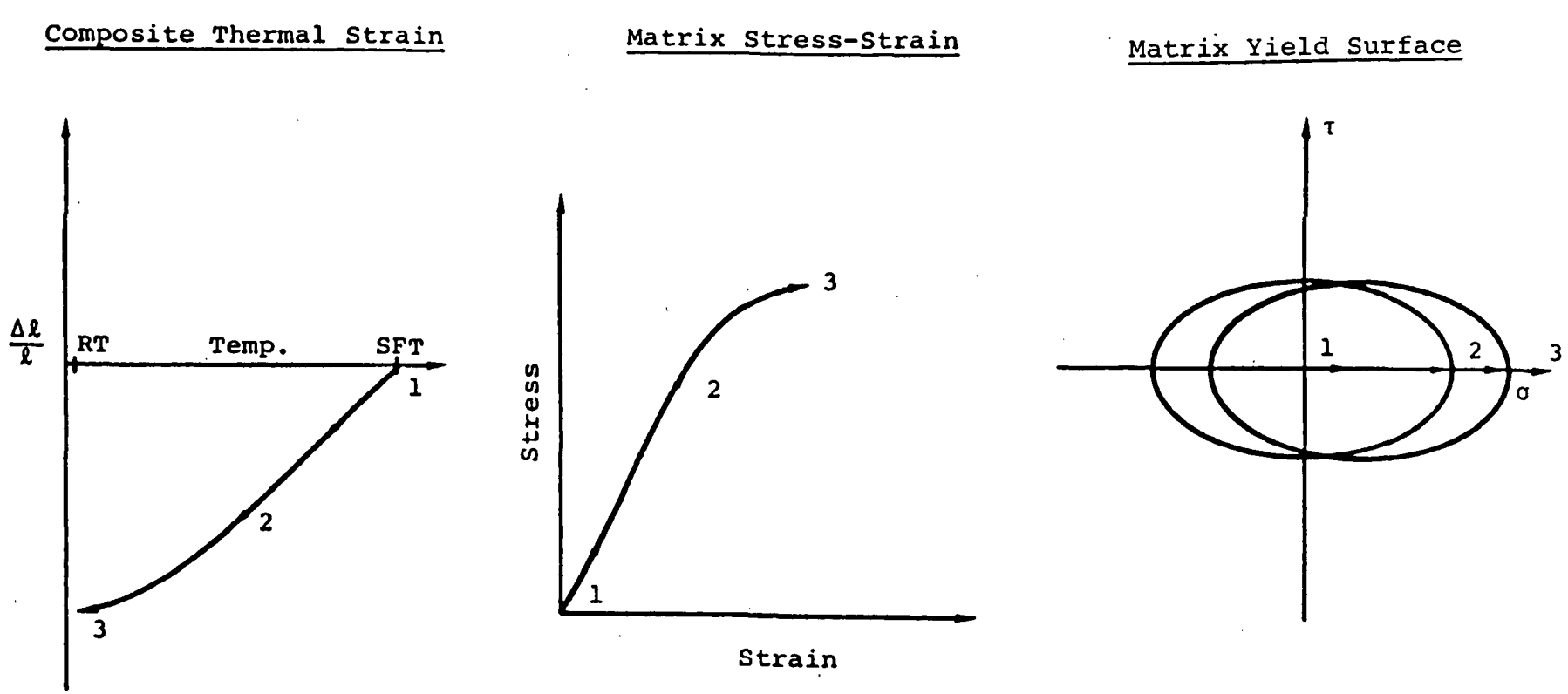

Figure 2. Nonlinear Behavior of Graphite Metal Matrix Composites and Matrix Due to Thermal Cycles. As composite is cooled from stress free temperature, the matrix yields in tension causing the thermal strain to be nonlinear and the matrix yield surface to shift.

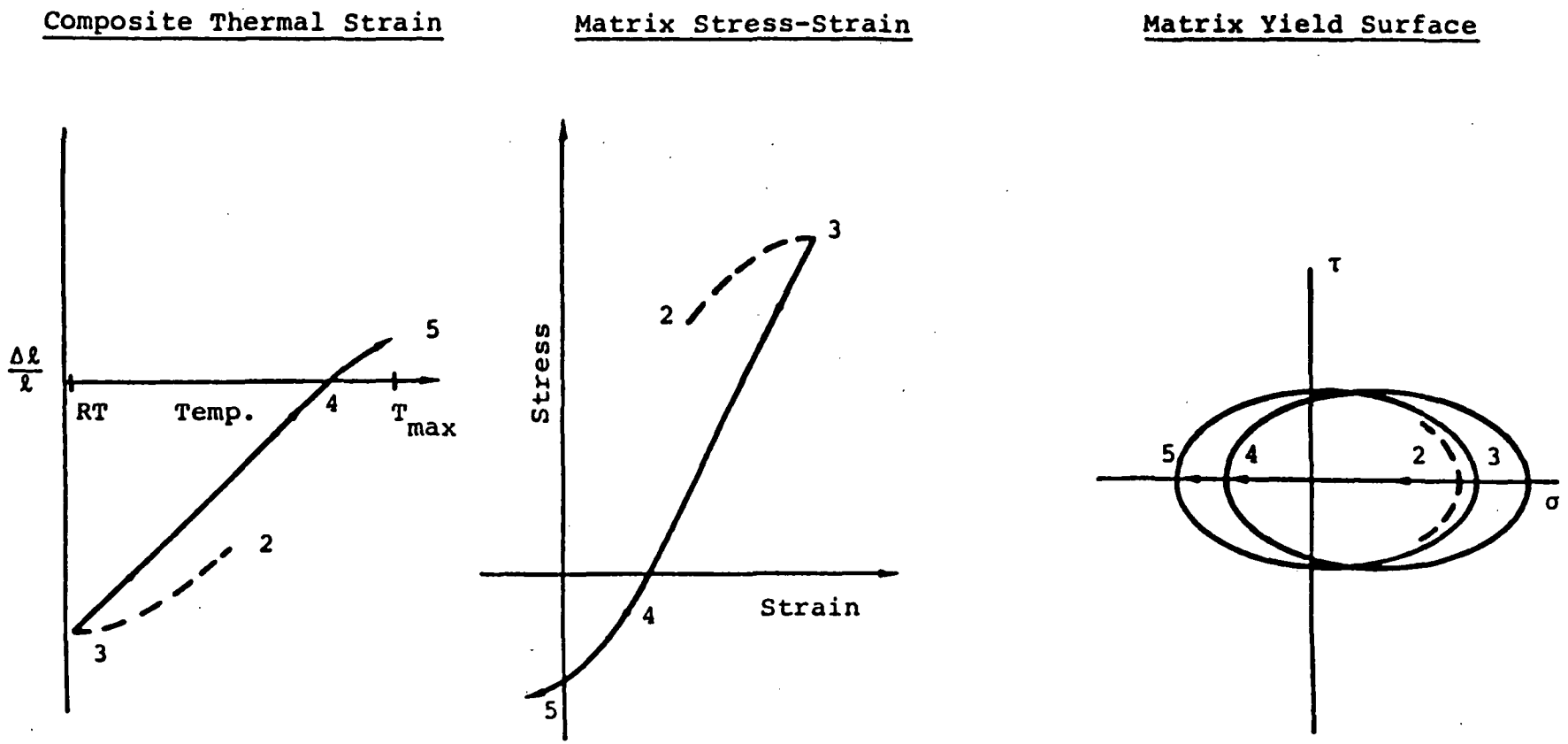

Figure 3. Nonlinear Behavior of Graphite Metal Matrix Composites and Matrix Due to Thermal Cycles. As composite is heated from room temperature matrix unloads elastically until it yields in compression. Yielding causes nonlinear thermal strain and matrix yield surface shifts again.

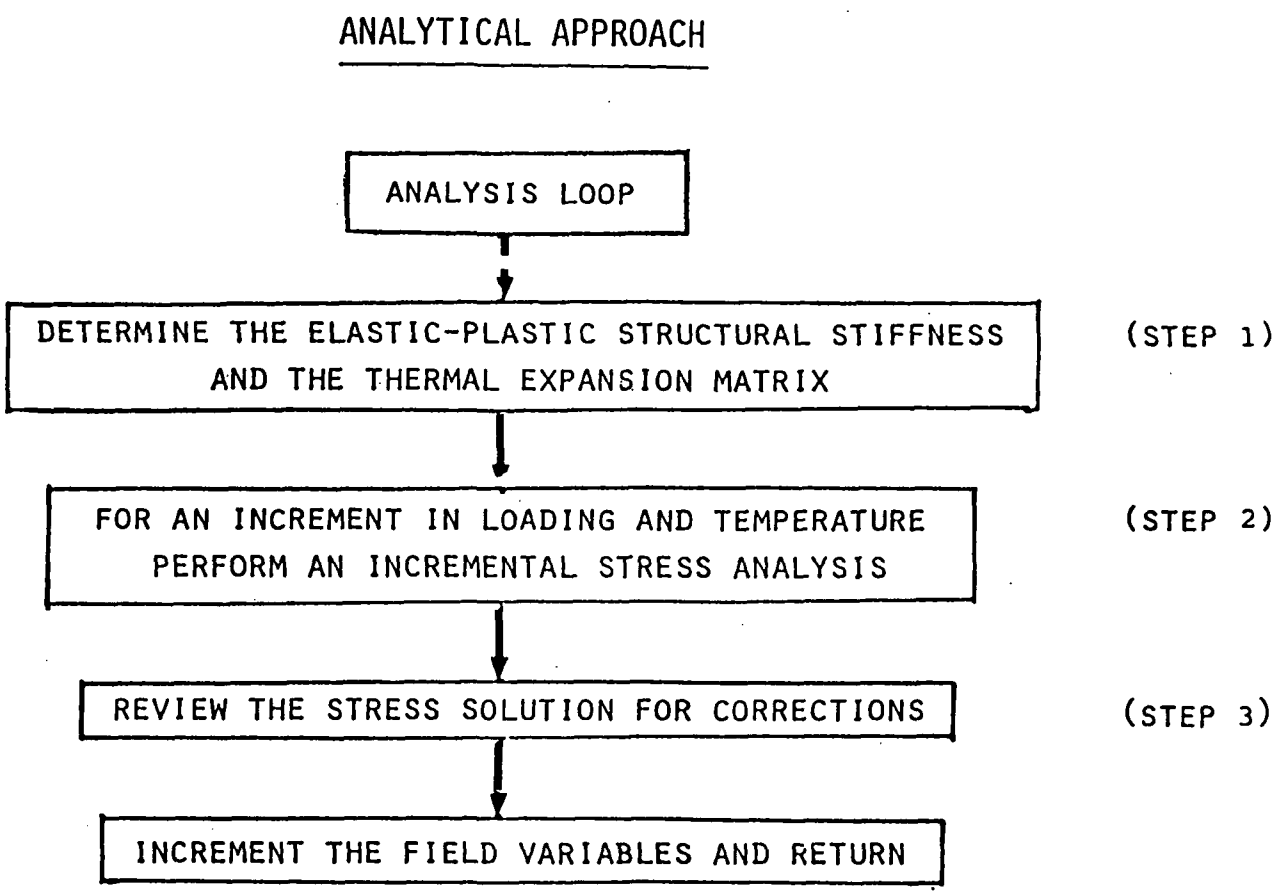

Figure 4. Flow Chart Showing Overall Approach To Incremental Laminate Analysis.

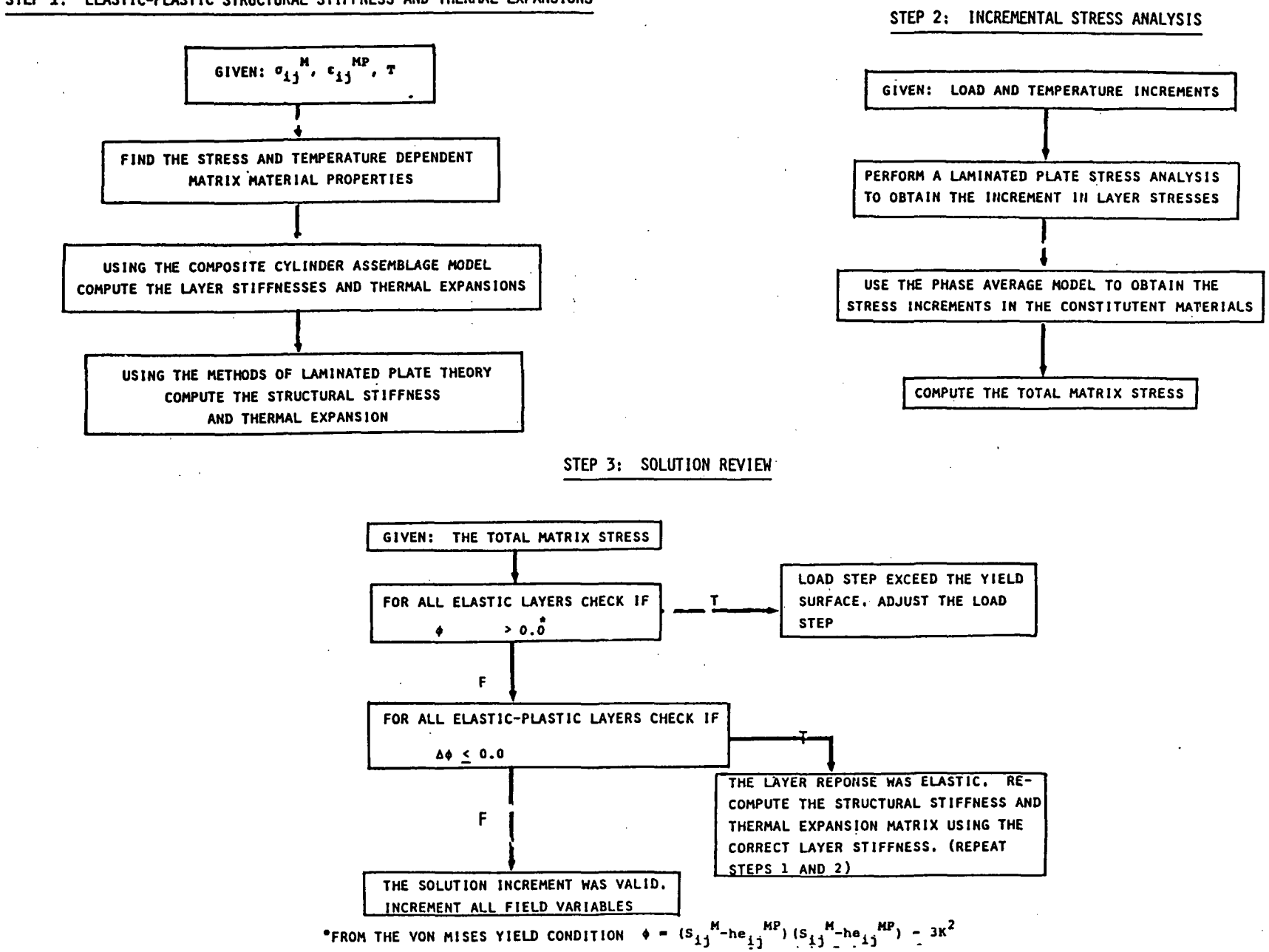

Figure 5. Detailed Flow Chart of Incremental Laminate Analysis.

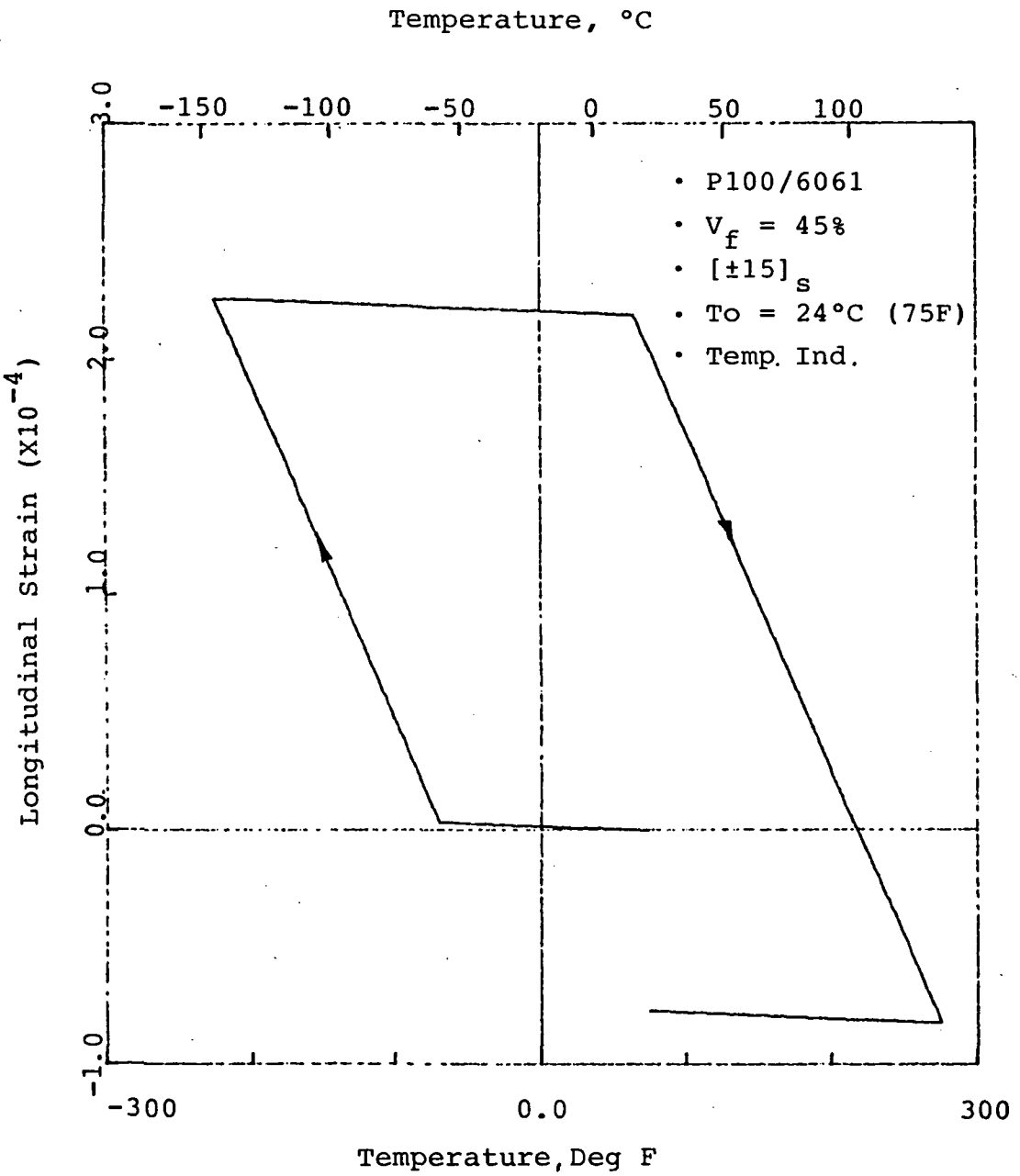

Figure 6. Computed Longitudinal Strain versus Temperature for a $[\pm 15]_s$ P100/6061 Laminate

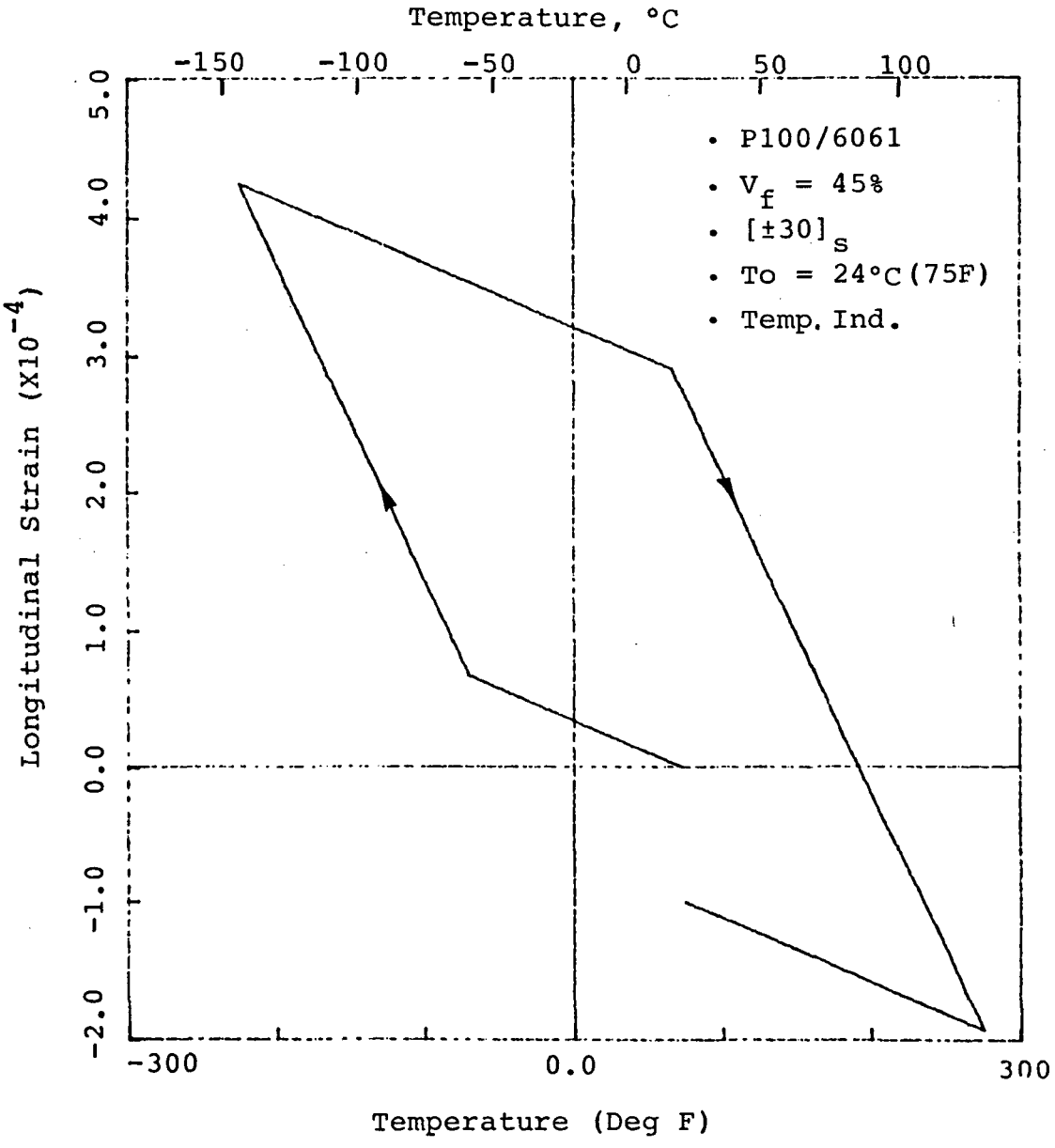

Figure 7. Computed Longitudinal Strain versus Temperature for a $[\pm 30]_s$ P100/6061 Laminate

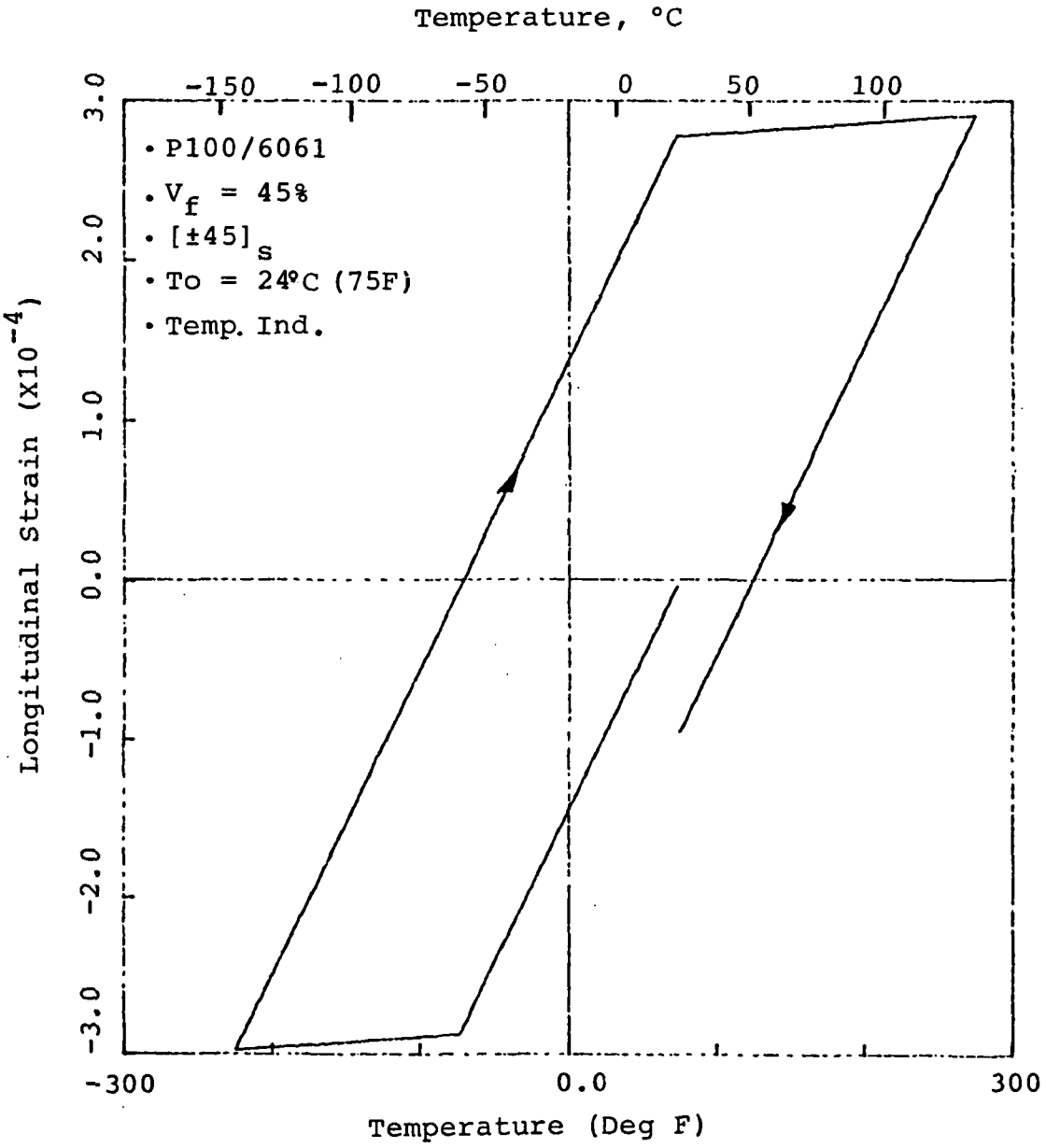

Figure 8. Computed Longitudinal Strain versus Temperature for a $[\pm 45]_s$ P100/6061 Laminate

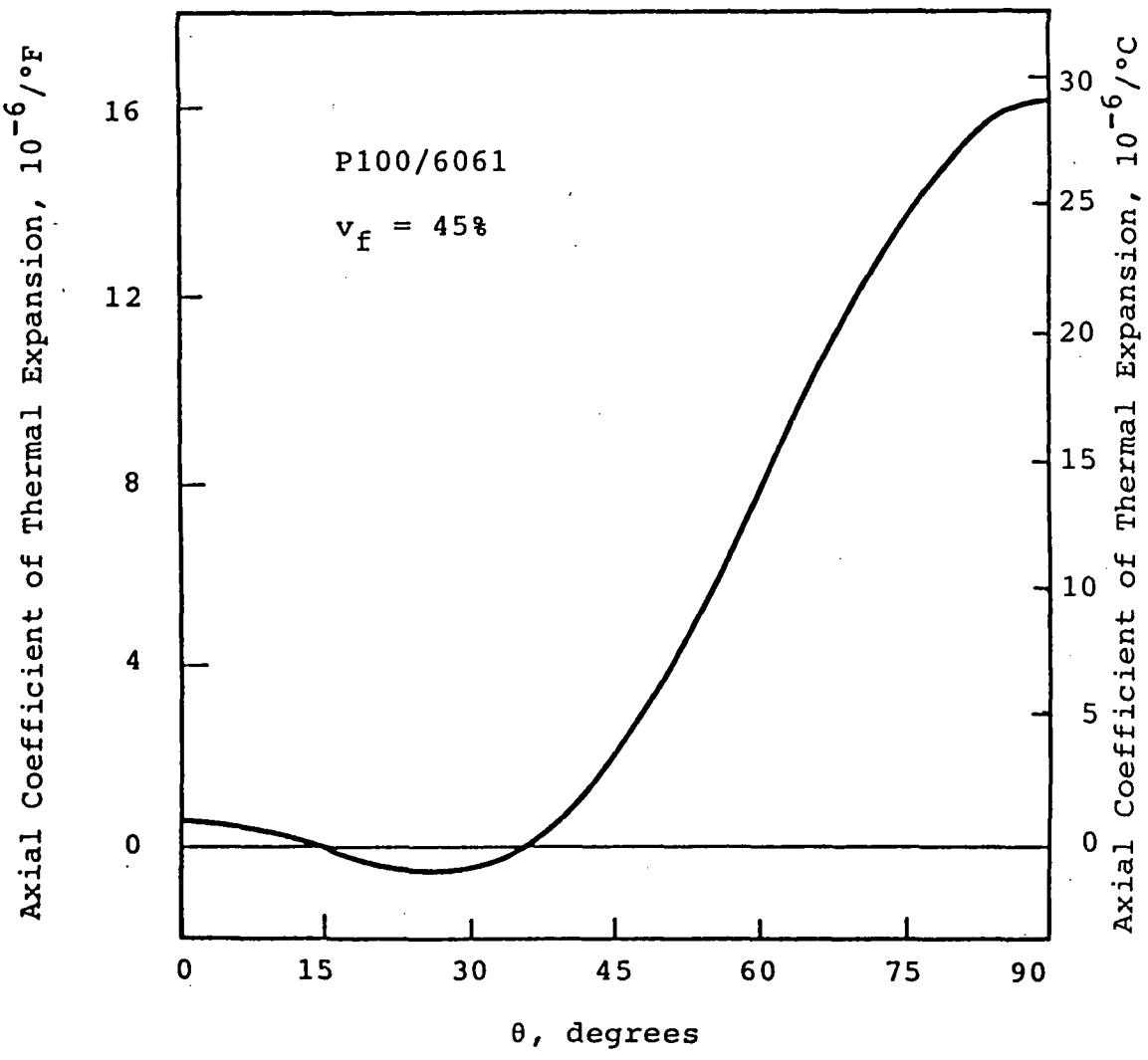

Figure 9. Axial Coefficient of Thermal Expansion versus Ply Angle for Balanced Symmetric Laminates

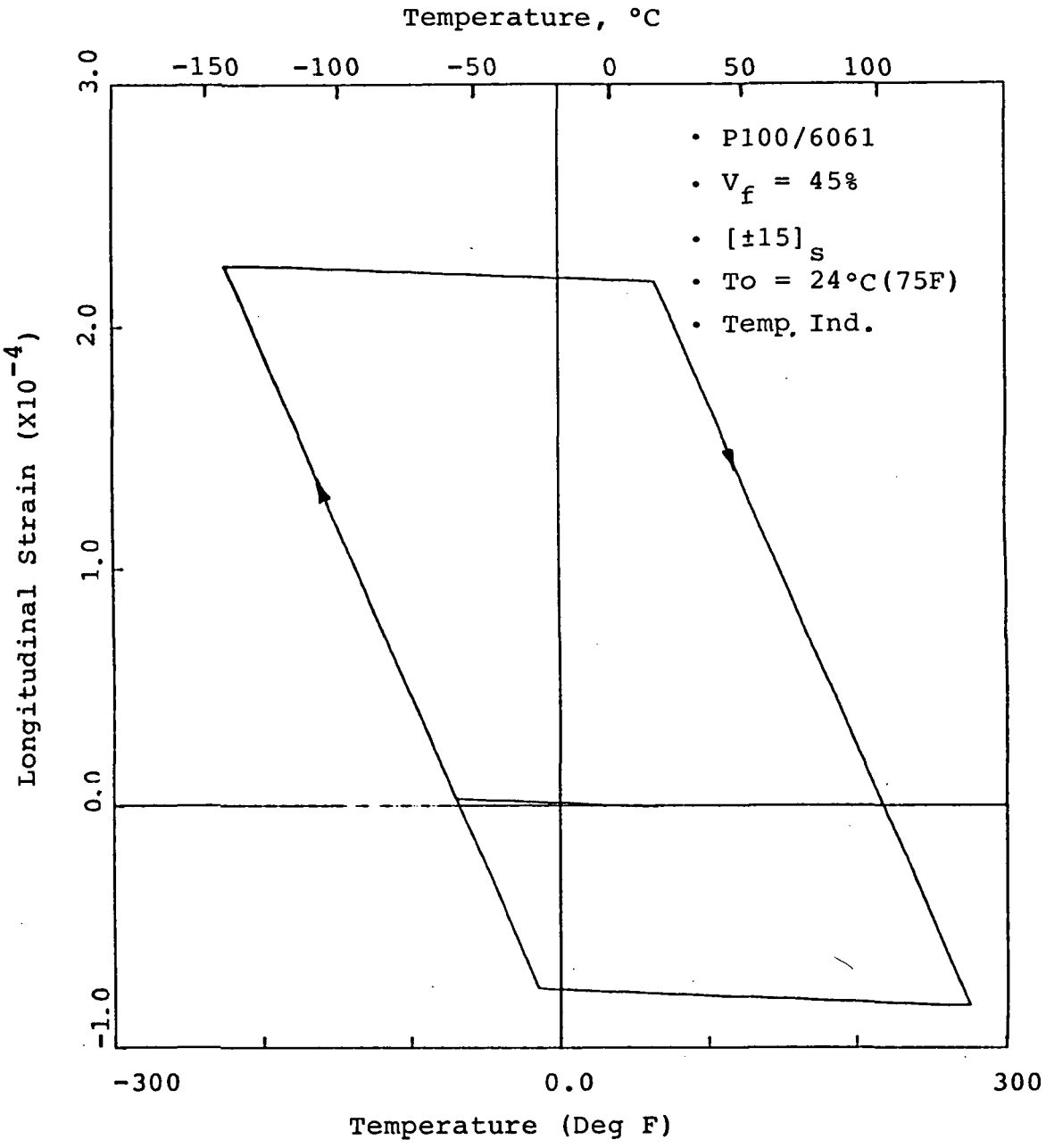

Figure 10. Computed Longitudinal Strain versus Temperature for a $[\pm 15]_s$ P100/6061 Laminate Subjected to Two Thermal Cycles (Temperature Independent)

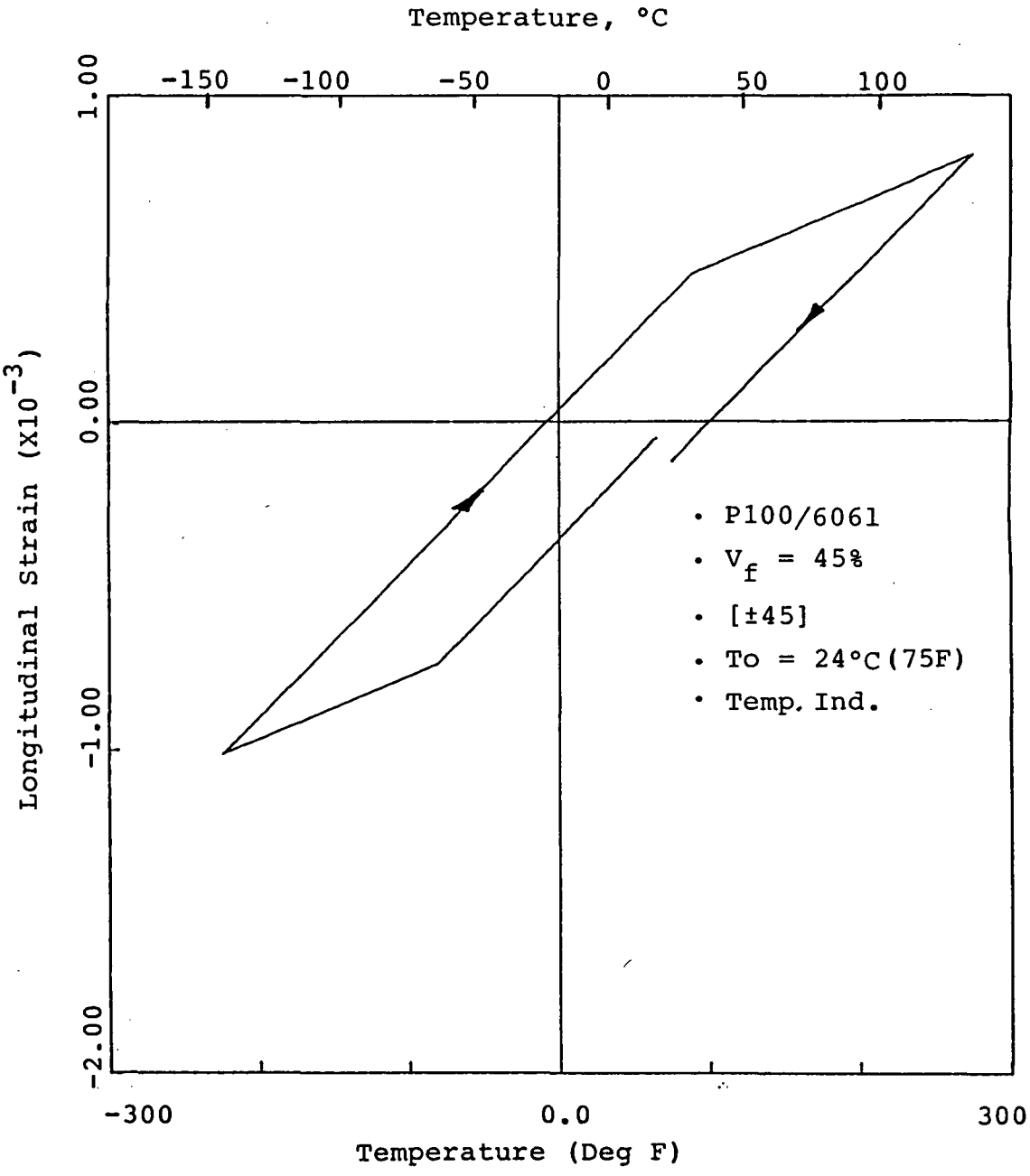

Figure 11. Computed Longitudinal Strain versus Temperature for a [±45] Unsymmetric P100/6061 Laminate

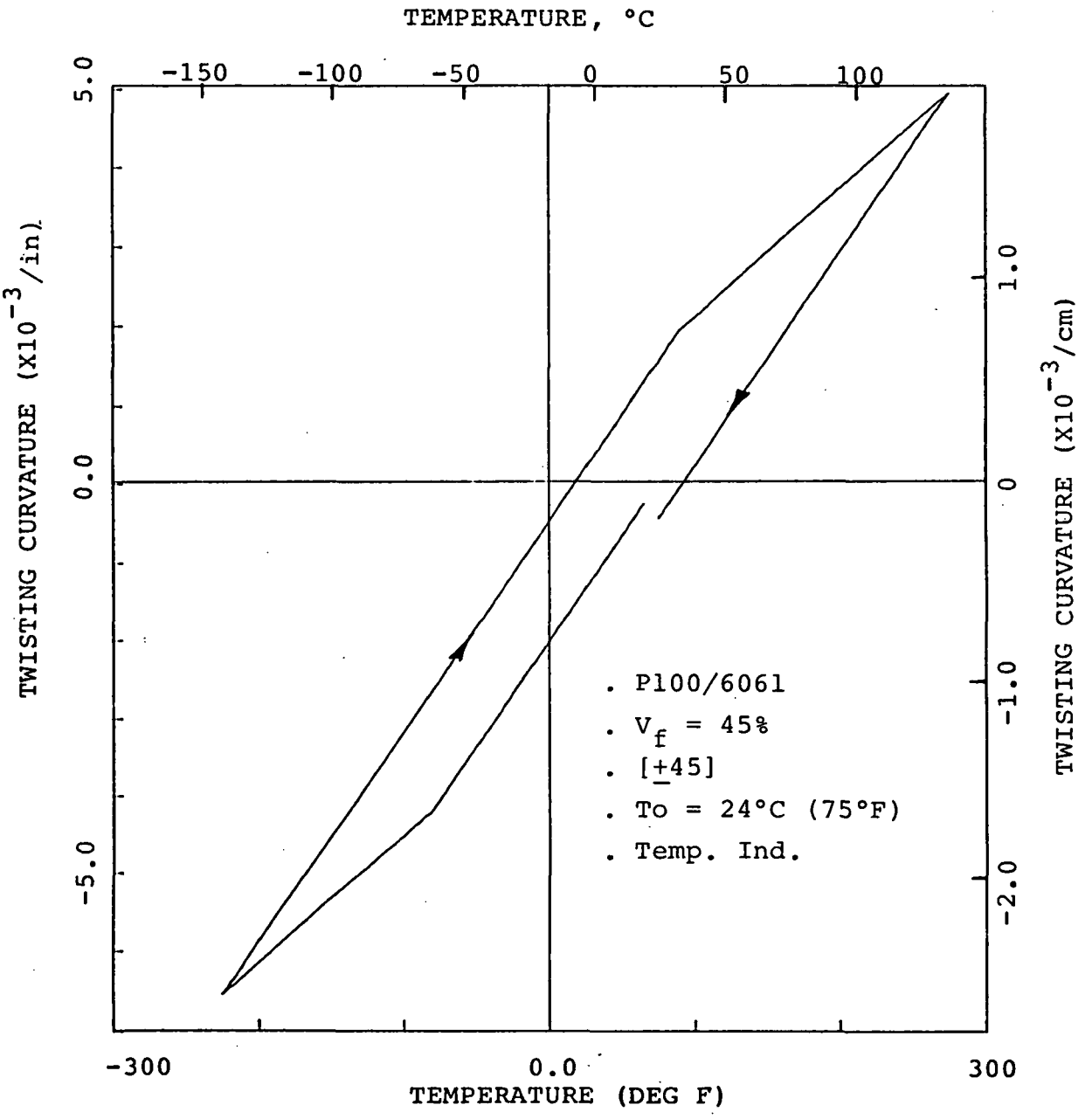

Figure 12. Computed Twisting Curvatures versus Temperature for a [±45] Unsymmetric P100/6061 Laminate

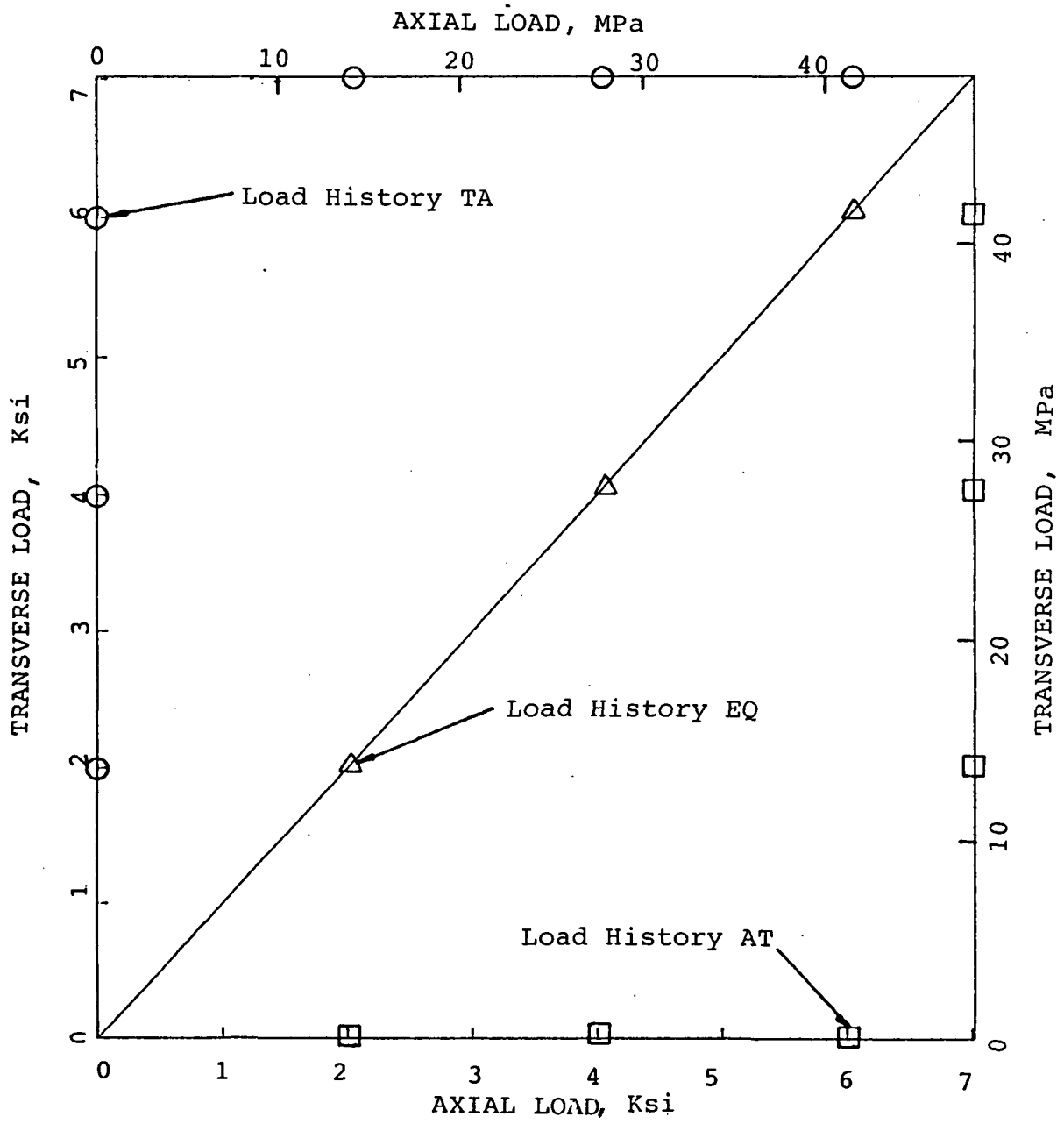

Figure 13. Mechanical Load Histories Used to Show Path Dependence of Nonlinear Solution

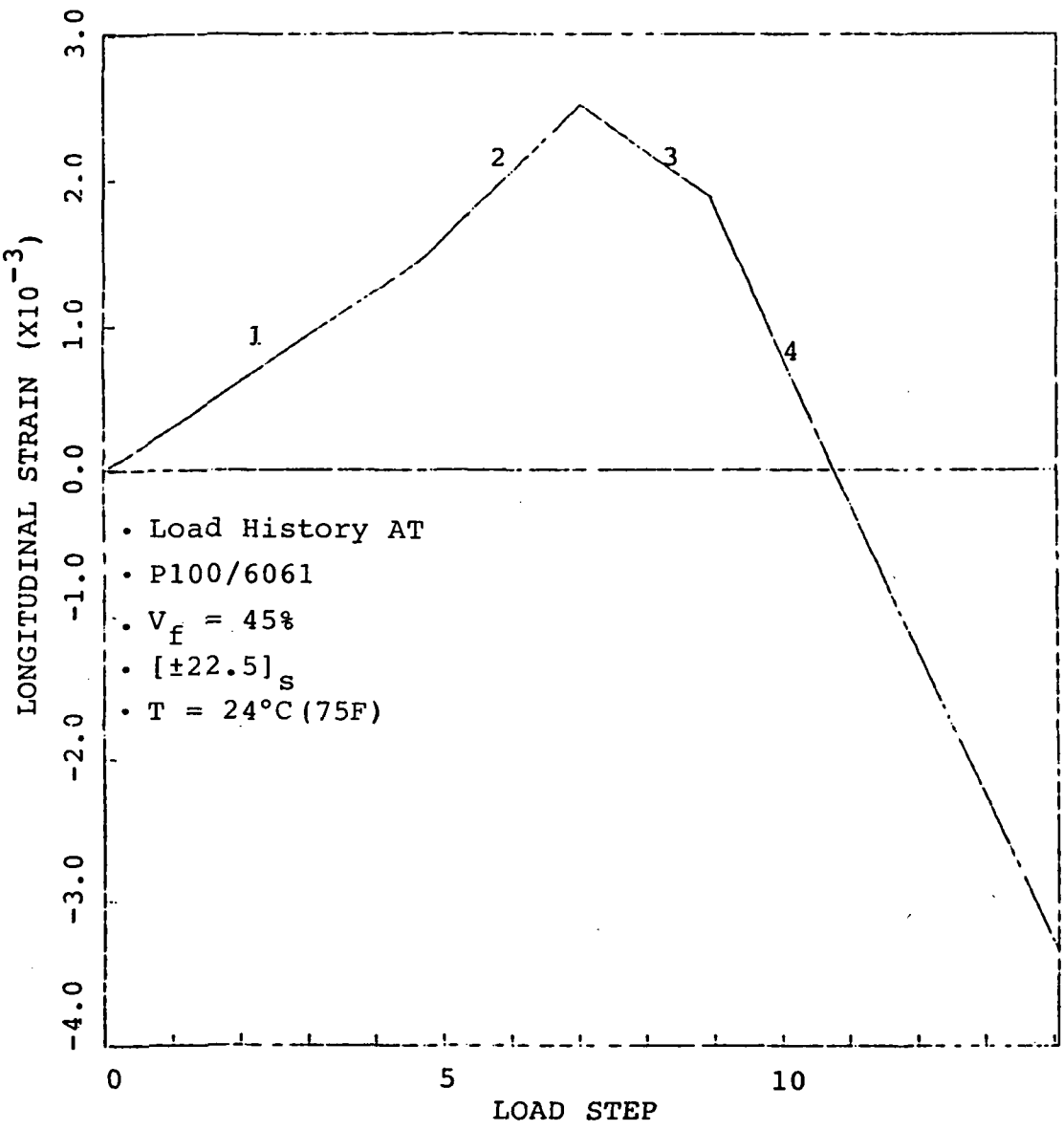

igure 14. Computed Longitudinal Laminate Strain versus Load Step for [±22.5], P100/6061 Laminate Subjected to Load History AT

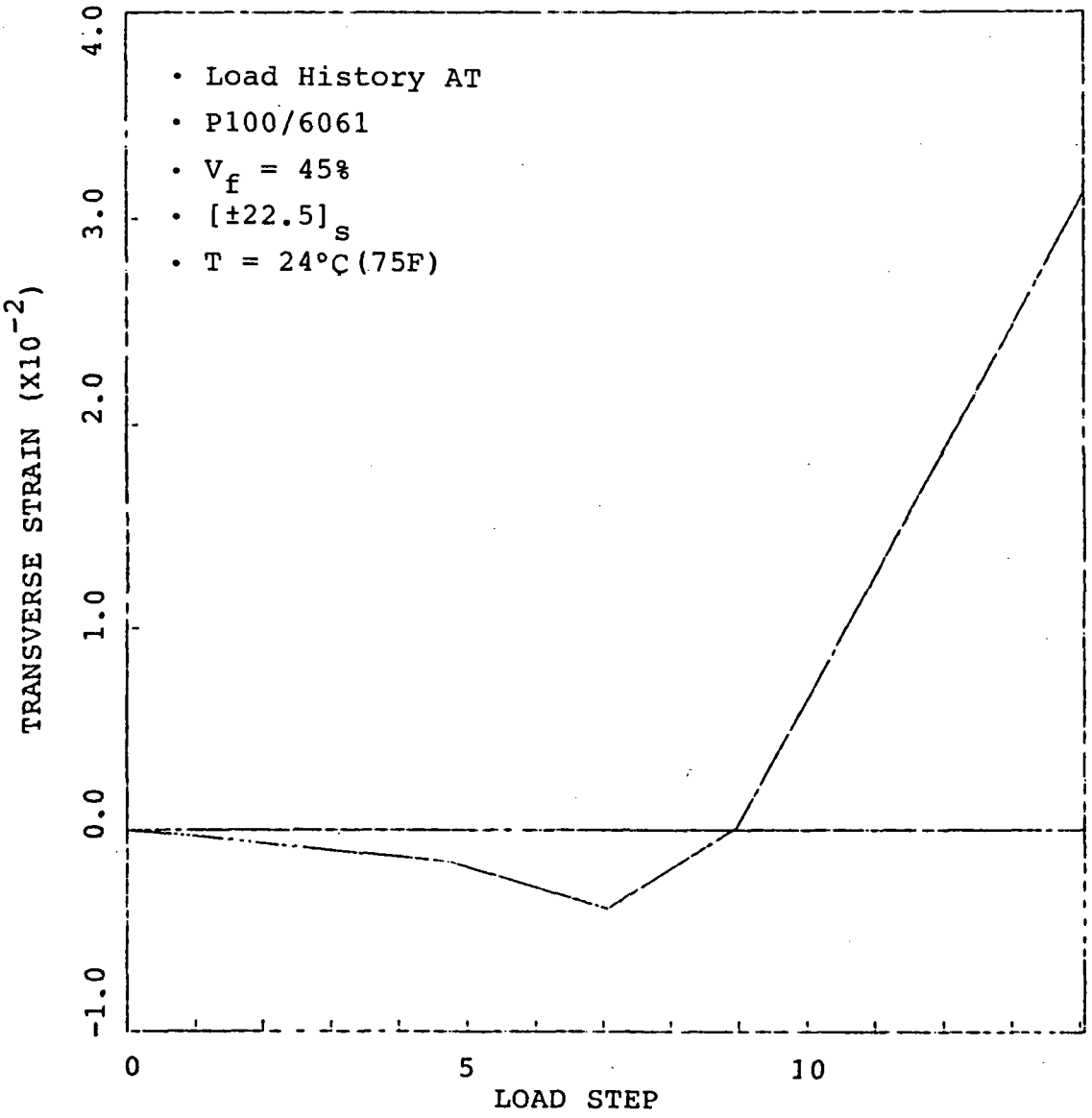

Figure 15. Computed Transverse Laminate Strain versus Load Step for a $[\pm 22.5]_s$ P100/6061 Laminate Subjected to Load History AT

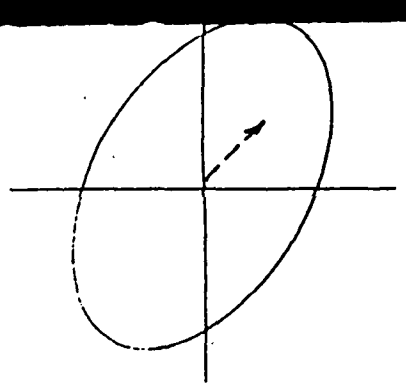

PHASE 1 ELASTIC RESPONSE
(AXIAL LOAD INCREMENTS)

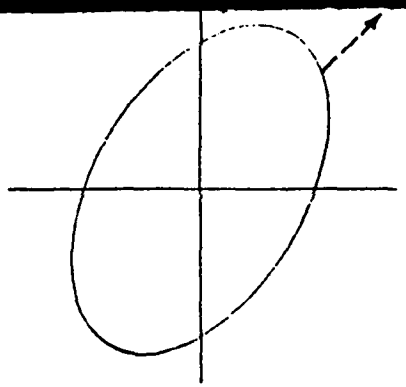

PHASE 2 ELASTIC-PLASTIC RESPONSE
(AXIAL LOAD INCREMENTS)

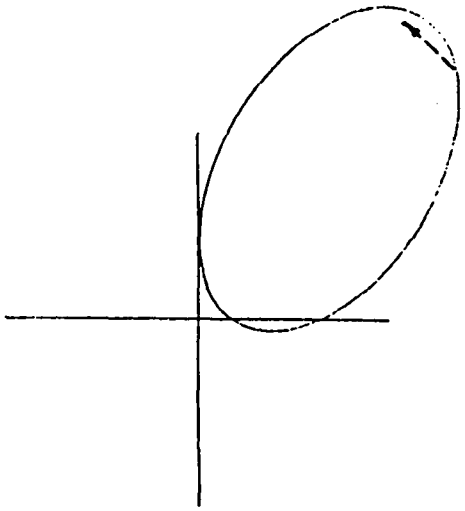

PHASE 3 ELASTIC RESPONSE
(TRANSVERSE LOAD INCREMENTS)

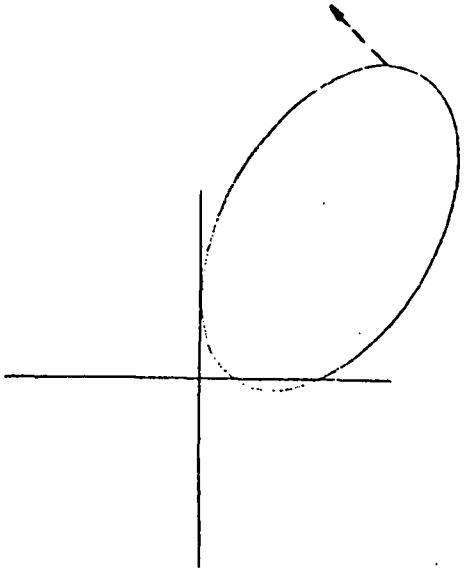

PHASE 4 ELASTIC-PLASTIC RESPONSE
(TRANSVERSE LOAD INCREMENTS)

Figure 16. Schematic Diagram Showing Motion of Matrix Stress Point and Yield Surface in $[\pm 22.5]_s$ P100/6061 Laminate Subjected to Load History AT

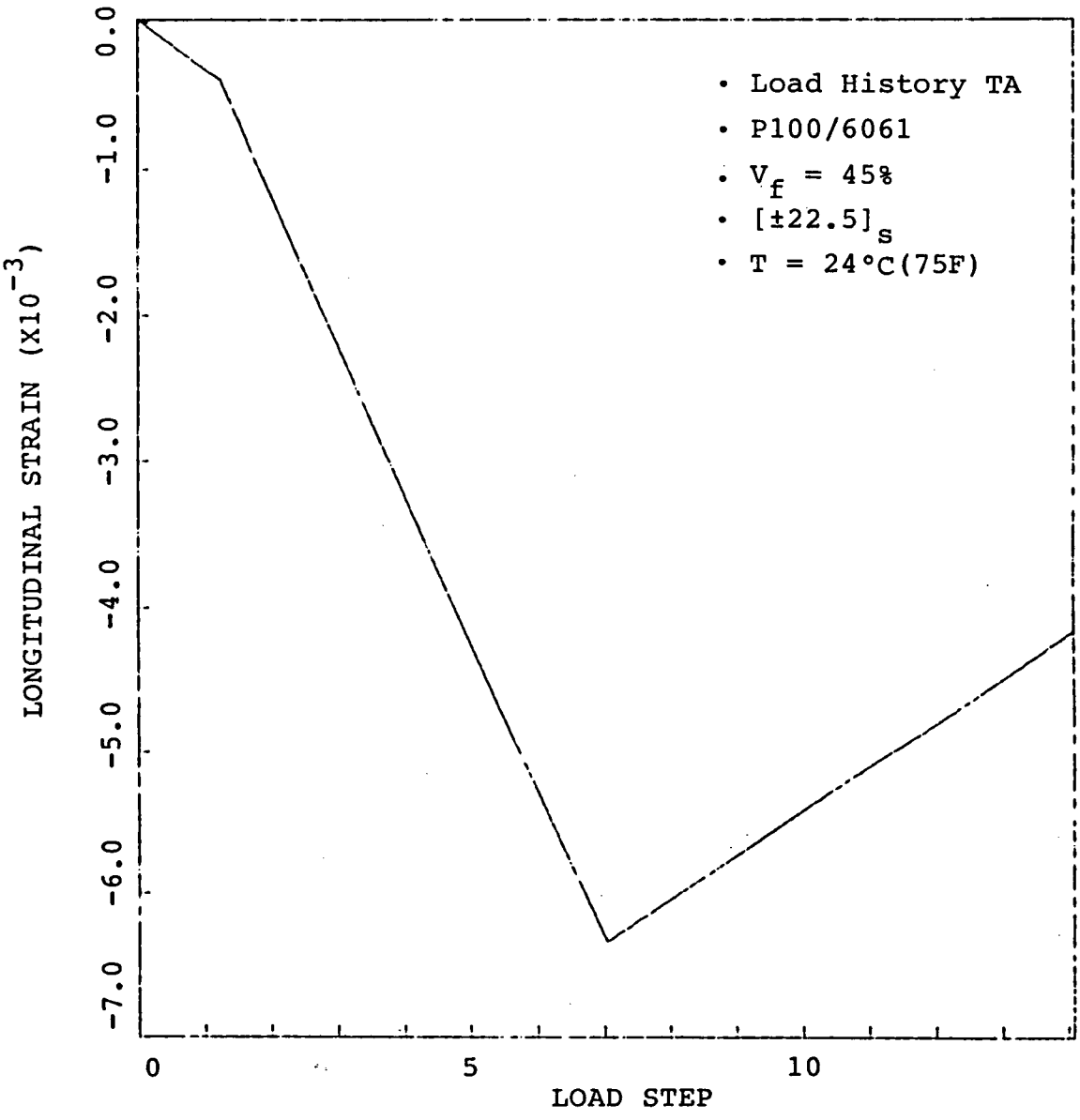

Figure 17. Computed Longitudinal Laminate Strain versus Load Step for a $[\pm 22.5]_s$ P100/6061 Laminate Subjected to Load History TA

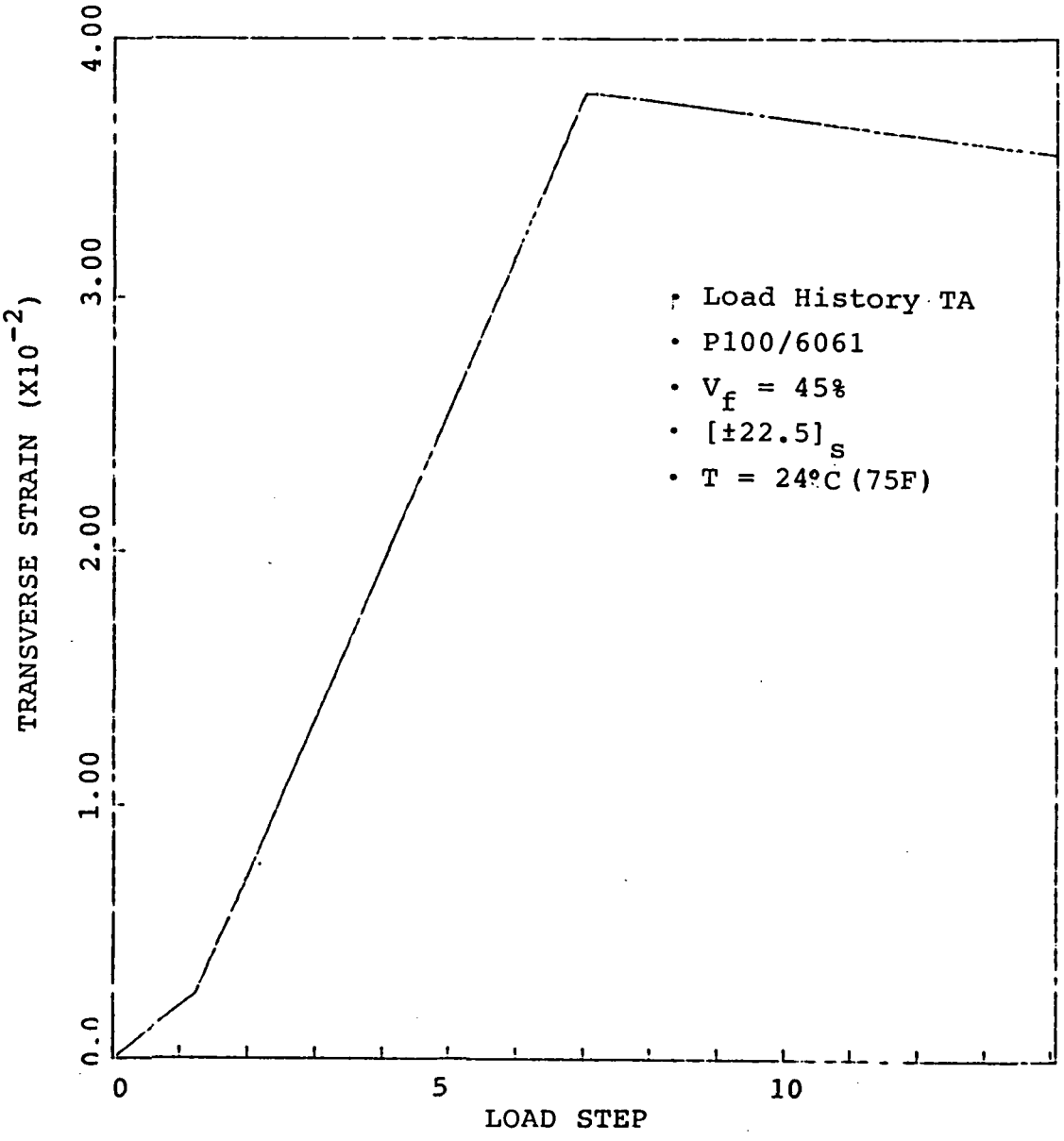

Figure 18. Computed Transverse Laminate Strain versus Load Step for a $[\pm 22.5]_s$ P100/6061 Laminate Subjected to Load History TA

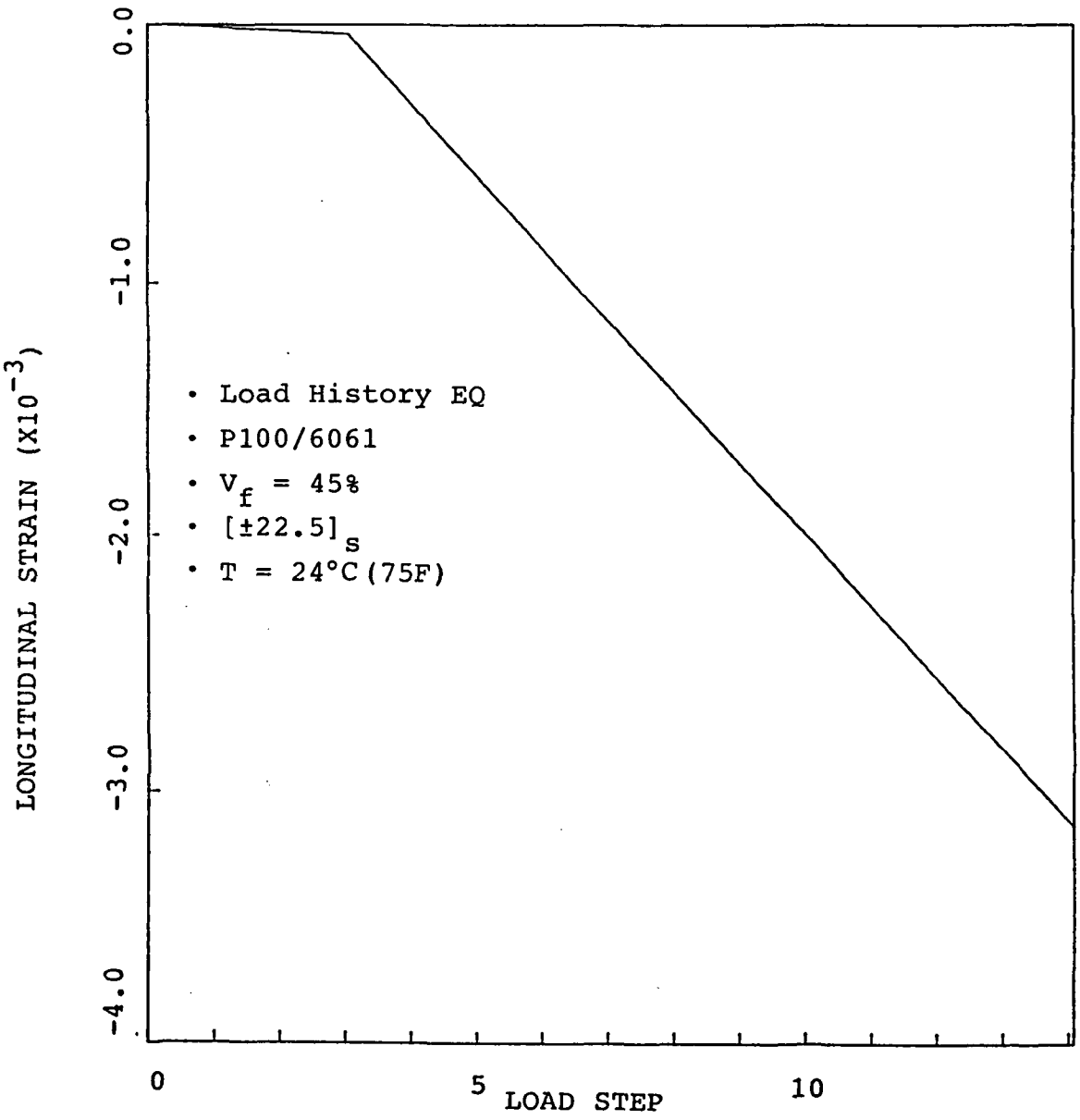

Figure 19. Computed Longitudinal Laminate Strains versus Load Step for a $[\pm 22.5]_s$ P100/6061 Laminate Subjected to Load History EQ

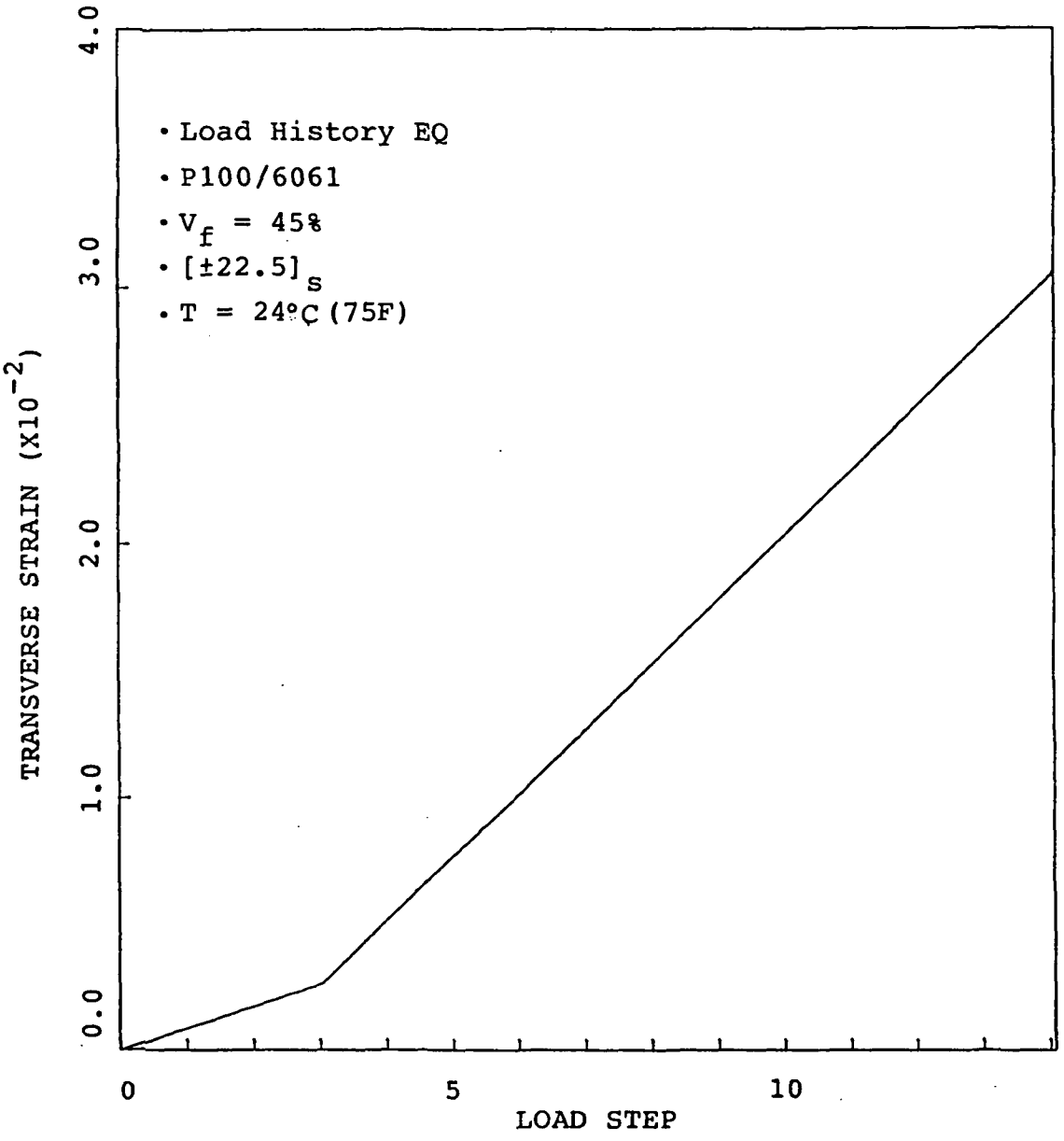

gure 20. Computed Transverse Laminate Strain versus Load Step for a $[\pm 22.5]_s$ P100/6061 Laminate Subjected to Load History EQ

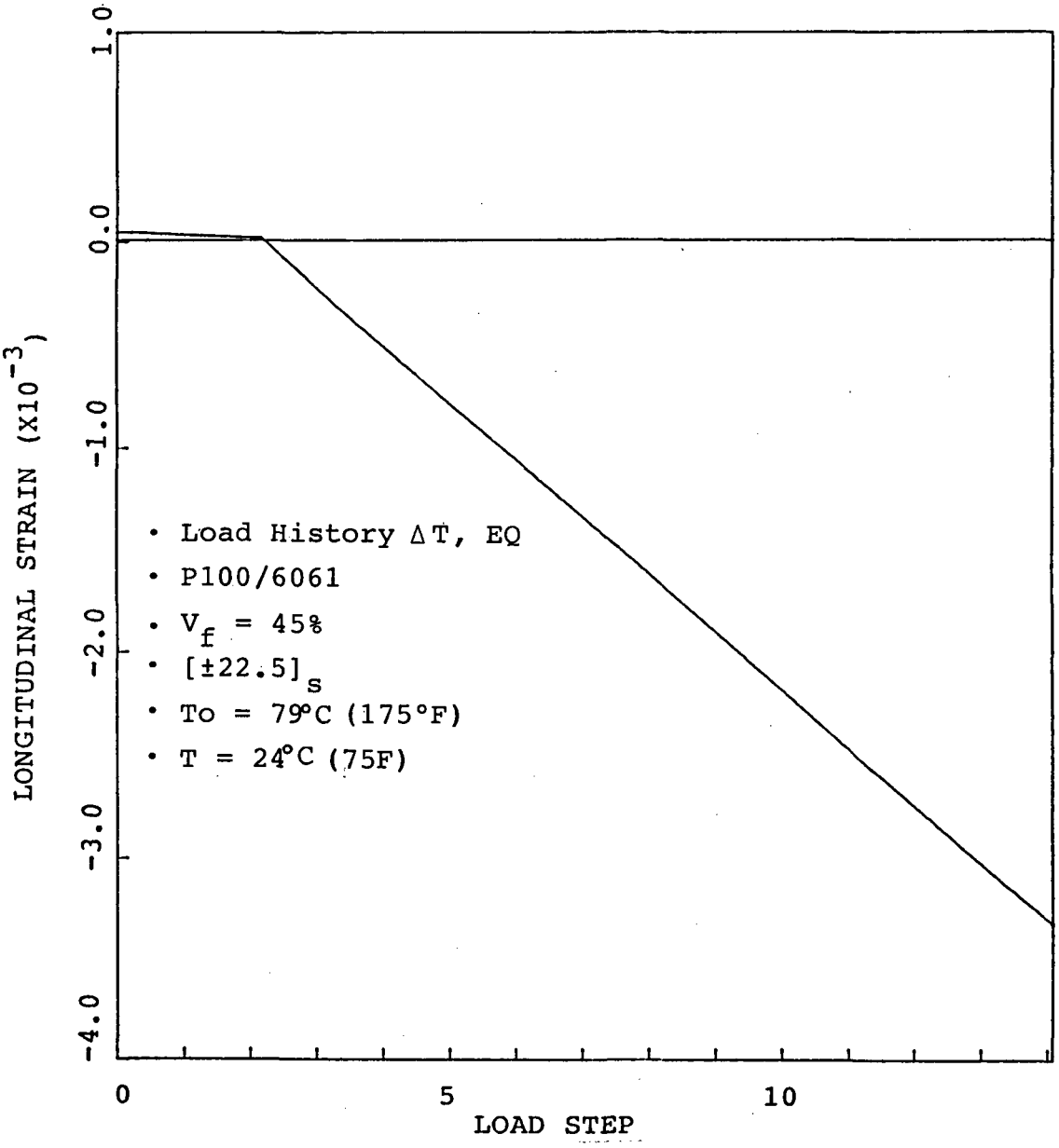

Figure 21. Computed Longitudinal Laminate Strains versus Load Step for $[\pm 22.5]_s$ P100/6061 Laminate Subjected to Cooldown followed by Load History EQ

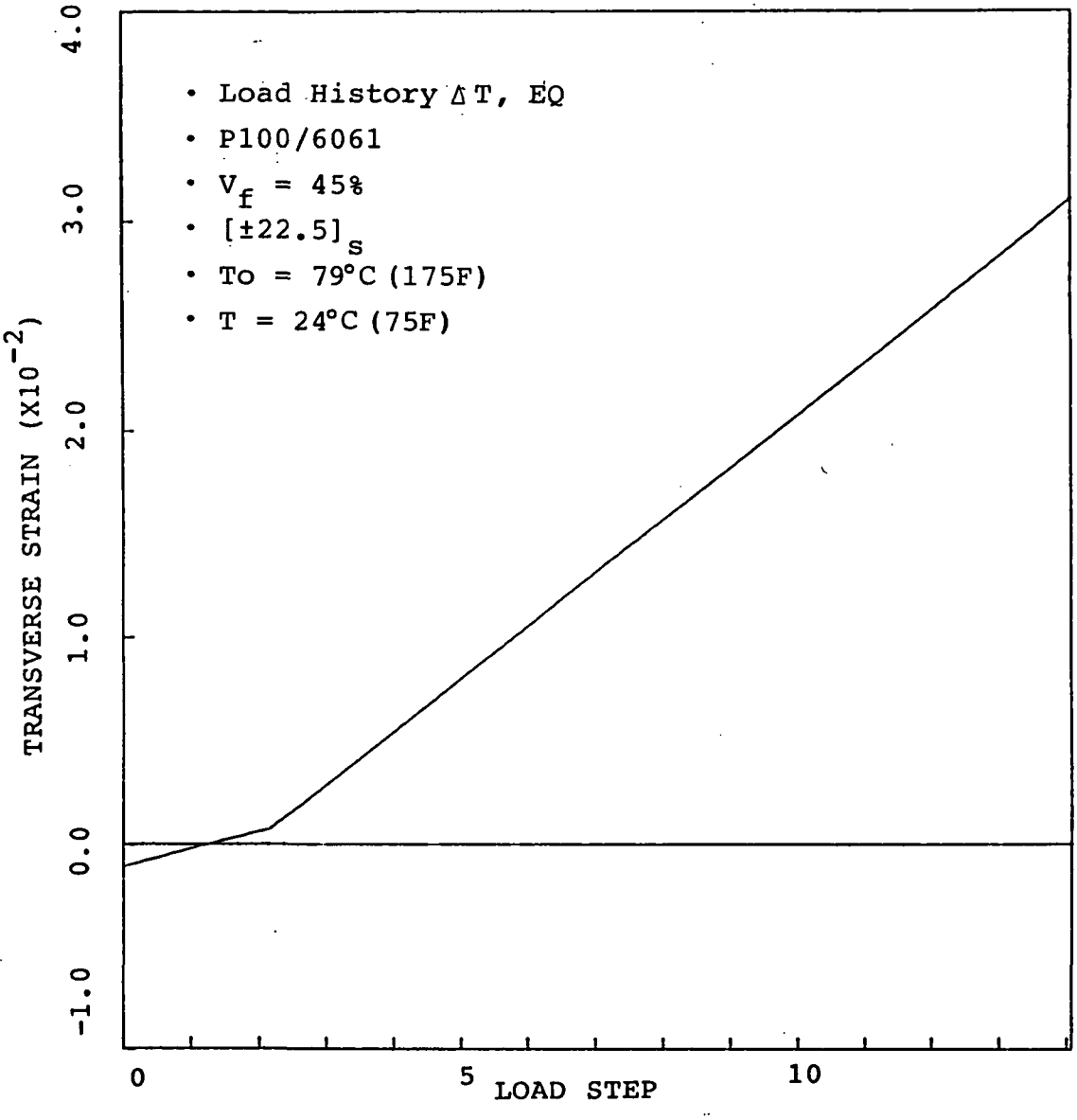

Figure 22. Computed Transverse Laminate Strain versus Load Step for a $[\pm 22.5]_s$ P100/6061 Laminate Subjected to Cooldown followed by Load History EQ

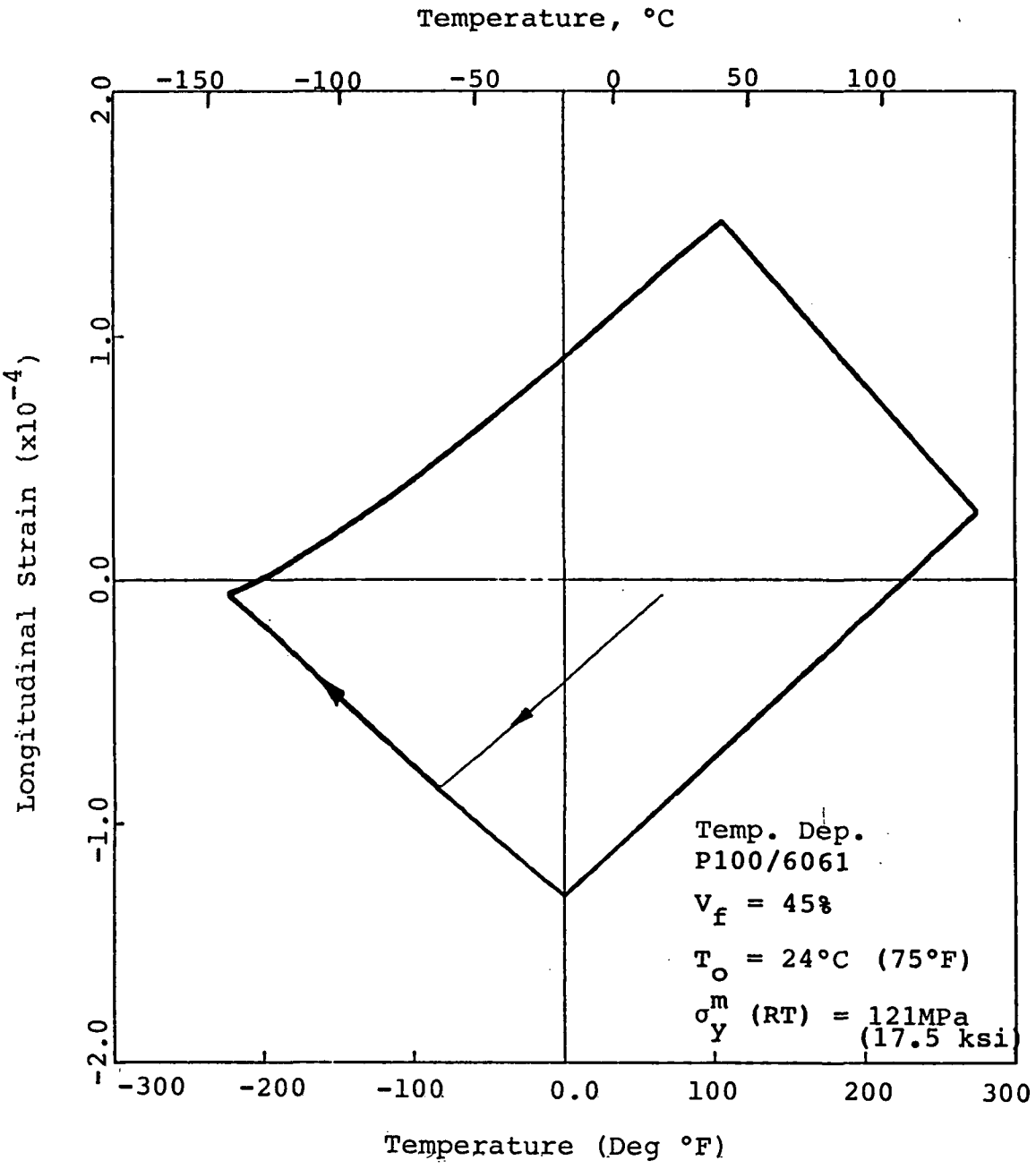

Figure 23. Computed Longitudinal Strain versus Temperature for a 0° P100/6061 Laminate

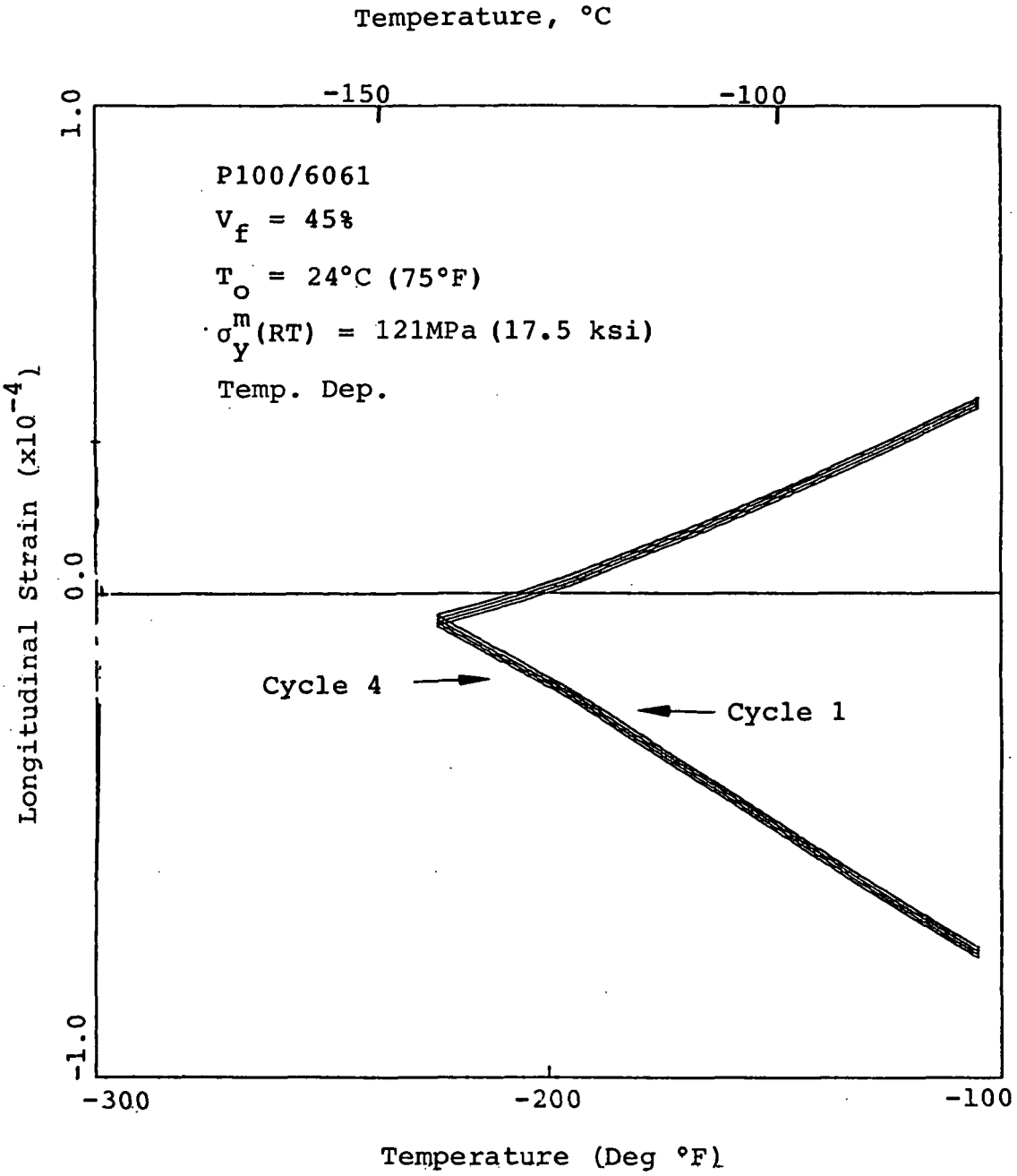

Figure 24. Exploded View of Low Temperature Region of Computed Strains versus Temperature for 0° P100/6061 Laminate

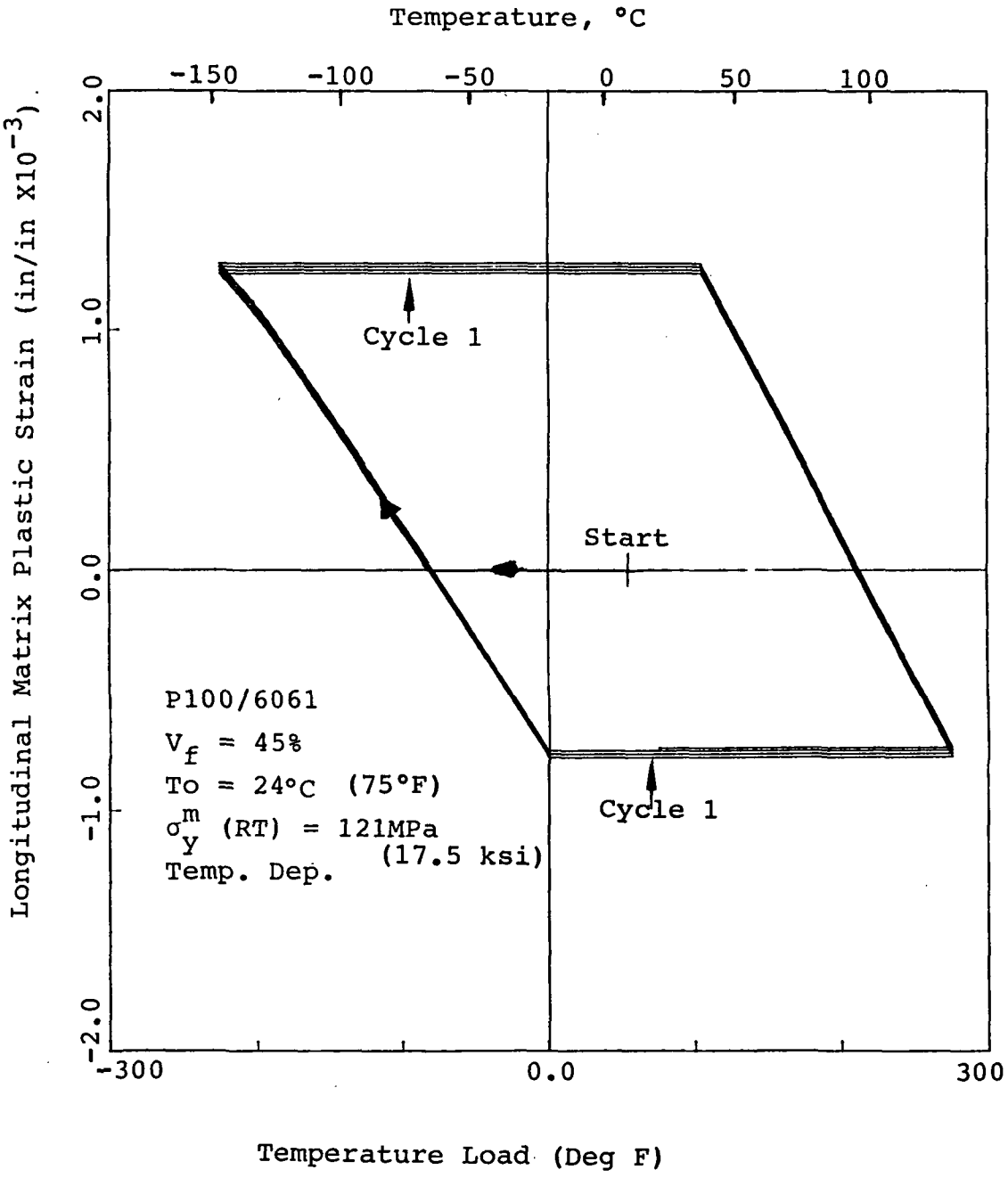

Figure 25. Computed Longitudinal Matrix Plastic Strain vs Temperature for a 0° P100/6061 Laminate

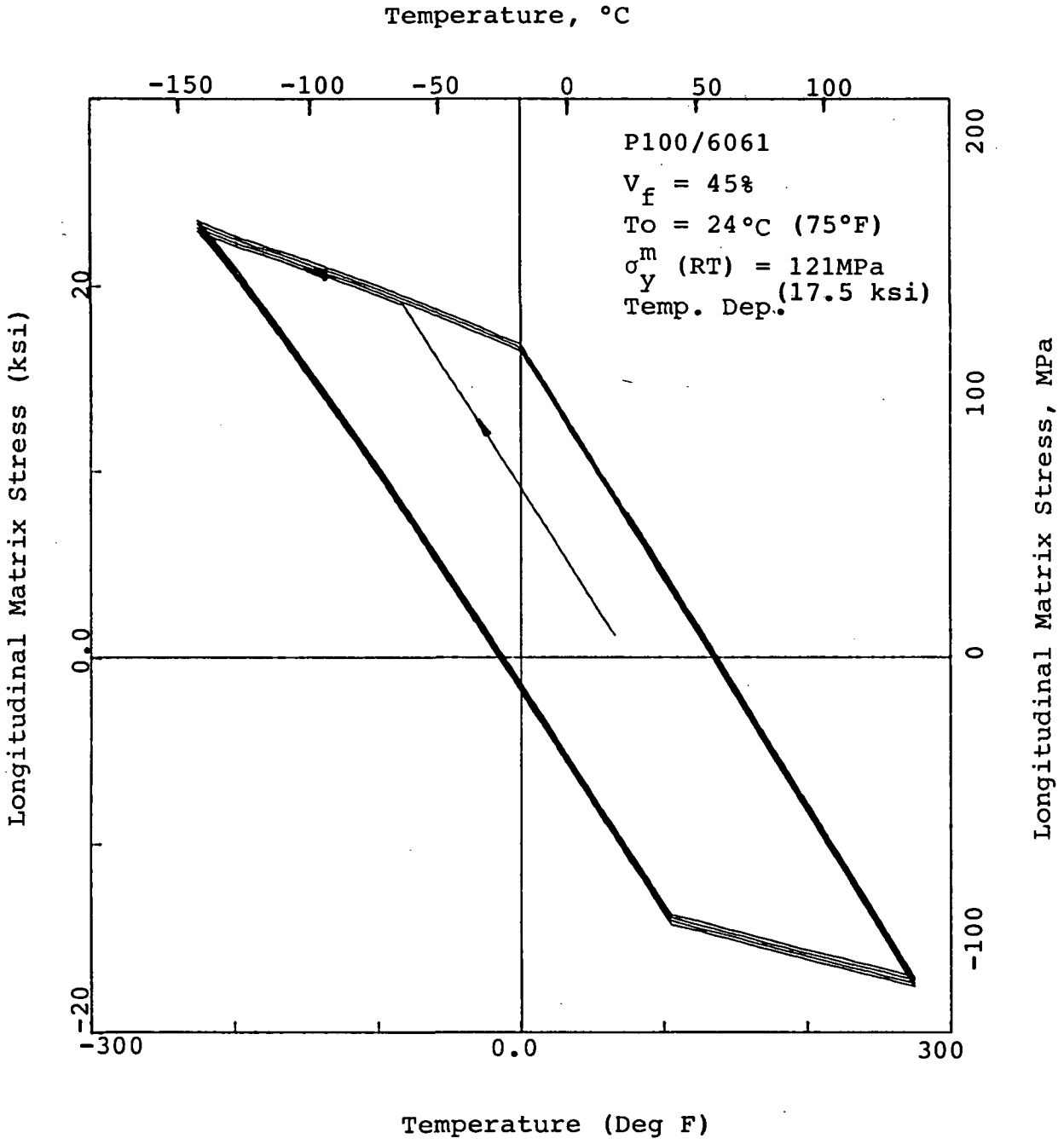

Figure 26. Computed Longitudinal Matrix Stress vs Temperature for a 0° P100/6061 Laminate

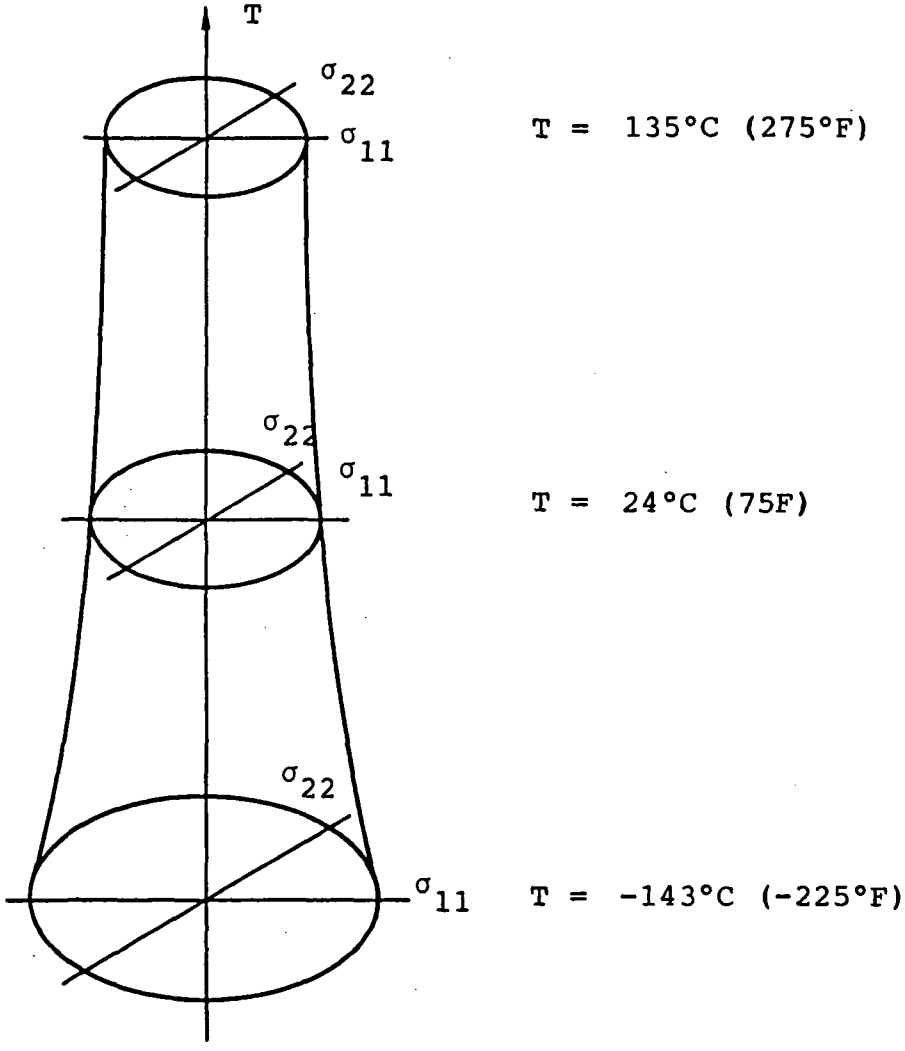

Figure 27. Schematic Diagram Showing Effect of Temperature Dependence on Matrix Yield Surface

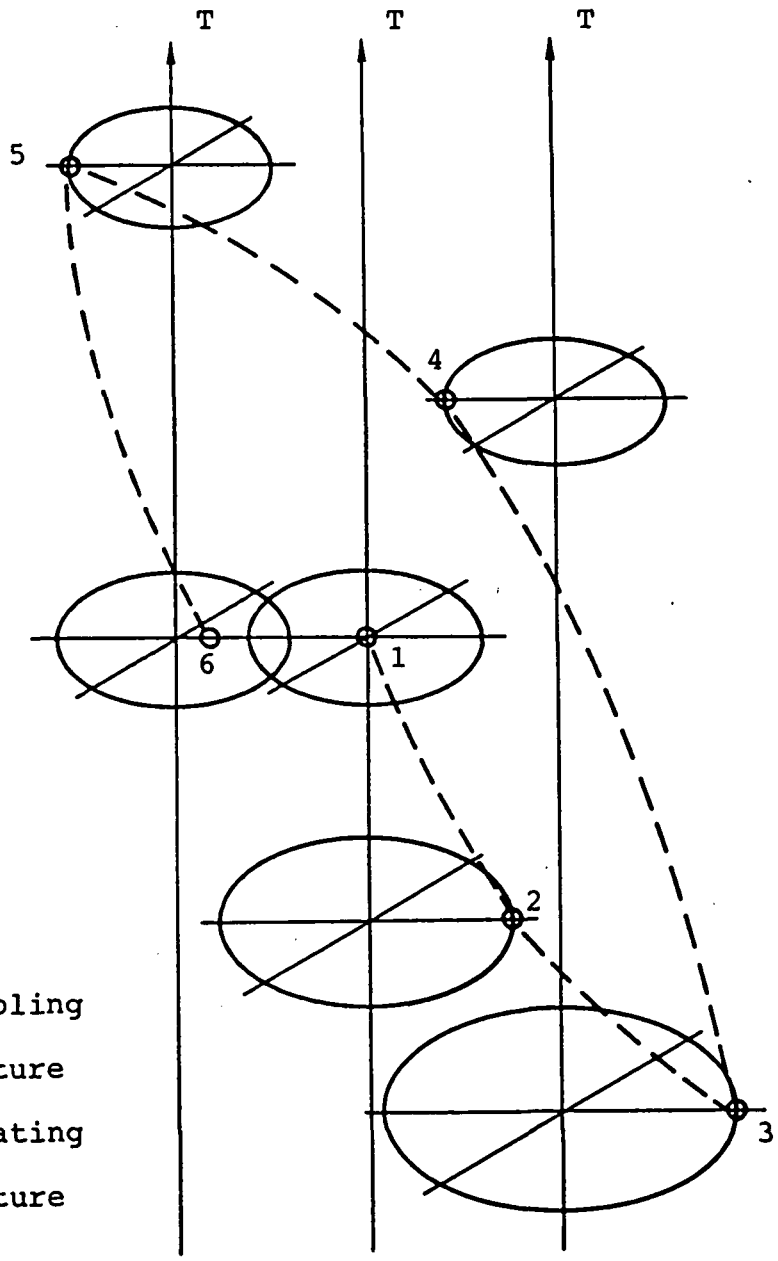

1. Initial State
2. Yield During Cooling
3. Minimum Temperature
4. Yield During Heating
5. Maximum Temperature
6. Final State

Figure 28. Schematic Diagram Showing Motion of Temperature Dependent Matrix Yield Surface During Thermal Cycle of Unidirectional Metal Matrix Layer

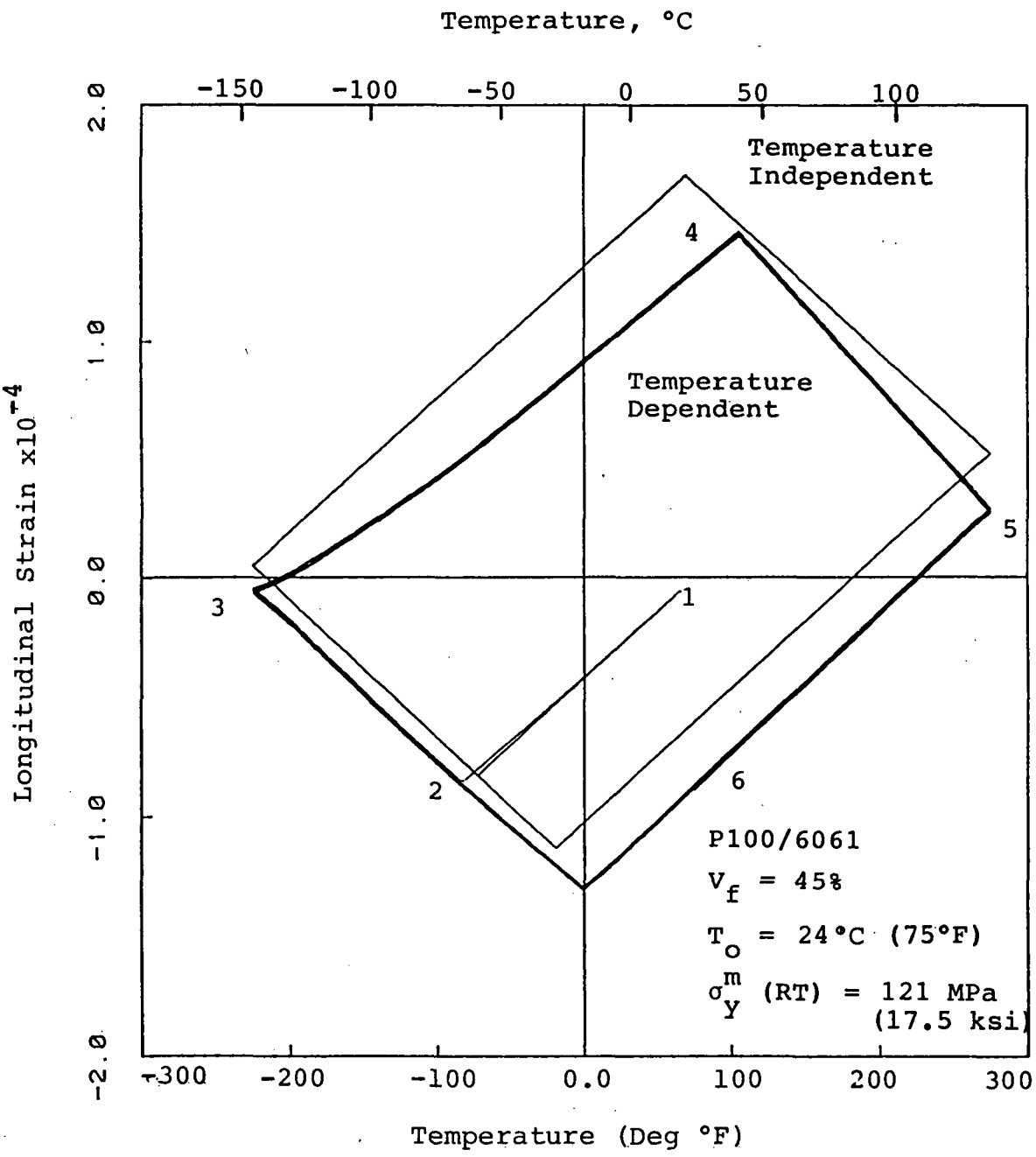

Figure 29. Comparison of Temperature Dependent versus Temperature Independent Solution for a 0° P100/6061 Laminate

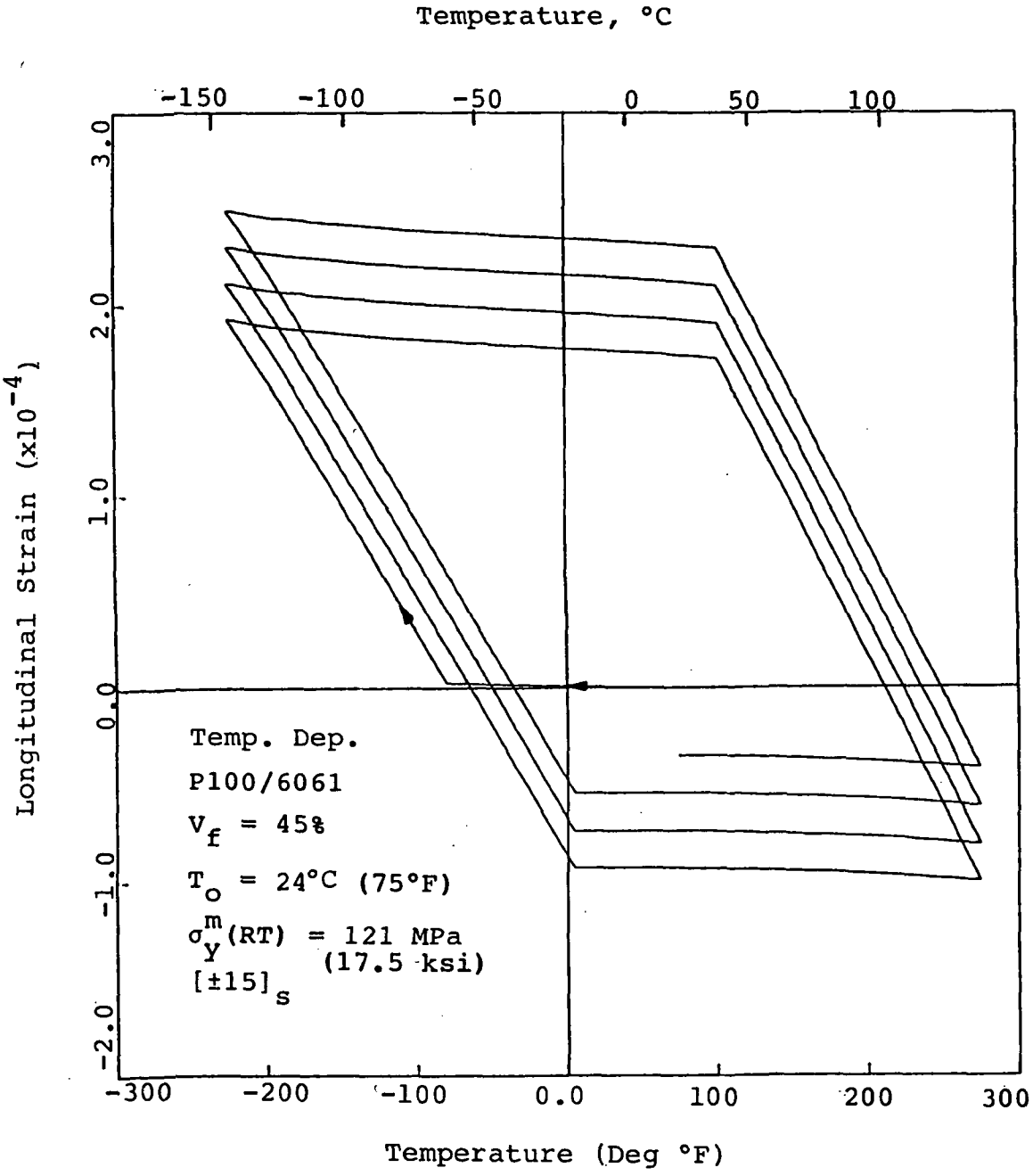

Figure 30. Computed Longitudinal Laminate Strain versus Temperature for a $[\pm 15]_s$ P100/6061 Laminate

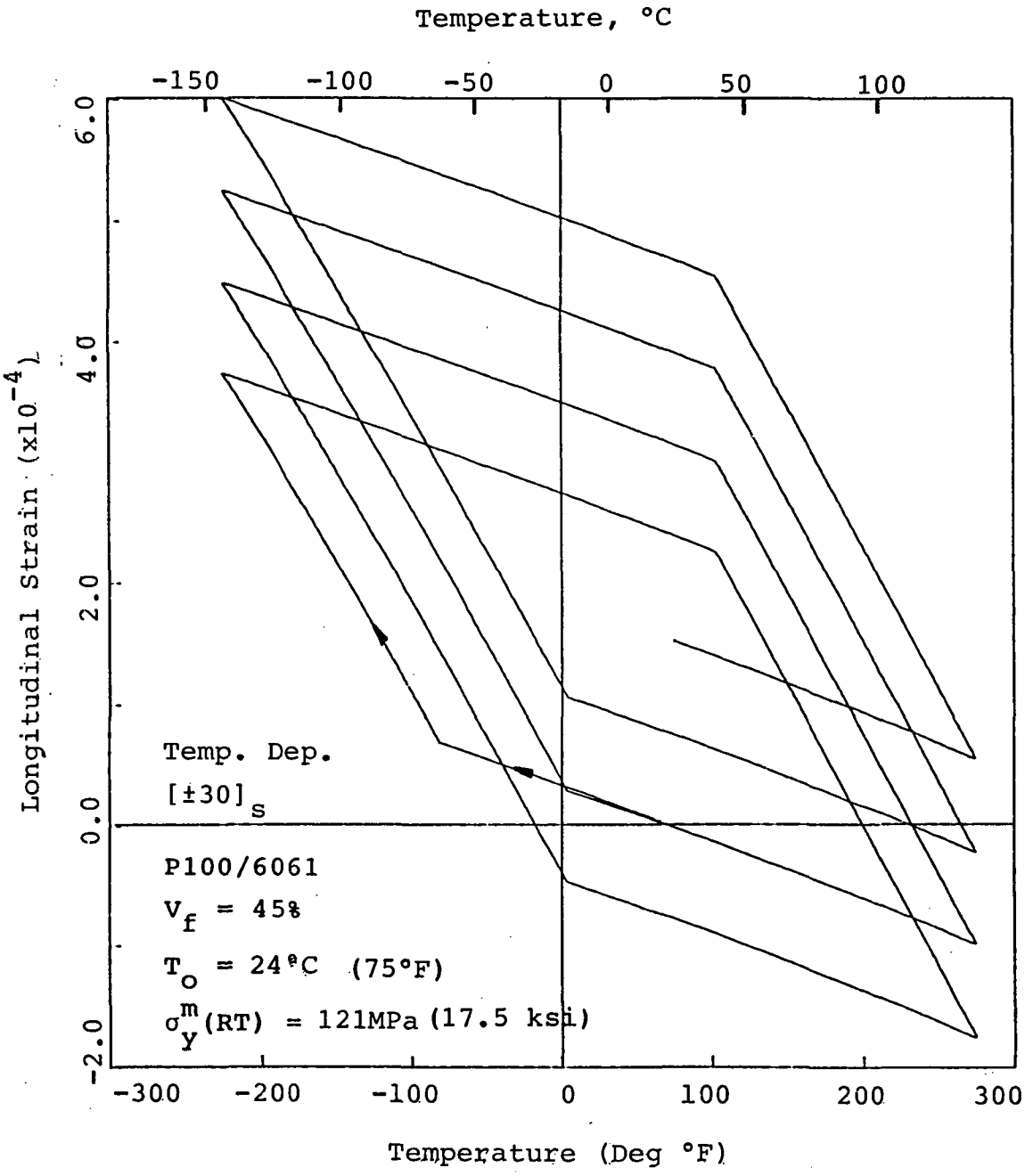

Figure 31. Computed Longitudinal Laminate Strain versus Temperature for a $[\pm 30]_s$ P100/6061 Laminate

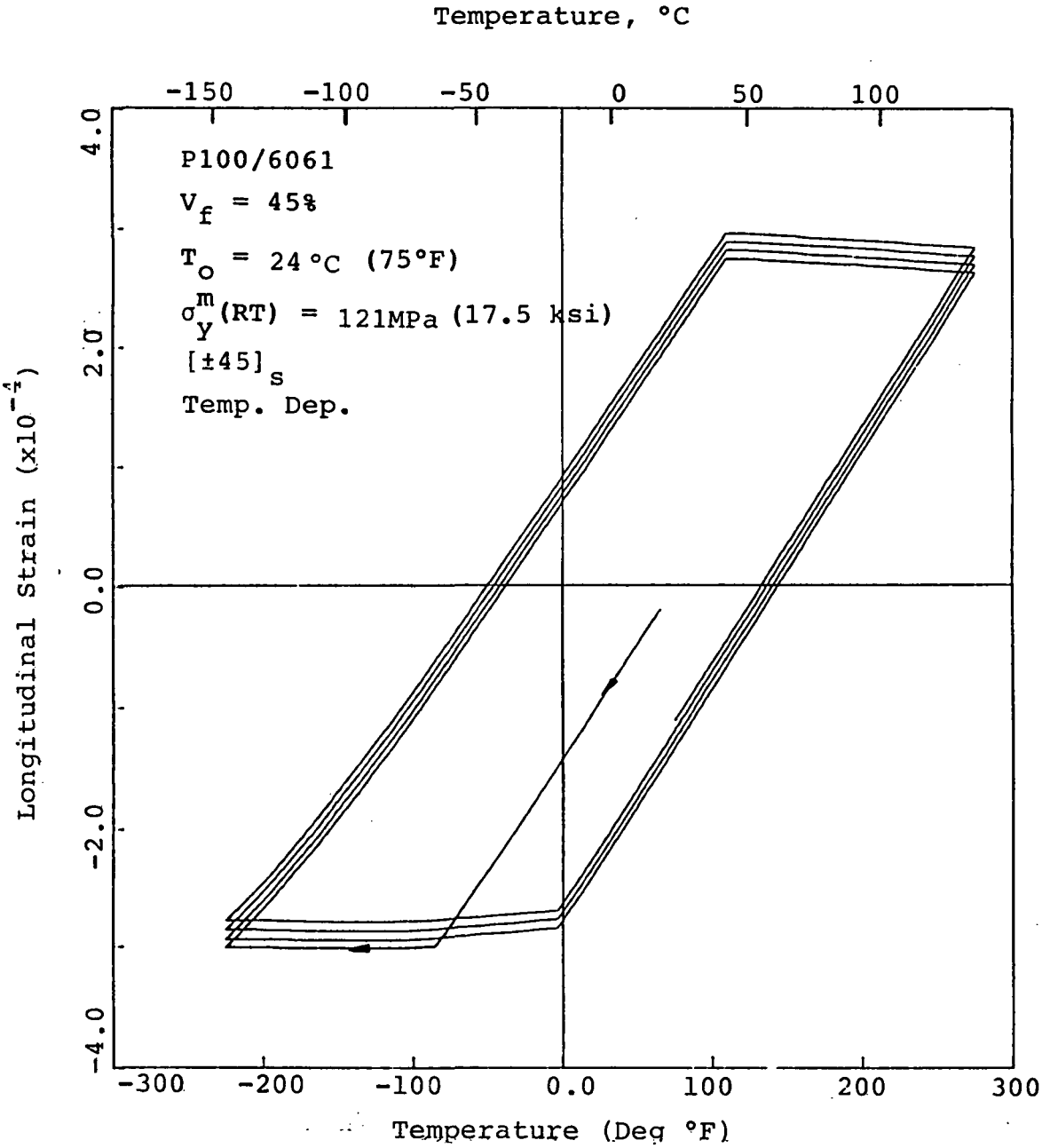

Figure 32. Computed Longitudinal Laminate Strain versus Temperature for a $[\pm 45]_s$ P100/6061 Laminate

APPENDIX - NONLINEAR TEMPERATURE DEPENDENT BEHAVIOR OF UNIDIRECTIONAL COMPOSITES

INTRODUCTION

The fundamental building block of the incremental laminate analysis is the theory which is employed to compute the properties of the layers based upon the properties of the fiber and matrix. For each load step in the laminate analysis, the layer material model is used to compute elastic lamina stiffnesses, to assess lamina yielding, and to calculate lamina post-yield behavior. The layer model utilized in this study is termed the temperature dependent phase average stress model. This theory is an extension of a temperature independent analysis which was developed for the Naval Surface Weapons Center, reference A-1. The following sections describe the approach, results, and limitations of the unidirectional composite model.

OBJECTIVES

The purpose of this task was to develop a material model which was capable of predicting the nonlinear temperature dependent behavior of a unidirectional composite based upon the properties of the constituent fiber and matrix. The model was designed to be compatible with an incremental laminate analysis. At the beginning of each load step it was used to compute effective stiffnesses for each layer. At the end of each load step, the layer stresses were employed to compute constituent stresses and assess yielding and post-yield behavior. The primary application of the layer model and the laminate analysis was to study the thermal hysteresis behavior of metal matrix composites. However, the layer model and laminate analysis were developed to include general combinations of thermal and mechanical loadings.

APPROACH

The layer model is used to determine effective properties of a unidirectional continuous fiber reinforced layer as shown in Figure A-1.

Because the layer is allowed to have nonlinear path dependent material properties, the model is incremental. Since the model is utilized primarily to study the response of graphite/aluminum composites to orbital temperature cycles, the analytical assumptions were chosen to best represent the behavior of graphite and aluminum in the temperature range of approximately -300°F to +300°F. The fibers were assumed to be elastic with properties that are independent of temperature. The matrix was assumed to be temperature dependent with stress-strain behavior that was represented as a bilinear kinematically hardening material.

The theoretical basis for the material model includes the composite cylinders assemblage, reference A-2, the concept of average constituent stresses, references A-3 and A-1, and the theory of thermoplasticity, reference A-4 and A-5. The composite cylinders assemblage provided the theory for computing effective layer properties from the known fiber and matrix properties. The average stress expressions were employed to determine the instantaneous average stress state within the fiber and matrix. The equations of thermoplasticity were utilized to define the yield point and the post yield behavior of the composite based upon the nonlinear response of the matrix.

The following sections describe the model in terms of its elastic behavior, the method utilized to define the composite yield point, and the post yield behavior of the composites.

Elastic Behavior

The incremental stress-strain relation for the temperature independent fiber is

$$d\epsilon_{ij}^{f} = S_{ijkl}^{f} \; d\sigma_{kl}^{f} + \alpha_{ij}^{f} \; dT \qquad (1)$$

where $d\epsilon_{ij}^{f}$ is the fiber incremental strain tensor, S_{ijkl}^{f} is the transversely isotropic fiber compliance, $d\sigma_{kl}^{f}$ is the fiber incremental stress tensor, α_{ij}^{f} is the transversely isotropic fiber thermal expansion and

dT is the increment in temperature. For the matrix, whose properties vary with temperature, the incremental stress-strain relation is

$$d\epsilon_{ij}^{m} = S_{ijkl}^{m}\, d\sigma_{kl}^{m} + \left[\frac{\partial S_{ijkl}^{m}}{\partial T}\ \sigma_{kl}^{m} + \alpha_{ij}^{m} + \frac{\partial \alpha_{ij}^{m}}{\partial T}\,(T - T_o) \right] dT \qquad (2)$$

where the superscript "m" signifies matrix properties and $\frac{\partial}{\partial T}$ represents the change in a property with respect to temperature. In this expression α_{ij}^{m} represents a secant thermal expansion coefficient defined by temperature T and T_o where T_o corresponds to the temperature at which the matrix thermal strain is assumed to be zero. Alternatively, the matrix stress-strain law can be written as

$$d\epsilon_{ij}^{m} = S_{ijkl}^{m}\, d\sigma_{kl}^{m} + \beta_{ij}^{m}\ dT \qquad (3)$$

where

$$\beta_{ij}^{m} = \left[\frac{\partial S_{ijkl}^{m}}{\partial T}\ \sigma_{kl}^{m} + \alpha_{ij}^{m} + \frac{\partial \alpha_{ij}^{m}}{\partial T}\,(T - T_o) \right] \qquad (4)$$

The quantity, β_{ij}^{m}, represents an effective incremental change in the matrix strain for a change in temperature. However, because β_{ij}^{m} contains a stress related term it is not equal to a tangent thermal expansion coefficient.

Once the constituent stress-strain relations are defined, the unidirectional composite properties can be written as

$$S_{ijkl}^{*} = f\,(v_m,\ S_{ijkl}^{f},\ S_{ijkl}^{m}) \qquad (5)$$

$$\beta^*_{ij} = g\ (v_m,\ S^f_{ijkl},\ S^m_{ijkl},\ \alpha^f_{ij},\ \beta^m_{ij}\ ) \qquad (6)$$

Here the functions f and g correspond to the operations associated with the composite cylinders assemblage, reference A-2, and v_m signifies the matrix volume fraction. S^*_{ijkl} represents the composite transversely isotropic compliance and β^*_{ij} represents the incremental change in composite strain for a unit change in temperature. Using these quantities the composite stress-strain relation is

$$d\epsilon^*_{ij} = S^*_{ijkl}\ \ d\sigma^*_{kl} + \beta^*_{ij}\ dT \qquad (7)$$

Notice that the composite properties are temperature dependent because of the matrix properties, although the above stress-strain law is not explicitly temperature dependent. The dependence arises through the matrix compliance, S^m_{ijkl}, and matrix thermal strain, β^m_{ijkl}, which are utilized to compute composite properties.

From reference A-1 and A-3, the average stress and strain increments in the constituents can be related to the average stresses and strains on the composite as

$$v_f\ d\sigma^f_{ij} + v_m\ d\sigma^m_{ij} = d\sigma^*_{ij} \qquad (8)$$

$$v_f\ d\epsilon^f_{ij} + v_m\ d\epsilon^m_{ij} = d\epsilon^*_{ij} \qquad (9)$$

These stresses and strains represent an average state within the constituent and are not the actual distributed fields. A fundamental assumption of this approach is that the actual heterogeneous states within the constituents can be approximated by average states which are uniform throughout the material. This is discussed more completely in references A-1 and A-3.

By substituting equations (1), (3), and (7) in equation (9) and utilizing that result in equation (8), the average matrix stress increment can be found as a function of the applied composite stresses, $d\sigma^*_{ij}$, and the change in temperature, dT,

$$d\sigma^m_{ij} = \frac{1}{v_m} S^I_{ijkl} \left[(S^f_{klmn} - S^*_{klmn})\, d\sigma^*_{mn} + (v_f\, \alpha^f_{kl} + v_m\, \beta^m_{kl} - \beta^*_{kl})dT \right] \quad (10)$$

where

$$S^I_{ijkl}\,(S^f_{klmn} - S^m_{klmn}) = I_{ijmn}$$

The tensor, S^I_{ijkl}, is simply the inverse of the matrix which is equal to the fiber compliance, S^f_{klmn}, minus the matrix compliance, S^m_{ijkl}.

For a load increment on the composite, $d\sigma^*_{ij}$ and dT, when the matrix is in an elastic state, these equations can be employed to compute the response of the composite. At the beginning of the load step, S^f_{ijkl}, α^m_{ij}, and S^m_{ijkl} are evaluated from the known constituent properties. β^m_{ij} are evaluated from the matrix properties and equation (4). The behavior of the composite during the load increment is computed using the composite cylinders assemblage, equations (5) and (6). The increment in matrix stresses during the load step is computed from equation (10) and that result is utilized in equation (8) to determine the increment in fiber stresses. Knowing the stress increments, the strain increments are computed for the fiber, matrix, and composite using equations (1), (3) and (7), respectively. The increments in stress and strain are added to the total values to completely define the state of the fiber, matrix and composite at the end of the increment. Another load step can then be applied and the process is repeated.

In order to check the validity of the elastic calculations a simple problem was analyzed. It is well known that the strain state in a linear, elastic material with temperature dependent properties is path independent, reference A-6. In other words the total elastic strains in a temperature

dependent material can be determined directly from Hooke's law if the compliance and thermal expansion are evaluated at the present temperature. The incremental elastic solution used in this analysis was checked by comparing the integrated results to total stresses and strains computed from elasticity theory.

The specific problem chosen was a unidirectional P100/6061 composite with 45% fiber content cooled from 75°F to 0°F. The constituent properties used in the analysis are shown in Tables A-1 and A-2. Table A-1 shows P100 fiber properties which were correlated with experimental data on epoxy, aluminum, and magnesium matrix composites. Table A-2 shows 6061 aluminum properties determined from MIL-HDBK-5, reference A-7. The strengths chosen for the 6061 matrix were determined from correlations with thermal hysteresis loops of P100/6061 composites, reference A-8, and are approximately equal to 6061 in a T4 temper condition.

A comparison of the axial composite strains and axial matrix stresses at 0°F computed from the total elastic solution or the incremental solution is shown in Table A-3. The table shows that as the stepsize in the incremental solution decreases from 15°F to 5°F to 1°F, the incremental solution converges to the total elastic solution. Therefore, the incremental solution computes the correct elastic behavior of the material and its accuracy increases with decreasing stepsize, as expected.

Composite Yield Surface

The composite is assumed to yield when the average matrix stresses satisfy the matrix yield function. The matrix was assumed to follow a von Mises yield function with the following form, reference A-4,

$$\phi = (S^m_{ij} - he^{mp}_{ij})(S^m_{ij} - he^{mp}_{ij}) - 3k^2 \qquad (11)$$

where

$$S^m_{ij} = \sigma^m_{ij} - 1/3\ \sigma^m_{kk}\ \delta_{ij} \text{ - deviatoric stresses}$$

$$e_{ij}^{mp} = \epsilon_{ij}^{mp} - 1/3\ \epsilon_{kk}^{mp}\ \delta_{ij} \text{ - deviatoric plastic strains}$$

$$h = 2/3\ \frac{E^m\ E_t^m}{E^m - E_t^m} \text{ - plastic modulus}$$

$$k^2 = k^2(T) = 2/9\ \sigma_y^{m\ 2}(T) \text{ - yield strength}$$

The form of the yield function is chosen to represent a kinematic, linear work hardening material. The yield function represents linear hardening (i.e. the stress-strain curve is bilinear) because, h, the plastic modulus is chosen to be a constant which depends upon the elastic modulus, E, and the tangent modulus, E_t. The yield function also represents a kinematically hardening material which means that during plastic flow, the yield function moves in stress space but does not change shape. The motion of the center of the yield function is described by the term, he_{ij}^{mp}.

At the end of each load step the matrix stress state was utilized in equation (11) to assess yielding. If the stress state resulted in a value of ϕ which was less than zero, the matrix was in an elastic state and the response of the composite could be computed using the elastic equations described in the previous section. However, if the matrix stresses resulted in a value of ϕ which equaled zero, the matrix and hence the composite were yielding and deforming plastically.

Since the position of the matrix yield surface in stress space depends explicitly on the matrix plastic strain, it was important that the final elastic load step resulted in a matrix stress point which fell precisely on the yield surface. It was, therefore, necessary to adjust the magnitude of the final elastic load step so that the matrix stresses satisfied the condition that $\phi = 0$. This procedure was complicated somewhat by the fact that the matrix strength, σ_y^m, was a function of temperature which meant that the yield function, ϕ, was capable of growing or shrinking during a load step.

The calculation of the size of the final elastic load step necessary to reach the matrix yield surface was accomplished using a Newton-Raphson

technique and equivalent matrix stresses and strengths. The technique is shown schematically in Figure A-2. From equation (11) it can be seen that ϕ will equal zero when the functions representing equivalent matrix stress and strength intersect. At load step I, an approximation of the intersection (point 1 in Figure A-2) can be determined from the values of stress and strength at step I and the respective slopes of the stress and strength functions determined from steps I and I-1. This intersection, point 1, can be utilized to reevaluate the stress and strength functions at load step $I+\lambda_1$. The new load step, $I+\lambda_1$, is then used to compute new slopes of the stress and strength functions which are then used to project a new intersection, point 2. This process continues until the difference between the equivalent stress and equivalent strength satisfy a specified convergence criterion. The value of λ at that point defines the magnitude of the load step necessary to reach the yield surface.

An example problem showing the behavior of the yield point finder and the effect of the convergence criterion is shown in Table A-4. The sample problem finds the yield temperature of a unidirectional P100/6061 panel with a 45% fiber volume. The panel is assumed to be stress free at 75°F, the matrix is assumed to have a room temperature yield strength of 17.5 ksi and the step size chosen for this analysis is 10°F. The composite is cooled from room temperature until it yields and the table shows the effect of the convergence criterion upon the solution for the yield point. For each value of the convergence criterion, the table shows the number of iterations required by the Newton-Raphson scheme, the equivalent matrix stress, the equivalent matrix strength, and the computed yield temperature. The results show that as the convergence value decreases, the number of iterations required increases and the agreement between stress and strength dramatically improves. The results show that the solution converges rapidly and a convergence value of 1×10^{-10} results in a very accurate solution for the magnitude of the load step necessary to cause yielding.

Post-Yield Behavior

Once the matrix stresses have reached the yield surface any further loading will cause the matrix to deform plastically which will affect the behavior of the composite. The approach utilized in computing the plastic

composite response is similar to that utilized in the elastic response. First the matrix incremental stress-strain relation is determined from the theory of plasticity. This stress-strain relation is utilized to define an effective matrix compliance and thermal expansion. These properties which represent the incremental response of the matrix are then utilized in the composite cylinders assemblage to predict the incremental response of the composite.

The post-yield behavior or flow rule of the matrix is determined by applying several conditions to the matrix yield surface. During plastic flow it is assumed that the stress point always remains on the yield surface, therefore, $\phi = 0$. It is also assumed that although the yield surface moves in stress space it does not change shape, therefore, $d\phi = 0$. Additionally, the matrix plastic strain increment is assumed to be in the direction of the outward normal to the yield surface, i.e. $d\epsilon_{ij}^{mp} = d\lambda \frac{\partial \phi}{\partial S_{ij}^{m}}$.

A further assumption is made in this model that, h, the plastic modulus is independent of temperature. This greatly simplifies the calculations of the motion of the yield surface and does not appear to be unreasonable when applied to actual aluminum data. Since h depends upon both the elastic and the tangent modulus, the assumption that h is constant with temperature implies that as the elastic modulus decreases with increasing temperature the tangent modulus also decreases. The tangent modulus at any temperature, however, is prescribed by the elastic modulus and some constant value of h. The constant can be evaluated from the measured elastic modulus and tangent modulus at one specific temperature such as 75°F.

Applying these conditions, the matrix plastic strain increment in terms of the material properties and stress state is:

$$de_{ij}^{mp} = \frac{1}{3hk^2}(S_{ij}^{m} - he_{ij}^{mp})(S_{kl}^{m} - he_{kl}^{mp})dS_{kl}^{m} - \frac{1}{hk}(S_{ij}^{m} - he_{ij}^{mp})\frac{\partial k}{\partial T}dT \qquad (12)$$

Since the total matrix strain increment is the sum of the elastic and plastic parts, the matrix stress-strain law can be written by combining equations (3) and (12),

$$d\epsilon_{ij}^{m} = S_{ijkl}^{m_{tan}} \, d\sigma_{kl}^{m} + \delta_{ij}^{m} \, dT \tag{13}$$

where $S_{ijkl}^{m_{tan}}$ is the tangent compliance of the matrix given by

$$S_{ijkl}^{m_{tan}} = S_{ijkl}^{me} + S_{ijkl}^{mp} \tag{14}$$

Here S_{ijkl}^{me} is the standard elastic compliance and S_{ijkl}^{mp} is defined by rewriting the first term of equation (12) in terms of stress increments $d\sigma_{kl}^{m}$ instead of stress deviator increments, dS_{kl}^{m}. The effective thermal expansion term, δ_{ij}^{m}, is defined as,

$$\delta_{ij}^{m} = \frac{\partial S_{ijkl}^{me}}{\partial T} \sigma_{kl}^{m} + \alpha_{ij}^{m} + \frac{\partial \alpha_{ij}^{m}}{\partial T} (T-T_o) - \frac{1}{hk} (S_{ij}^{m} - he_{ij}^{mp}) \frac{\partial k}{\partial T} \tag{15}$$

Notice that this expression is simply, β_{ij}^{m} plus an additional term which can be thought of as the plastic thermal strain.

Having defined a matrix incremental stress-strain law, the composite incremental stiffness and thermal expansion can be computed from the composite cylinders assemblage such that

$$S_{ijkl}^{*_{tan}} = f(v_m, S_{ijkl}^{m_{tan}}, S_{ijkl}^{f}) \tag{16}$$

and,

$$\delta_{ij}^{*} = g\,(v_m, S_{ijkl}^{m_{tan}}, S_{ijkl}^{f}, \alpha_{ij}^{f}, \delta_{ij}^{m}). \tag{17}$$

Here the symbols S^{*tan}_{ijkl} and δ^{*}_{ij} are used to represent composite properties in which the matrix is deforming plastically. The functional relationships, f and g, however, are the standard composite cylinder relations. This procedure, in effect, computes incremental composite properties by writing the matrix stress-strain law in a form which appears to be elastic and then uses the composite model which was developed for an elastic response. Eventhough the model uses effective elastic relationships, the nonlinear behavior is retained explicitly in the matrix calculations and implicitly in the composite through the incremental formulation.

The matrix stress increment during plastic flow is evaluated using the same procedure which was applied to the elastic material except that the composite and matrix properties are changed to reflect plastic flow. Specifically,

$$d\sigma^{m}_{ij} = \frac{1}{v_m} S^{I_{tan}}_{ijkl} \left[(S^{f}_{klmn} - S^{*tan}_{klmn}) d\sigma^{*}_{mn} + (v_f \alpha^{*}_{kl} + v_m \delta^{m}_{kl} - \delta^{*}_{kl}) dT \right] \qquad (18)$$

where

$$S^{I_{tan}}_{ijkl} (S^{f}_{klmn} - S^{m_{tan}}_{klmn}) = I_{ijmn}$$

Notice that equation (18) is identical to its elastic counterpart, equation (10), except that the matrix and composite properties have been modified.

Equations (12) through (18) can be employed to represent the post yield behavior of the matrix and composite. The equations are based upon infinitesimal changes, however, they are applied numerically as discrete increments. The numerical approximation becomes apparent at the end of a plastic load step when the stress point is no longer on the yield surface. That is, the matrix stresses at the end of the step no longer satisfy the condition that $\phi = 0$. This implies that there is an error in the matrix plastic strain increment, $d\epsilon^{mp}_{ij}$ which must be corrected before the next load step can be applied.

The correction is accomplished numerically through a Newton-Raphson scheme as shown in Figure A-3. At the end of the load step, the magnitude of the plastic strain increment is computed as $d\lambda$. Using this plastic strain in the expression for ϕ results in a value of ϕ_1 which is not equal to zero although a requirement of the plastic flow is that the stress point and yield surface coincide. The error can be corrected by modifying the magnitude of the plastic strain increment. The modified magnitude, $d\lambda_2$, can be evaluated by using the value of ϕ and $d\phi$ at $d\lambda$, to project forward. This procedure is repeated until the correct magnitude of $d\lambda$ is chosen so that ϕ equals zero at the end of the load step.

An example of this convergence behavior is shown in Table A-5. The table shows the behavior of the plastic strain converger at a typical load step in the plastic range. Specifically, the results are shown for a 45% P100/6061 unidirectional plate at -105°F. The stress free temperature was chosen as 75°F, the room temperature yield strength was chosen as 17.5 ksi and the step size was -10°F. It can be seen from the previous discussion on the yield point, Table A-4, that the material yielded at about -82.5°. Therefore, the response at -105°F, shown in Table A-5, is well into the plastic regime. The results shown in the table describe how the value of ϕ converges to zero and the effect that this has upon the matrix plastic strain increment. At each plastic step in the analysis, this convergence procedure is required so that at the end of the step the total matrix strains are consistent with the matrix stress-strain law.

The equations which have been derived, completely define the behavior of the composite material for arbitrary load histories. The equations were utilized to create a computer program following the logic shown in the flow chart, Figure A-4. The flow chart shows that at some initial state, it is assumed that the stresses and properties of the constituents are known. This, for example, could be the stress free state. For a specified load increment, the model first assumes that the matrix is elastic and computes matrix properties from equation (2), (3), and (4), and composite properties from equations (5), (6), and (7). The composite load increment, which can be any combination of stress and temperature, is applied in terms of $d\sigma_{ij}^{*}$ and dT. Equation (10) is utilized to compute the resulting increment in matrix stress. The matrix stresses are then employed in the yield function,

equation (11), to assess yielding. If equation (11) shows that ϕ is less than zero, then the material is elastic and the initial assumption of elastic matrix propertries was correct. Therefore, the values of $d\sigma_{ij}^{m}$ are correct and the increment in fiber stresses $d\sigma_{ij}^{f}$ can be computed from equilibrium, equation (8). The strain increments in the composite, matrix, and fiber are computed from the appropriate stress-strain laws, equations (7), (3), and (1), respectively. The total values of stress and strain in the composite and constituents are summed and the state at the end of the increment is completely defined. The process can then repeat itself.

On the other hand, if ϕ is not less than zero, then the assumption of an elastic matrix was incorrect. In this case the matrix properties are determined from equations (12) through (15) and the composite properties are determined from equations (16) and (17). The composite load increment $d\sigma_{ij}^{*}$ and dT is applied and the matrix stresses are evaluated using equation (18). The solution procedure then continues as before with the fiber stress increments computed from equation (8). The strain increments are then evaluated using the plastic stress-strain laws for the matrix and composite, the total stresses and strains are computed and the solution continues.

RESULTS

The theory described in the previous section was utilized to create a computer code named TPLAS, Thermo-Plastic Layer Analysis. TPLAS was exercised briefly to verify the analysis and to examine the behavior of the composite. The following sections describe computations of thermal hysteresis behavior and the response of the model to mechanical loads including the effects of changing temperature.

Thermal Loads

Since the major objective of this effort was to develop an analytical model capable of predicting the response of metal matrix composites to thermal load histories, TPLAS was utilized to investigate three different problems. The first analysis investigated the behavior of the composite during its initial orbital cycle. The second problem, compared the theoretical effects of a temperature dependent versus a temperature

independent solution. The third problem analyzed several sequential thermal cycles to track the history dependence of the composite. Each of these analyses are discussed in the following paragraphs.

The response of the composite to an initial orbital load cycle resulted in a very strong theoretical check on the computer code. Recall from the flow chart, Figure A-4, that once the constituent stresses are computed, the constituent strains are calculated from their appropriate stress-strain laws. If the computer model is behaving correctly, the strains in the axial direction, for the fiber, matrix, and composite must all be identical because of the fundamental assumption of uniform axial strain in a composite.

The axial strains computed by TPLAS for the composite, fiber, and matrix for an initial orbital cycle are shown in Figures A-5, A-6, and A-7, respectively. This thermal cycle contains an initial elastic response during cooldown until the matrix yields. During further cooling the matrix flows plastically. When the material is subsequently heated, the response is elastic again until the matrix yields. Further heating causes additional plastic straining until the maximum temperature is reached. Subsequent cooling results in the final elastic response. Therefore, the composite and matrix go through various states of elastic and plastic behavior. The fiber, however, remains elastic through the entire thermal cycle. If the strain histories shown in Figures A-5 through A-7 are overlayed or examined closely it can be seen that the figures are identical. The fact that the axial strains in the fiber, matrix, and composite are equal verifies that the model is behaving properly and that the theoretical basis is valid for this analysis.

A comparison of the temperature dependent solution with a simpler temperature independent solution is shown in Figure A-8. Each analysis was performed for the same P100/6061 plate which was stress free at room temperature and contained a 45% volume fraction of fibers. The temperature dependent solution used the properties shown in Table A-2 whereas the temperature independent solution assumed the properties were constant at their room temperature values. The predicted thermal cycles shown in Figure A-8 show a significant effect of temperature dependent matrix properties upon the thermal hysteresis. The temperature dependent model requires greater temperature changes to cause yielding both during cooling and

heating. The temperature dependent model also shows a larger magnitude of residual strain at the end of the cycle. The comparison clearly shows that the aluminum matrix properties which change during the thermal cycle have a measurable effect upon the thermal strain behavior of the composite.

The theoretical response of the composite to subsequent thermal cycles is shown in Figure A-9. The dashed line in the figure shows the thermal strain history of the composite on the first cycle, i.e. beginning at a stress free state. At the end of the cycle, the material is no longer stress free, the yield surface has been shifted in stress space and the response of a subsequent cycle is expected to be different. The solid line shows that the subsequent cycle does indeed have a different strain history. Notice that on the first cycle the composite yielded at about -80°F whereas during the second cycle the composite yielded much earlier, at about 0°F. As the subsequent thermal cycle continues, the composite response is similar to that of the first cycle except for a slight offset due to a shift in residual stress (see the main text chapter on thermal hysteresis). Although the residual stress shift is theoretically slight, changes in the temperature extremes of as little as ±5°F, will significantly alter the response. This is true because altering the temperature extremes will change the amount of plastic strain in the matrix which will change the position of the yield surface. These changes in load history will cause the thermal hysteresis curve to move so that subsequent cycles no longer approximately repeat themselves. This fact may explain some of the shifts in the thermal hysteresis curves seen in experimental data.

Mechanical Loads

Since the layer model is employed in a laminate analysis it must be able to account for mechanical as well as thermal loads. The layer model is capable of predicting the response of mechanical loads consisting of all six stress components. Since laminated plate theory assumes a state of plane stress sample problems are presented for the three stress components of interest, σ_{11}^{*}, σ_{22}^{*}, and τ_{12}^{*}. Results were computed for a P100/6061 plate with a 45% fiber volume fraction. The plates were loaded axially, transversely, and in shear. In each case, mechanical loads were applied at

room temperature. The load paths were chosen so that the matrix yielded, deformed plastically and then unloaded.

The results for the axial, transverse, and shear loads are shown in Figures A-10 through A-12, respectively. Each composite stress-strain curve shows the expected elastic behavior, plastic flow and elastic unloading. As expected, the transverse and shear curves show much stronger nonlinearity than the axial curve since the transverse and shear response is dominated by the matrix whereas the axial response is dominated by the fiber. These results are identical to those determined for the temperature independent model, reference A-1. In reference A-1, the phase average predicted stress-strain curves were compared to more complex finite element solutions. The comparisons showed that the agreement between the solutions was good and that the phase average model, although approximate, was a more cost effective tool for incorporation in a laminate analysis.

In order to investigate the effects of temperature dependent properties on mechanical behavior, two problems were analyzed with combined mechanical and thermal loads. Each problem used a 45% P100/6061 layer as the composite. The material was assumed to be stress free at room temperature. In the first problem the material was loaded axially at the same time that it was cooled from room temperature to -25°F. In the second problem the material was loaded transversely while it was cooled to -25°F.

The results for the axial loads are shown in Figure A-13 and the results for the transverse loads are shown in Figure A-14. Each figure shows a comparison of the temperature dependent solution and the temperature independent solution. Notice first by comparing Figure A-13 and A-10 that the temperature change results in a much lower axial yield stress. The axial response shows a composite with no temperature change having a yield strength of about 90 ksi whereas the composite with a temperature change has a strength of about 45 ksi. The reduction in axial yield stress is due to the additional stresses that arise in the matrix because of the mismatch in fiber and matrix thermal expansion coefficients. Figure A-13 also shows that since the axial loads are dominated by the fiber, the difference between the temperature dependent and temperature independent solutions are very slight. On the other hand, the transverse loads presented in Figure A-14 show an effect of temperature dependent properties. Notice that as the temperature decrease the matrix modulus increases, which translates into a

somewhat higher elastic modulus for the temperature dependent response. Also notice that as the temperature decreases the matrix yield strength increases which results in a higher yield strength for the temperature dependent response.

The final mechanical load case which was analyzed was a comparison of the transverse stress-strain behavior of the composite at room temperature and at an elevated temperature. In this case an attempt was made to study the effect that processing may have on the mechanical behavior of the composite. In each case the composite was assumed to be stress free at 295°F. This temperature was chosen arbitrarily since actual processing temperatures are on the order of 800°F to 900°F. However, because of creep in the aluminum the stress free temperature is much lower than the processing temperature so that 295°F is not a totally unrealistic stress free state. For each load case the material was initially cooled to room temperature. In one case the material was then loaded transversely to represent a room temperature stress-strain curve. In the other case, after cooling, the material was first heated to 175°F and then loaded transversely to represent an elevated temperature stress-strain curve.

A comparison of the results is shown in Figure A-15. It may be expected that, since the transverse behavior is dominated by the matrix and the matrix becomes weaker at elevated temperatures, the elevated temperature composite would have a lower yield strength then the room temperature composite. The analysis, however, shows just the opposite effect. This can be explained by the thermally induced residual stresses in the matrix. Cooling from elevated temperatures causes a large build up of residual stresses in the matrix so that subsequent mechanical loading at room temperature results in a low composite yield point. However, if the material is heated before it is loaded some of the residual stresses will be relieved explaining the higher yield point in the elevated temperature response.

The results presented in this section show that the temperature dependent phase average stress model is capable of predicting nonlinear layer behavior which can be utilized in a study of nonlinear laminated composites. The results have shown that the temperature dependence of the matrix properties is significant, Figure A-8. The analysis has also shown that the response of the composite material depends strongly on both the

load history, Figure A-9, and the interaction between the constituents, Figure A-15.

MODEL LIMITATIONS

The approximations used in the temperature dependent phase average stress model impose certain limitations upon the accuracy of the solution. There appear to be three areas in which the approximations may cause concern. These include the computation of initial yielding, the anisotropic plastic behavior of the matrix and the assumption that the matrix plastic modulus, h, is temperature independent. Note that the remaining matrix properties, i.e. Young's modulus, Poisson's ratio, thermal expansion, and yield strength, may all be arbitrary functions of temperature. Each of these limitations is discussed in the following paragraphs.

The layer model does not compute the actual heterogeneous stress field within the fiber and matrix but approximates these stresses with uniform field based upon average values. This assumption is shown explicitly in Figure A-16 where the phase average model is compared to a concentric cylinder model of a P100 fiber in a 6061 matrix under a negative temperature change. The comparison shows that the two models give identical results for axial matrix stress shown as σ_{zz} in Figure A-16. The results presented in Figure A-16 also show that the transverse stresses computed by the phase average model approximate the actual hoop and radial stress components. Under a general loading condition, the actual distributed stresses in the matrix will cause yielding at some points in the material before yielding will be predicted by the phase average model. This will result in the phase average model overpredicting the composite yield surface, as shown in Figure A-17. In terms of a stress-strain curve, Figure A-18 shows the comparison of the transverse behavior predicted using either the phase average model or a more accurate finite element solution. Here it can be seen that the phase average model overpredicts the yield point and neglects some of the local nonlinearity caused by the growth of the plastic zone in the matrix. However, once the matrix has fully yielded, the two solutions parallel each other during further plastic loading. This effect will be most noticeable in transverse loading where the actual stress field in the matrix is far from uniform. In axial, thermal, or shear loadings, however, the matrix

stress state is more nearly homogeneous and the phase average model provides an excellent approximation.

An additional limitation of the phase average model is that the matrix must be treated in the composite as if it is transversely isotropic during plastic flow. By examining the matrix flow rule, equation (12), it can be seen that in general the matrix plastic compliance may be fully populated so that during yielding the matrix may behave as if it is completely anisotropic. Therefore, under a general loading condition (i.e. not uniaxial) the matrix may be deforming anisotropically while the composite model at best must treat the matrix as transversely isotropic. For axial, thermal, or shear loads the stresses in the matrix can be divided between a hydrostatic and a uniaxial component. In these cases the assumed isotropy in the matrix is exact and the phase average model is an accurate approximation of the matrix behavior.

To assess the effects of this assumption a problem was analyzed where the composite was assumed to contain no fibers and was simultaneously loaded axially and transversely with different magnitudes of stress. In reality, the response of the composite and the matrix should be identical since there are no fibers. However, the model assumes the composite is transversely isotropic and the computed composite strains are based upon that assumption. On the other hand, the matrix flow rule is programmed explicitly so that the matrix strains are computed for an anisotropic material.

The comparison of the matrix and composite strains after a significant amount of plastic straining is shown in Figure A-19 and Table A-6. Figure A-19 compares the axial and transverse load-strain histories computed using either the composite equations or the matrix equations. The composite contains no fibers and is loaded with a stress of σ_o in the axial direction and 1/2 σ_o in the transverse direction. The composite and matrix strains are shown to coincide in the elastic region. During plastic flow, however, the matrix flow rule results in what appears to be a slightly stiffer material. Notice that this effect appears to be more significant in the direction of the smaller load increments. That is, the error appears to be more significant in the transverse strains than in the axial strains. The numerical values of the composite and matrix strains at the end of this load path are shown explicitly in Table A-6. For this particular problem the error is seen to be on the order of 1 to 2%. Once again this effect will be

strongest for transverse loads where the matrix is in a general state of loading.

The other limitation of the layer model is the assumption that the plastic modulus is temperature independent. Based upon 6061 stress-strain data from MIL-HDBK-5, reference A-7, the plastic modulus is seen to vary by approximately 15% over the range of room temperature to 300°F. This assumption may be improved in the future, however, it significantly complicates the computations of plastic strain and motion of the yield surface.

SUMMARY

Based upon the results presented here the temperature dependent phase average stress model appears to be an excellent tool for studying the nonlinear behavior of metal matrix composites. The model was shown to give expected elastic results and to converge rapidly and accurately for the plastic response of the composite. Sample problems were run which showed that the temperature dependence of the matrix has a significant effect and that the response of the composite will be strongly history dependent.

The limitations of the model were shown to have the strongest effect on the transverse stress-strain behavior which is not unexpected since that loading condition creates the most heterogeneous stress field in the composite. Comparisons of transverse stress-strain curves computed using the phase average model and a more exact finite element model showed that the limitations are most significant near the yield point. In the elastic range or after the matrix has fully yielded the phase average model was seen to approximate the composite response well. For axial, thermal, or shear loads the stresses in the matrix can be divided between a hydrostatic and a uniaxial component. In these cases the assumed isotropy in the matrix is exact and the phase average model is an accurate approximation of the matrix behavior.

SYMBOLS

E	-	Young's modulus
E_t	-	Tangent modulus when $\sigma > \sigma_y$
e_{ij}	-	Deviatoric strain tensor
h	-	Plastic modulus parameter used in matrix yield surface
k	-	Yield strength parameter used in matrix yield surface
S_{ijkl}	-	Compliance tensor
s_{ij}	-	Deviatoric stress tensor
T	-	Temperature
T_o	-	Reference temperature
dT	-	Temperature increment
v_m	-	Matrix volume fraction
α_{ij}	-	Thermal expansion vector
β_{ij}	-	Effective elastic thermal expansion vector, defined in equation 4
δ_{ij}	-	Kronecker's delta
δ_{ij}^m, δ_{ij}^*	-	Effective plastic matrix (m) or composite (*) thermal expansion vector, defined in equations (15) and (17)
$d\epsilon_{ij}$	-	Strain tensor increment
σ_y	-	Yield strength
$d\sigma_{ij}$	-	Stress tensor increment
ϕ	-	Yield surface

SUPERSCRIPTS

f	-	Fiber
m	-	Matrix
*	-	Composite
I	-	Inverse
tan	-	Tangent property

REFERENCES

A-1. Buesking, K.: "Nonlinear Unidirectional Metal Matrix Composite Behavior." Presented at Air Force Mechanics of Composites Review, Dayton, OH, October, 15-17, 1984.

A-2. Hashin, Z.: "Analysis of Properties of Fiber Composites with Anisotropic Constituents." JAM, Vol. 46, No. 3, pp. 543-550, September, 1979

A-3. Hashin, Z.: "Theory of Fiber Reinforced Materials." NASA CR-1974, March 1972.

A-4. Martin, J. B.: Plasticity; Fundamentals and General Results. MIT Press, Cambridge, MA 1975.

A-5. Naghdi, P. M.: "Stress-Strain Relations in Plasticity and Thermoplasticity." in Plasticity, Proceedings of Second Symposium on Naval Structural Mechanics, Pergamon Press, New York, 1960.

A-6. Fung, Y. C.: Foundations of Solid Mechanics. Prentice-Hall, Englewood Cliffs, NJ, 1965

A-7. "Military Standardization Handbook, Metallic Materials and Elements for Aerospace Vehicle Structures." MIL-HDBK-5C, September 1982.

A-8. Dries, G. A.; and Tompkins, S. S.: "Thermal Processing of Graphite Reinforced Aluminum to Minimize Thermal Strain Hysteresis." NASA TP-2402, March 1985.

Constituent Properties Used in Nonlinear Metal Matrix Laminate Analysis

Table A-1. P100 Fiber Properties

E_a		E_t		G_a		ν_a	ν_t	α_a		α_t	
GPa	Msi	GPa	Msi	GPa	Msi	–	–	$10^{-6}/°C$	$10^{-6}/°F$	$10^{-6}/°C$	$10^{-6}/°F$
690	100	3.45	0.50	17.2	2.50	0.41	0.45	-1.62	-0.90	20.3	11.3

Table A-2. 6061 Aluminum Matrix Properties

Temperature		E		ν	α		σ_y		E_{tan}*	
°C	°F	GPa	Msi	–	$10^{-6}/°C$	$10^{-6}/°F$	MPa	Ksi	GPa	Msi
-184	-300	75.9	11.0	0.33	18.7	10.4	140	20.3	13.9	2.020
-129	-200	73.8	10.7	0.33	20.3	11.3	130	18.9	13.9	2.010
- 73	-100	71.0	10.3	0.33	21.6	12.0	128	18.6	13.8	1.995
- 18	0	69.6	10.1	0.33	22.3	12.4	124	18.0	13.7	1.983
24	75	68.3	9.9	0.33	22.9	12.7	121	17.5	13.7	1.980
38	100	67.6	9.8	0.33	23.0	12.8	119	17.3	13.6	1.976
93	200	66.9	9.7	0.33	23.4	13.0	111	16.1	13.6	1.973
149	300	64.9	9.4	0.33	23.9	13.3	101	14.7	13.5	1.960

* Tangent modulus when $\sigma \geq \sigma_y$

Table A-3. Comparison of Elastic Composite Strains and Matrix Stresses for P100/6061 Plate Cooled from 24°C (75°F) to -18°C (0°F), V_f = 45%

Elastic Solution	ε_{11}^{*} με	σ_{11}^{m} MPa	σ_{11}^{m} psi
--	-41.67	63.00	9138

Incremental Solution	ε_{11}^{*} με	σ_{11}^{m} MPa	σ_{11}^{m} psi
Stepsize = 8.3°C(15°F)	-41.76	63.90	9148
Stepsize = 2.8°C(5°F)	-41.70	63.03	9141
Stepsize = (0.6°C)(1°F)	-41.68	63.00	9138

Table A-4. Effect of Convergence Criterion on Solution for Temperature Dependent Yield Point

[P100/6061, V_f=45%, T_o=24°C(75°F), σ_y^m(RT)=121MPa(17.5ksi), ΔT = -5.6°C(-10°F)]

Convergence Criterion	No. of Iterations	$\sqrt{(S_{ij}-he_{ij}^{mp})(S_{ij}-he_{ij}^{mp})}$ MPa	$\sqrt{3k^2}$ MPa	T_y °C
1×10^{-2}	1	104.1090090	104.1223009	-63.62619361
1×10^{-4}	2	104.1230308	104.1230313	-63.62619411
1×10^{-6}	2	"	"	"
1×10^{-10}	3	104.1230313	104.1230313	-63.62619411

-	-	ksi	ksi	°F
1×10^{-2}	1	15.099203626	15.101131381	-82.527148545
1×10^{-4}	2	15.101237241	15.101237321	-82.527149439
1×10^{-6}	2	"	"	"
1×10^{-10}	3	15.101237325	15.101237325	-82.527149439

Table A-5. Example of Plastic Strain Convergence Scheme Used to Insure Yield Surface Coincides With Stress Point

P100/6061, V_f = 45%, T_o = 24°C(75°F), σ_y^m(RT)=121MPa(17.5ksi), T=-76°C(-105°F)

Iteration	ϕ		$d\varepsilon_{11}^{mp}$
-	$(Pa)^2$	$(psi)^2$	με
1	-1986	-41.79	94.176218919
2	8.94×10^{-5}	1.88×10^{-6}	94.175538578
3	1.77×10^{-7}	3.73×10^{-9}	94.175538578

Table A-6. Comparison of Composite and Matrix Strains in Plastic Range Computed Using Phase Average Stress Model for Composite with 0% Fibers Under General Load [σ_{11} = 275 MPa (40 ksi), σ_{22} = 138 MPa (20 ksi)]

Strain Component	Matrix Strain %	Composite Strain %	Error %
ε_{11}	0.9332	0.9328	0.0429
ε_{22}	0.0697	0.0706	1.29

Note: Error is caused by the fact that the composite computations must treat the matrix as transversely isotropic

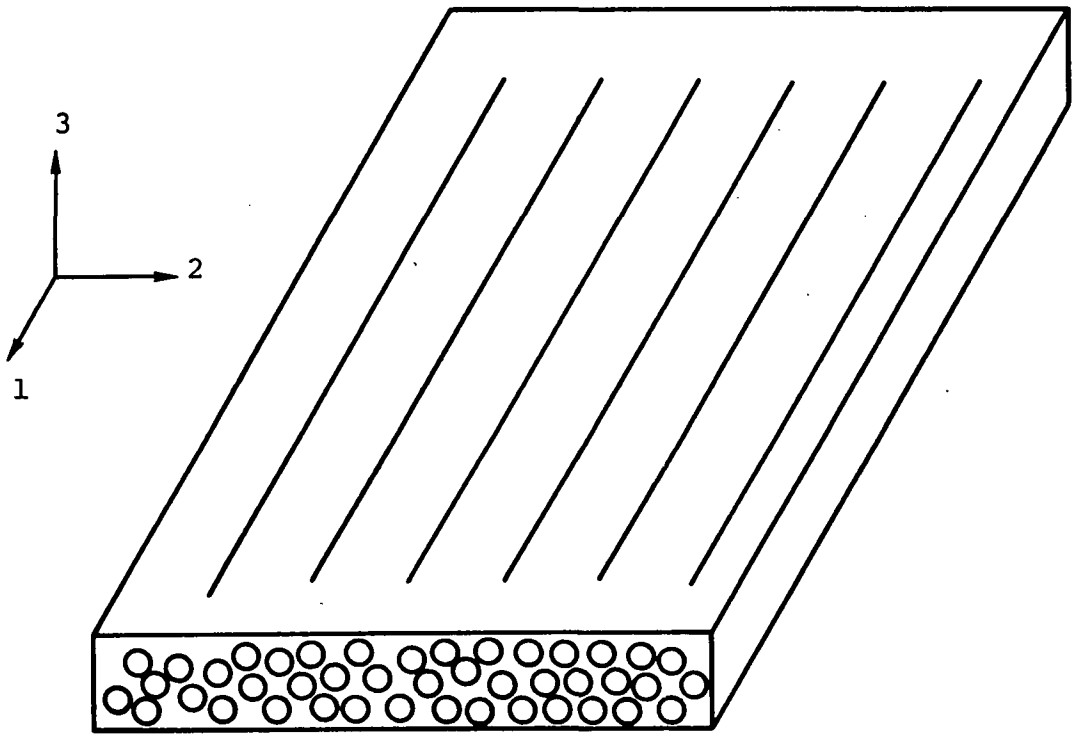

Figure A-1. Schematic Diagram of Unidirectional Fiber Reinforced Layer

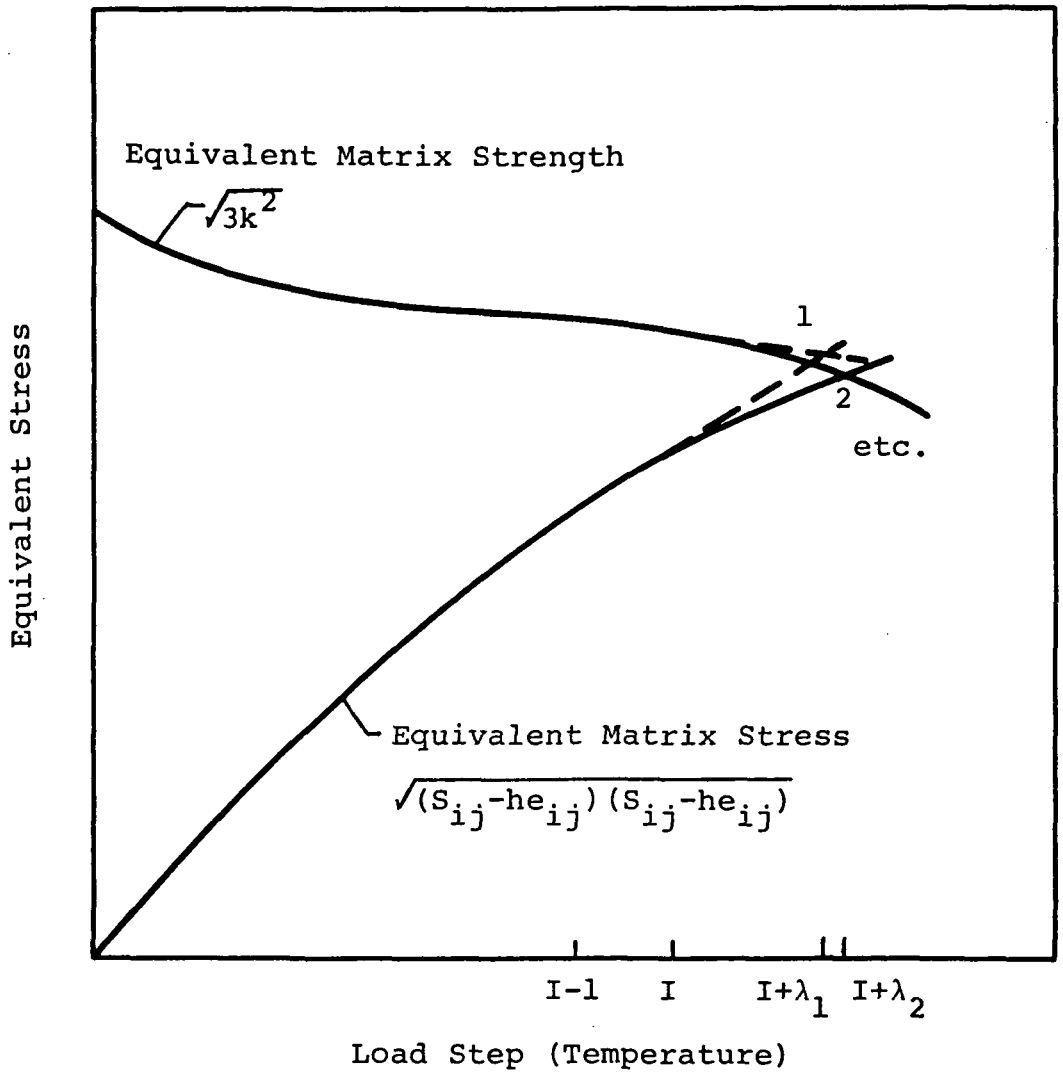

Figure A-2. Schematic Diagram Showing Procedure Used to Converge to Temperature Dependent Matrix Yield Point

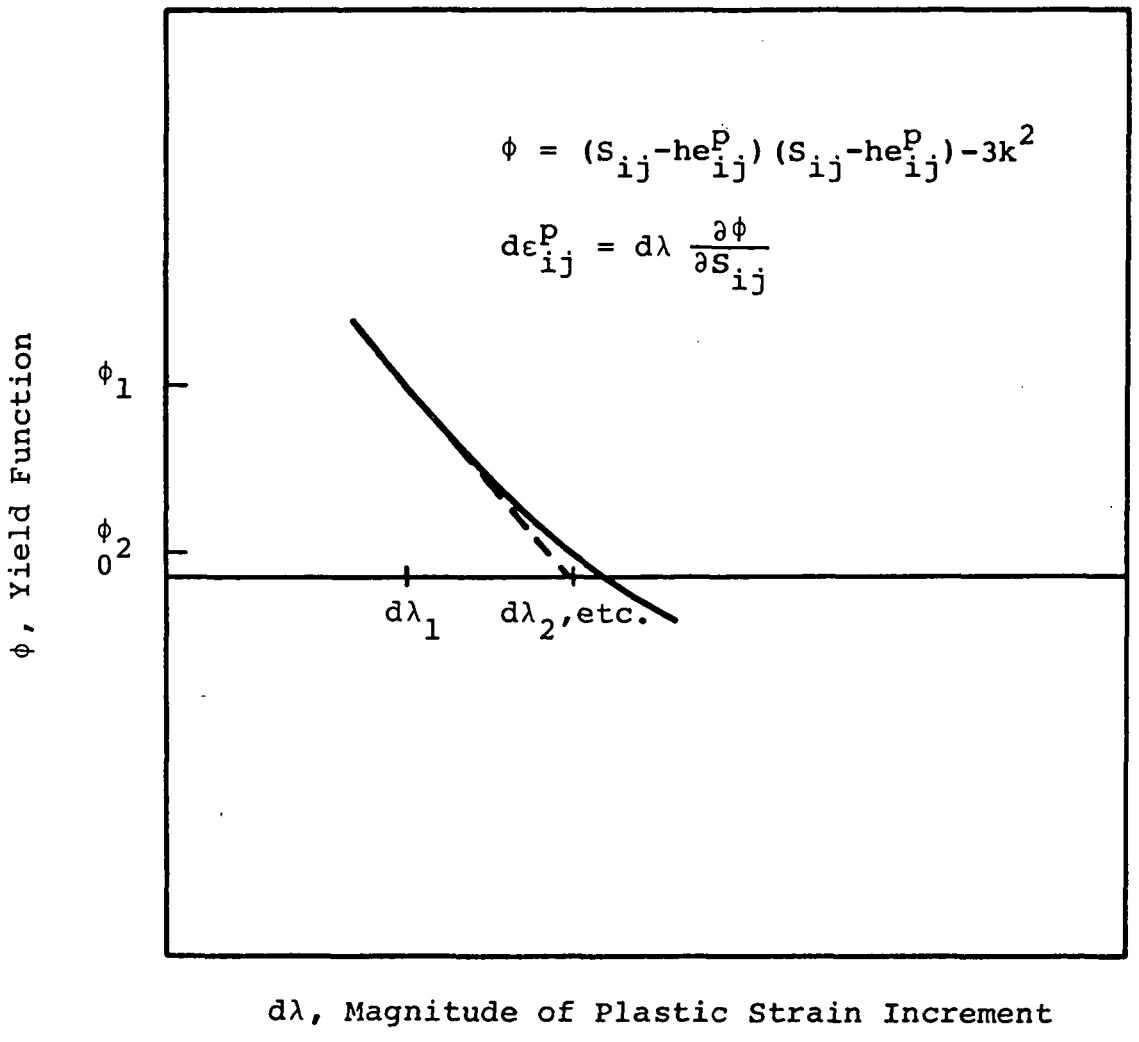

Figure A-3. Schematic Diagram Showing Procedure Used to Converge to Magnitude of Matrix Plastic Strain Increment

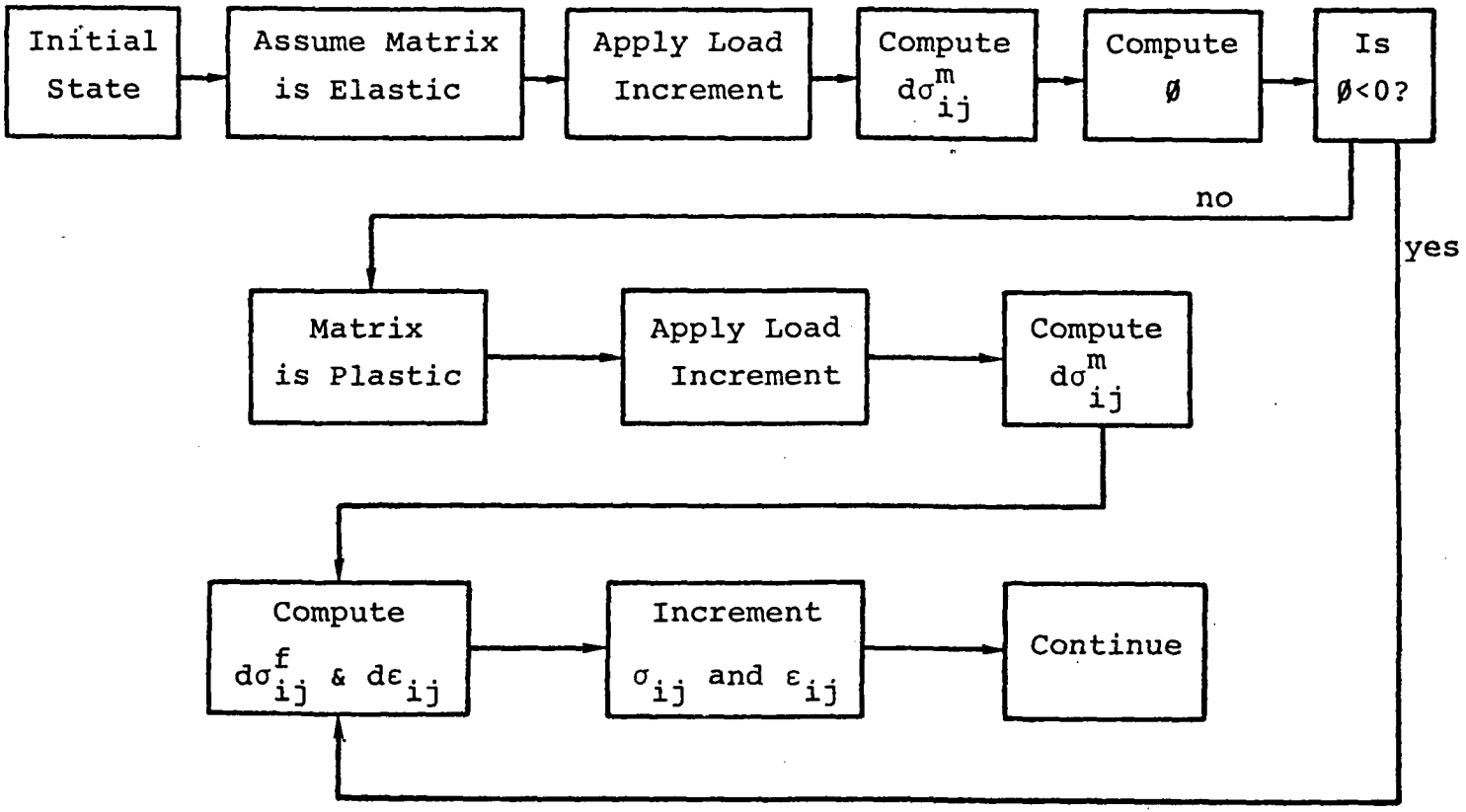

Figure A-4. Flow Chart Showing Overall Logic Used in Temperature Dependent Layer Model

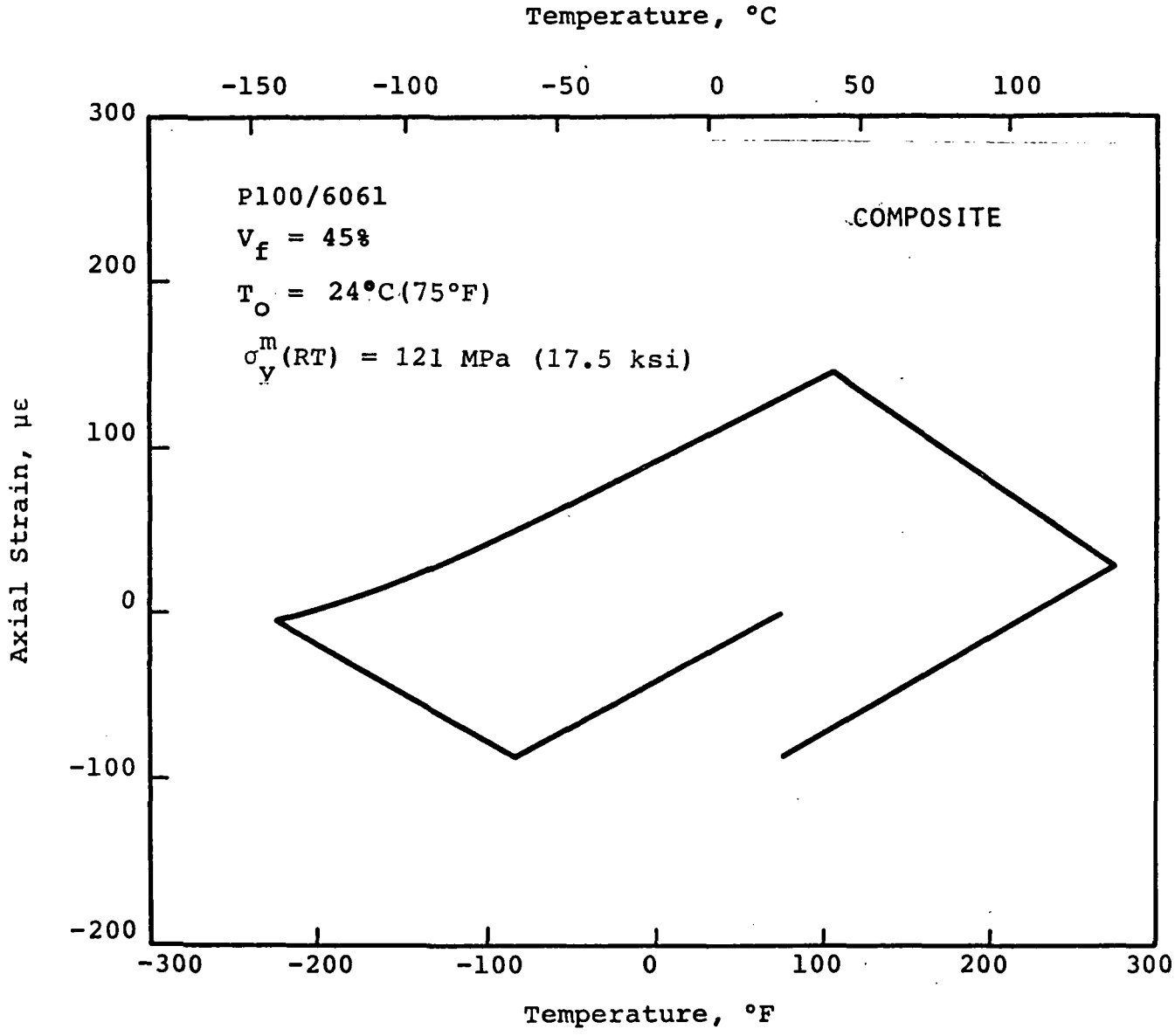

Figure A-5. Predicted Composite Thermal Strains in P100/6061 Unidirectional Plate Based Upon Temperature Dependent Phase Average Stress Model

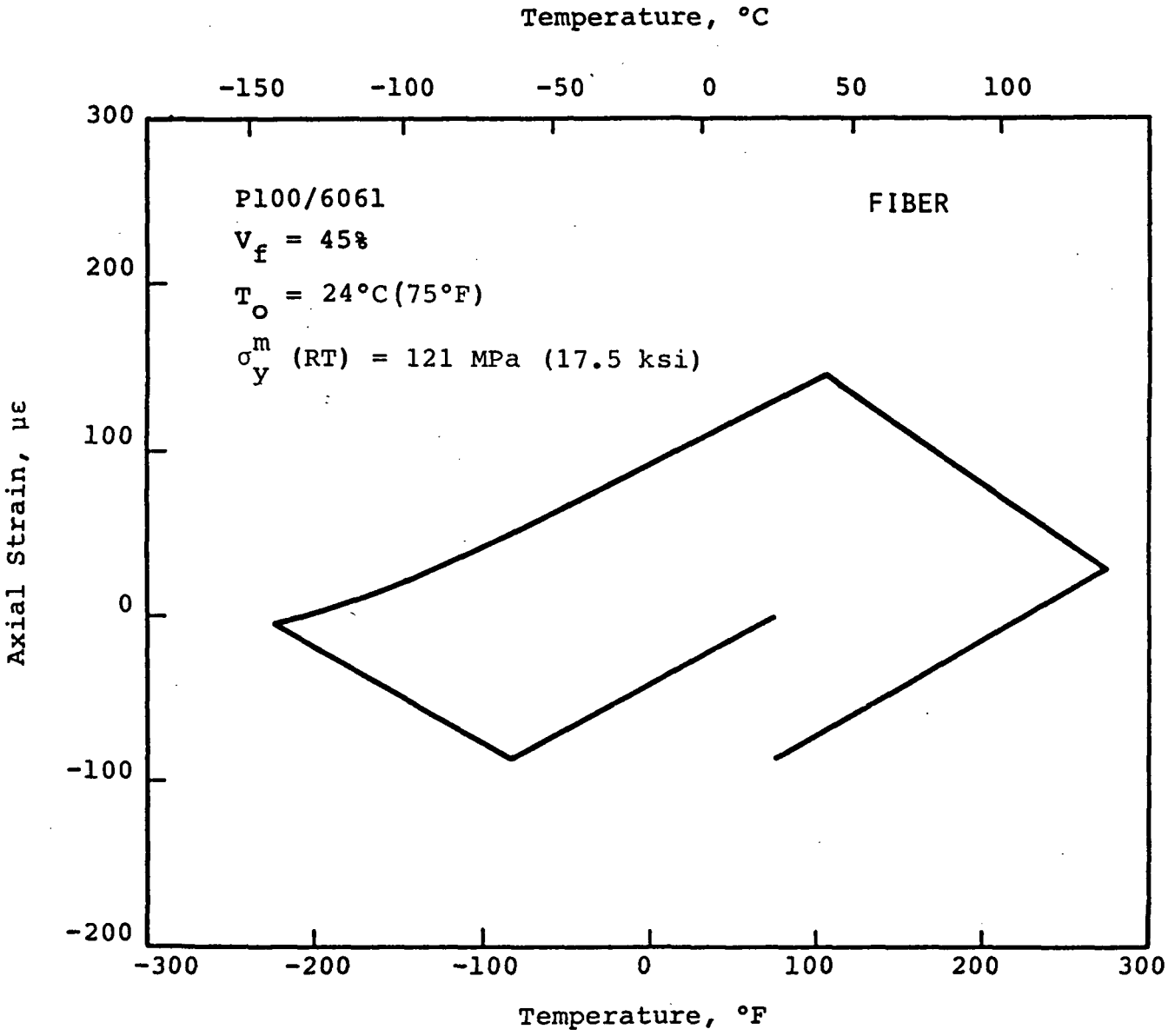

Figure A-6. Predicted Fiber Thermal Strains in P100/6061 Unidirectional Plate Based Upon Temperature Dependent Phase Average Stress Model

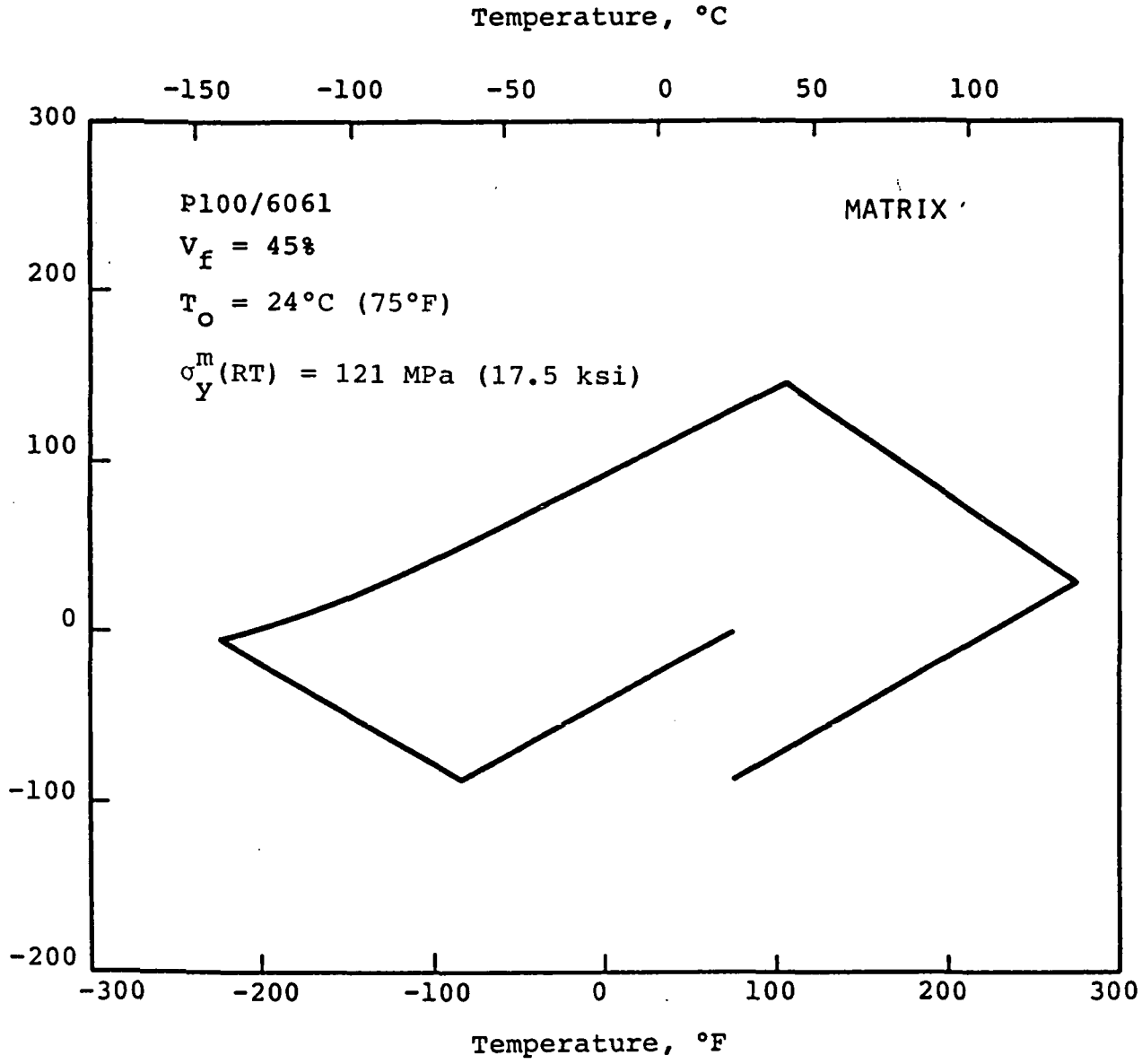

Figure A-7. Predicted Matrix Thermal Strains in P100/6061 Unidirectional Plate Based Upon Temperature Dependent Phase Average Stress Model

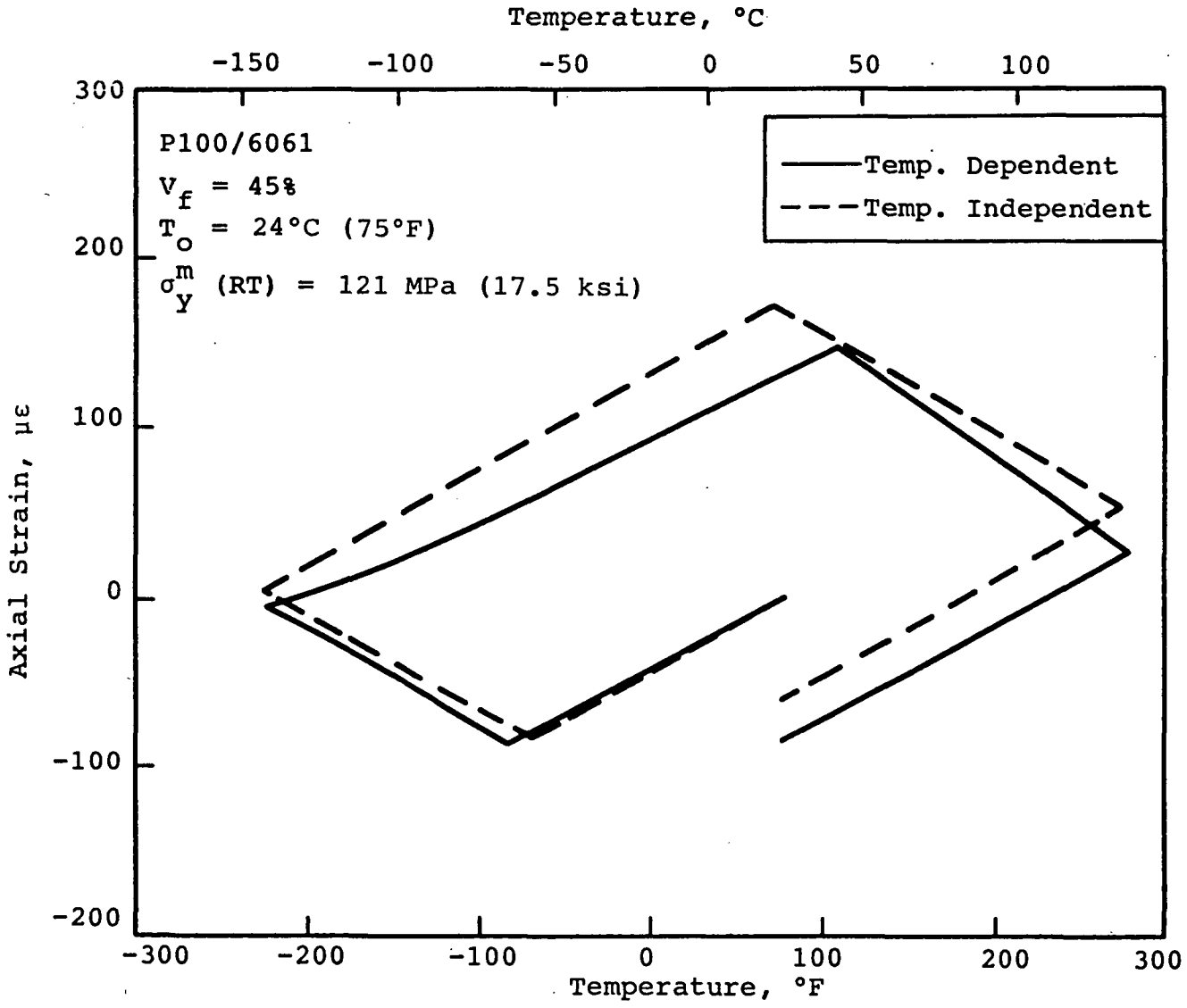

Figure A-8. Comparison of Predicted Thermal Strains in P100/6061 Unidirectional Plate Assuming that the Matrix Properties are either Temperature Dependent or Temperature Independent

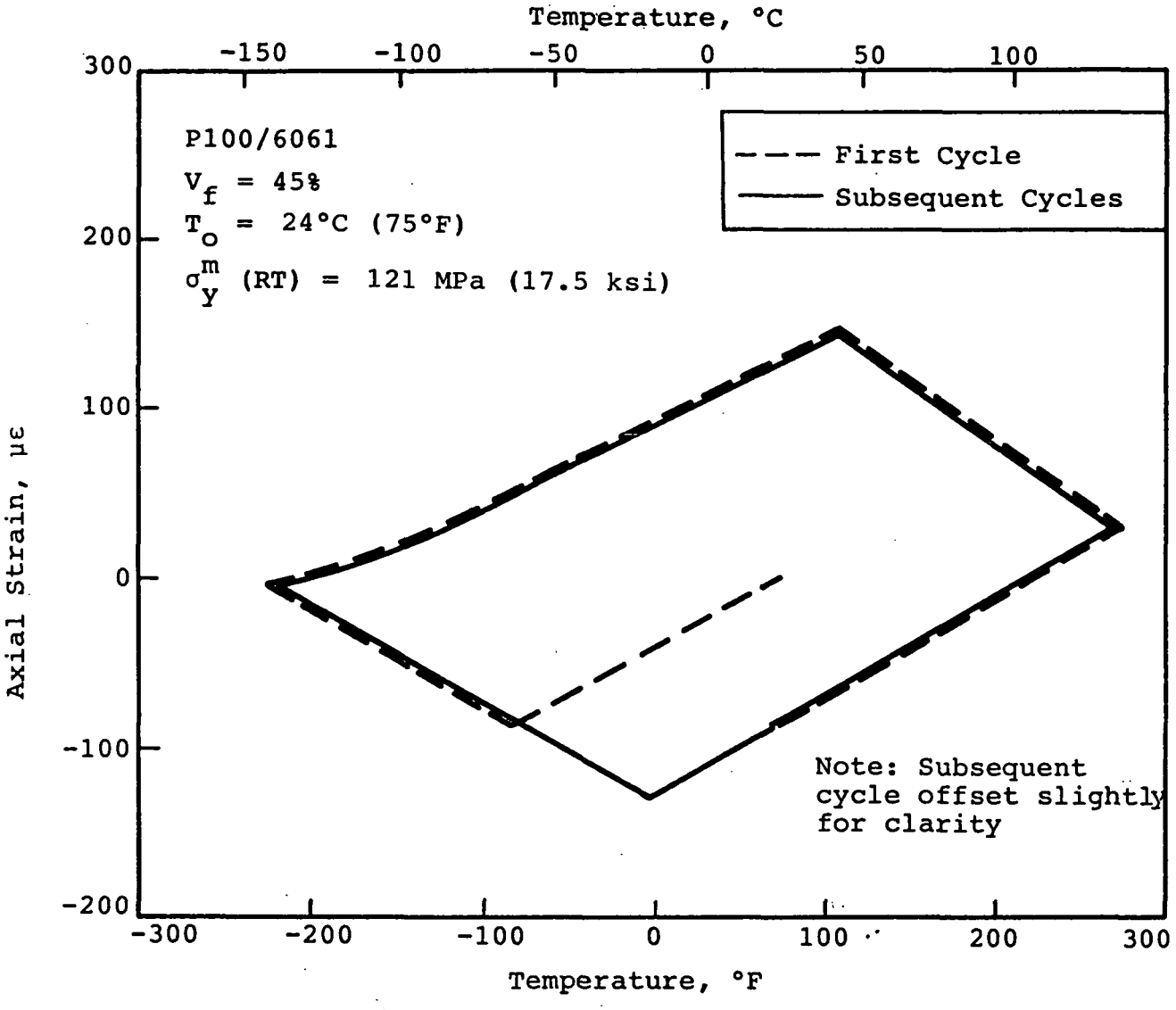

Figure A-9. Predicted Thermal Strains in P100/6061 Unidirectional Plate Based Upon Temperature Dependent Phase Average Stress Model.

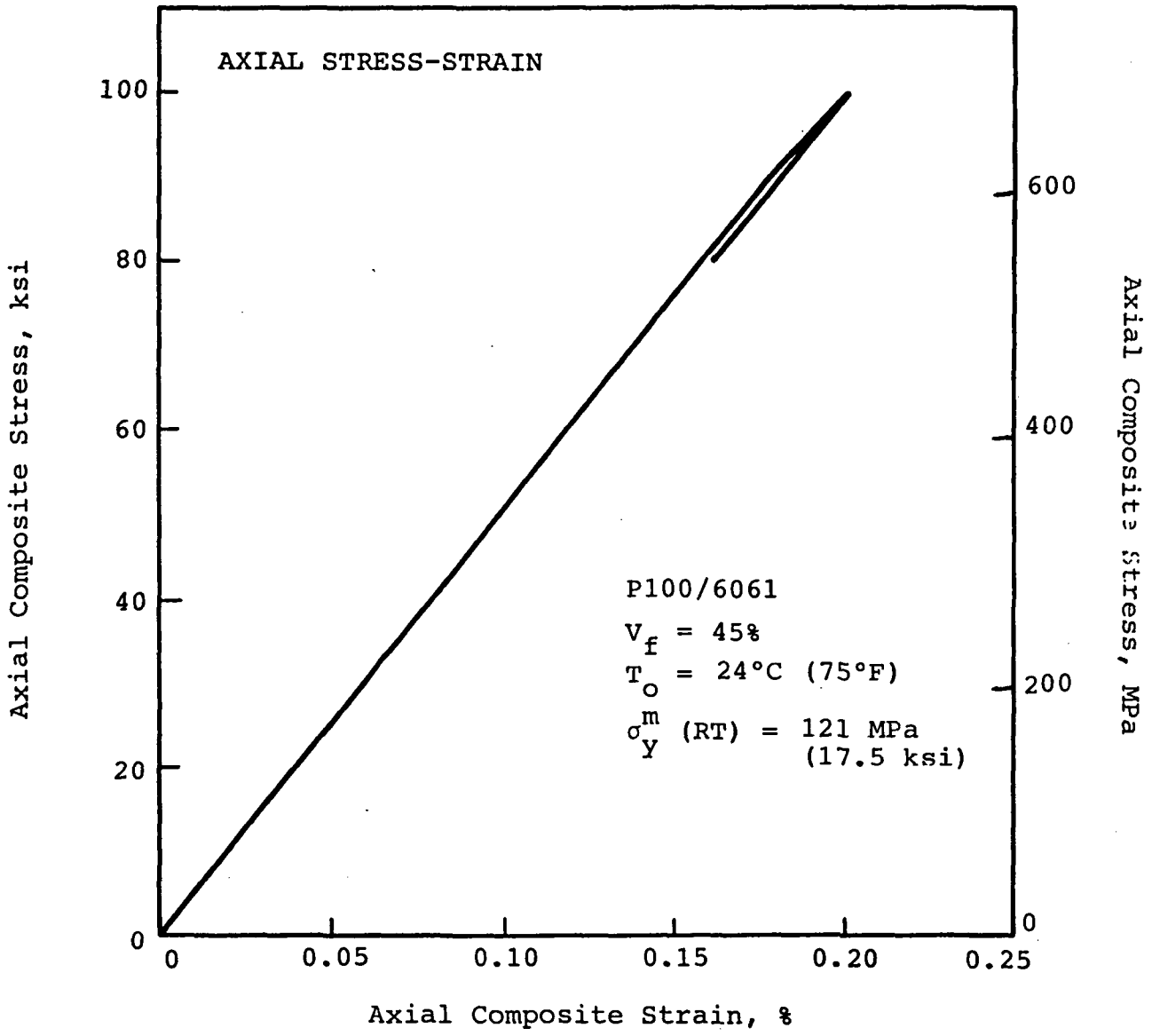

Figure A-10. Computed Room Temperature Axial Stress Strain Curve for a P100/6061 Unidirectional Plate. Analysis includes predictions of loading and unloading behavior

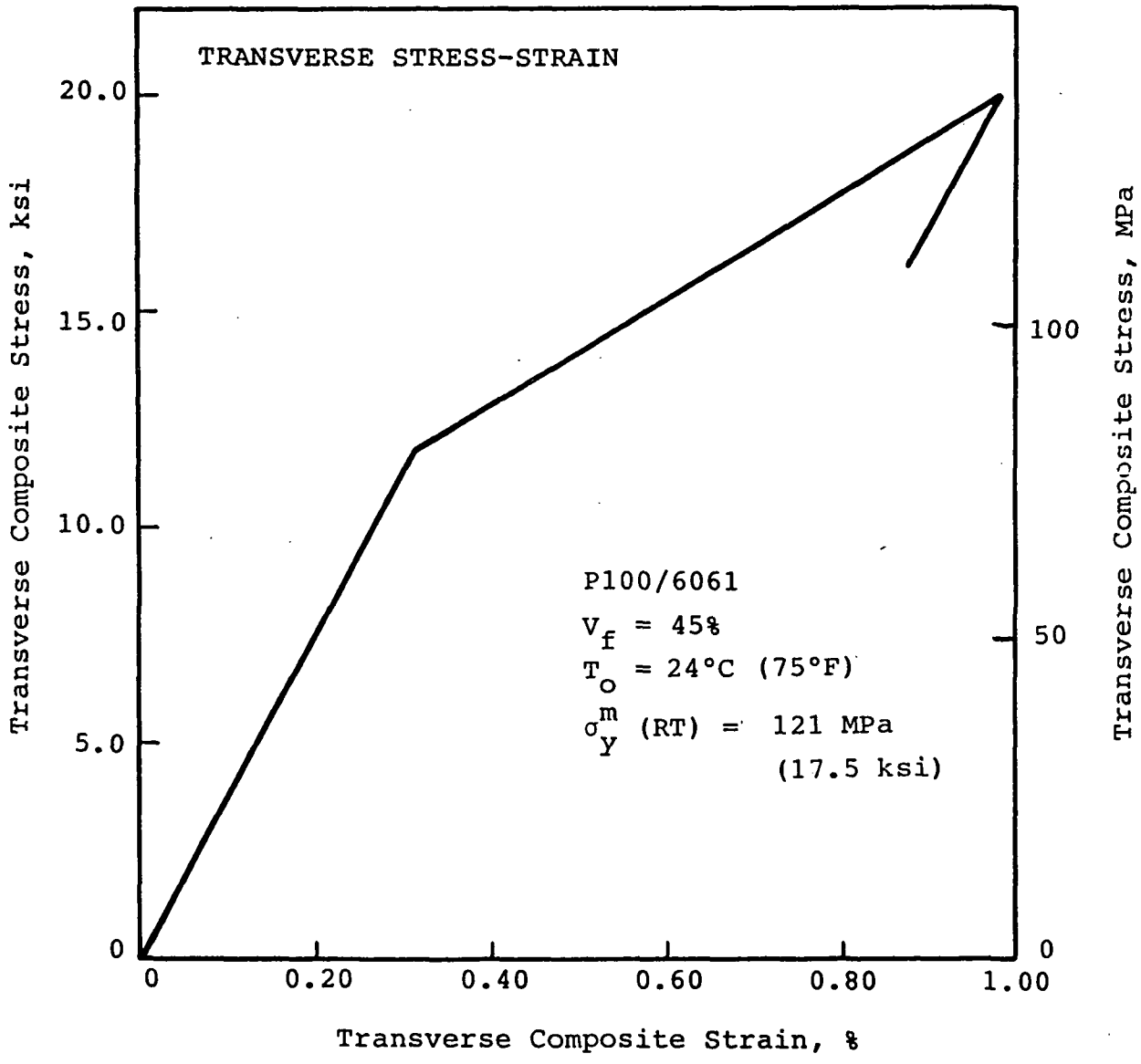

Figure A-11. Computed Room Temperature Transverse Stress Strain Curve for a P100/6061 Unidirectional Plate. Analysis includes predictions of loading and unloading behavior

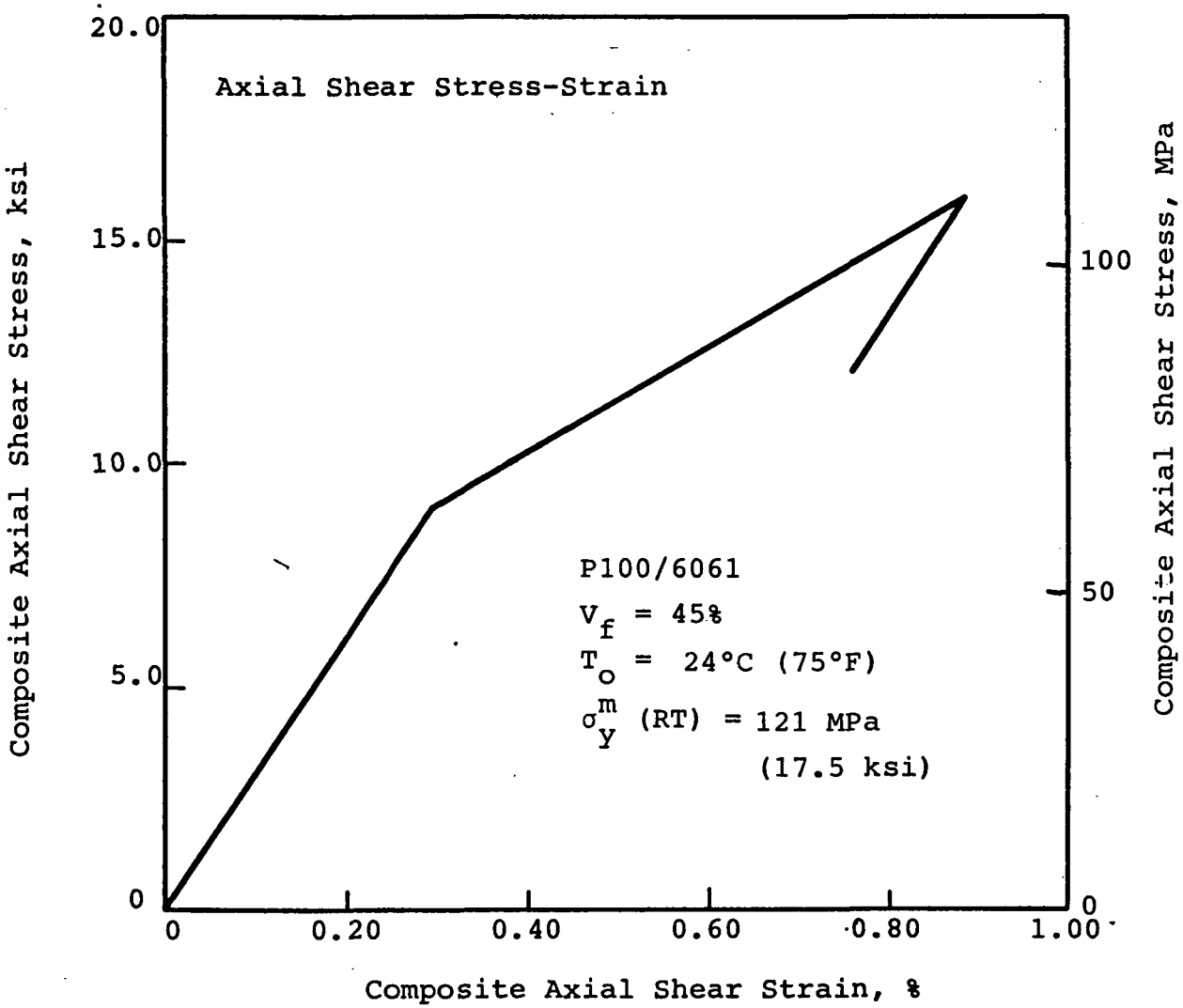

Figure A-12. Computed Room Temperature Axial Shear Stress Strain Curve for a P100/6061 Unidirectional Plate. Analysis includes predictions of loading and unloading behavior

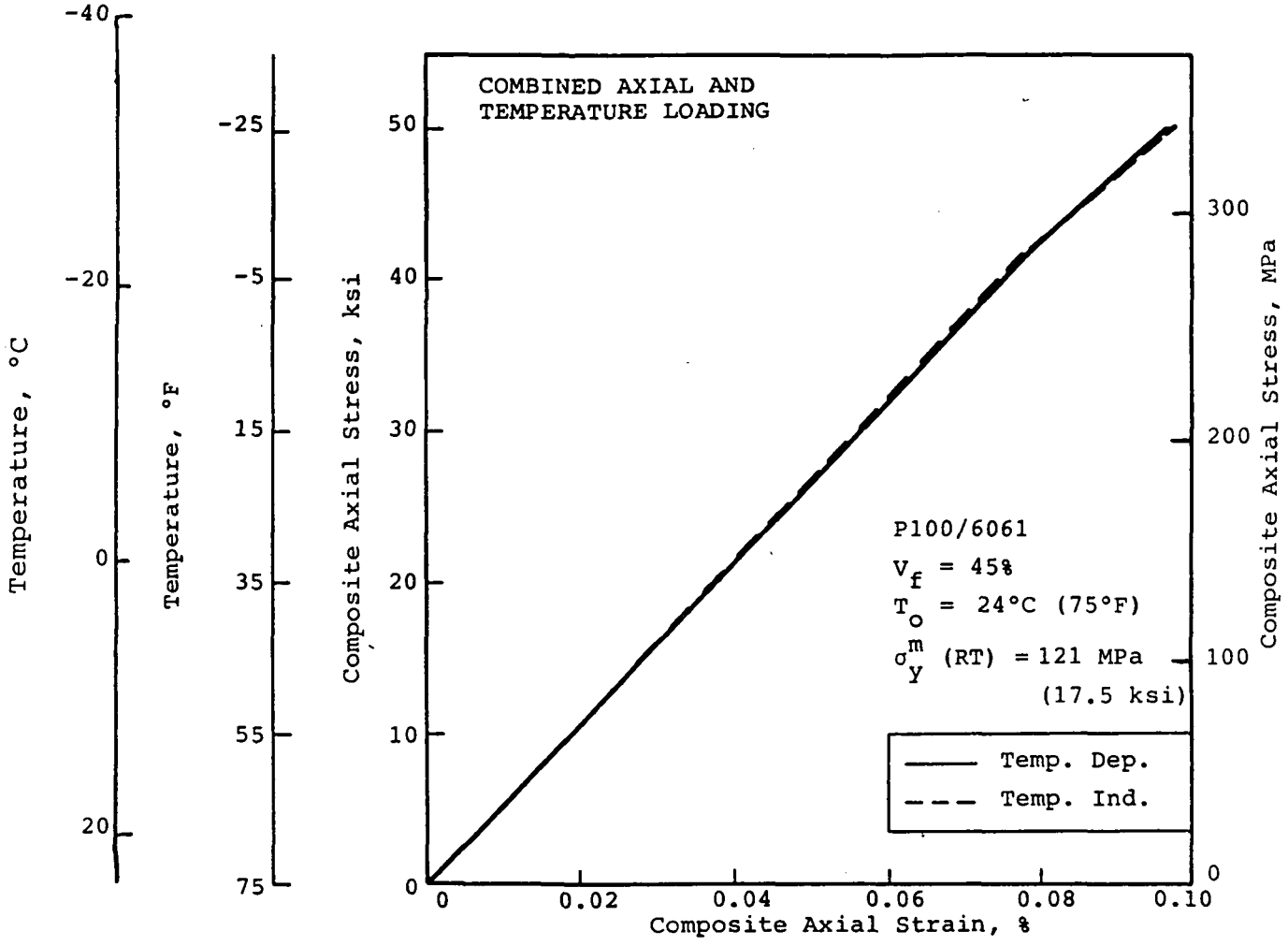

Figure A-13. Predicted Load-Strain Curve for P100/6061 Unidirectional Plate Under Combined Axial and Temperature Loads. Results shown for temperature dependent and independent solutions

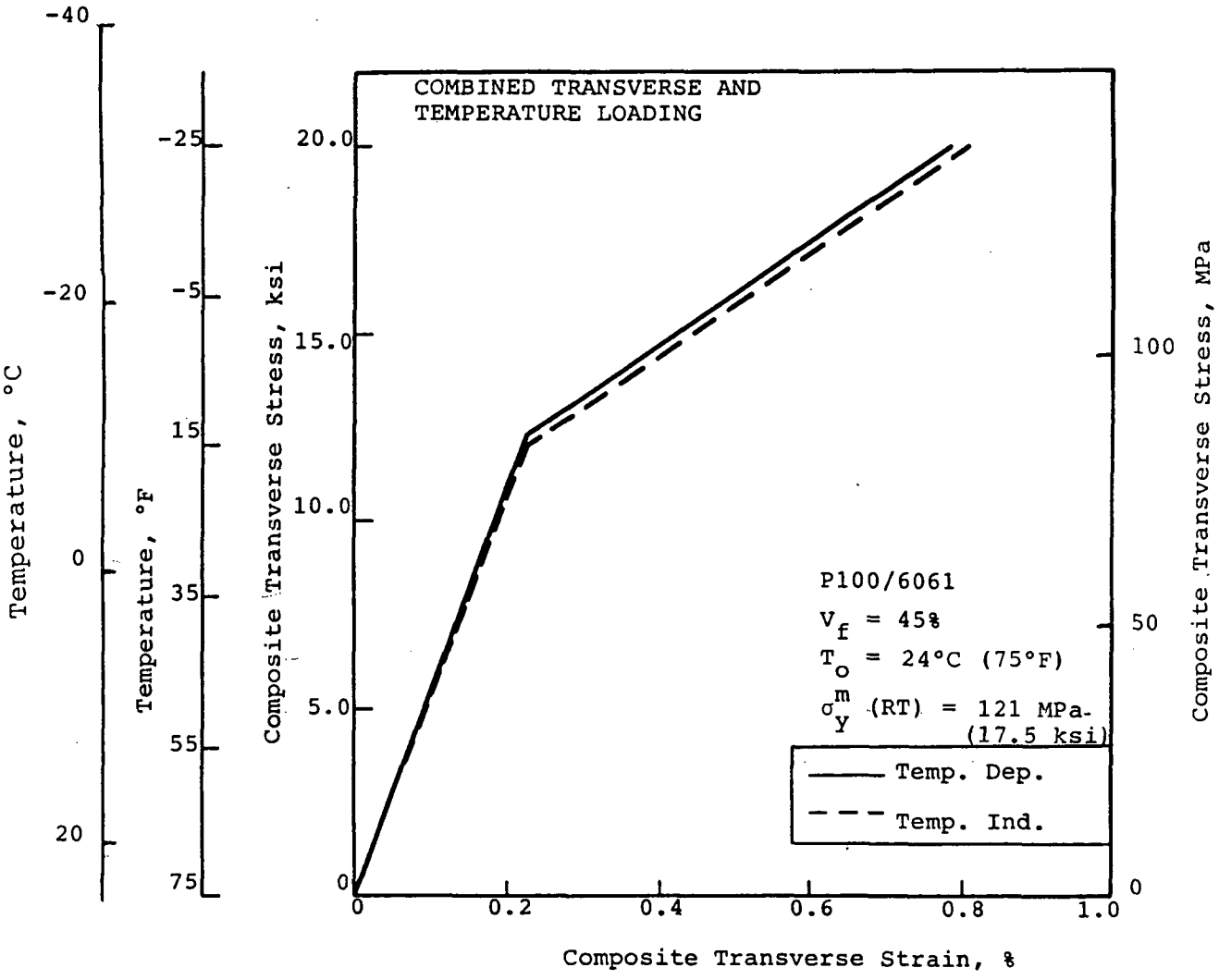

Figure A-14. Predicted Load Strain Curve for a P100/6061 Unidirectional Plate under Combined Transverse and Temperature Loading. Results shown for temperature dependent and independent solutions

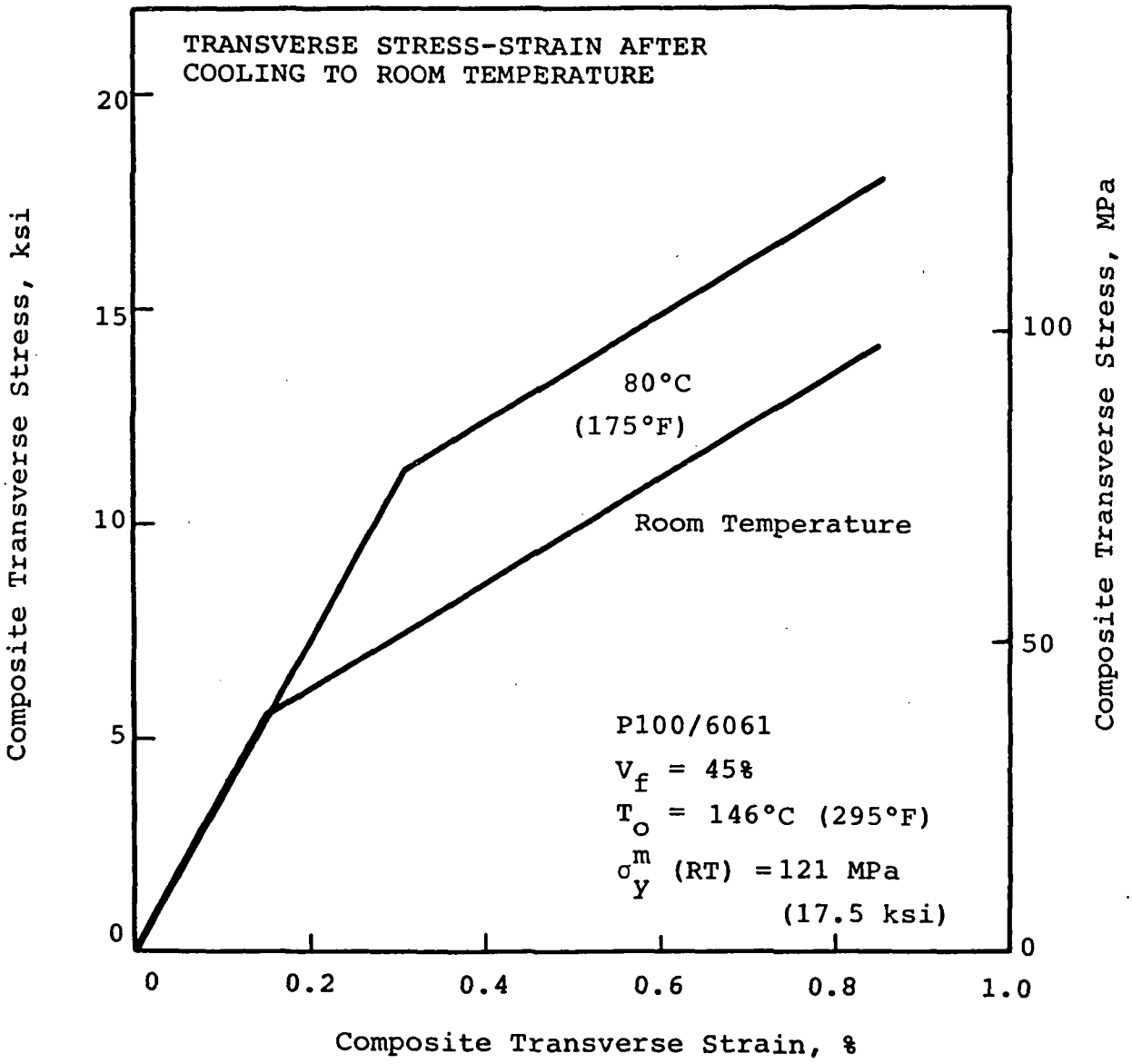

Figure A-15. Predicted Transverse Stress-Strain Curves for a P100/6061 Unidirectional Plate After Cooling to Room Temperature. Results show that elevated temperature material is stronger because the heating cycle has relieved residual matrix stresses.

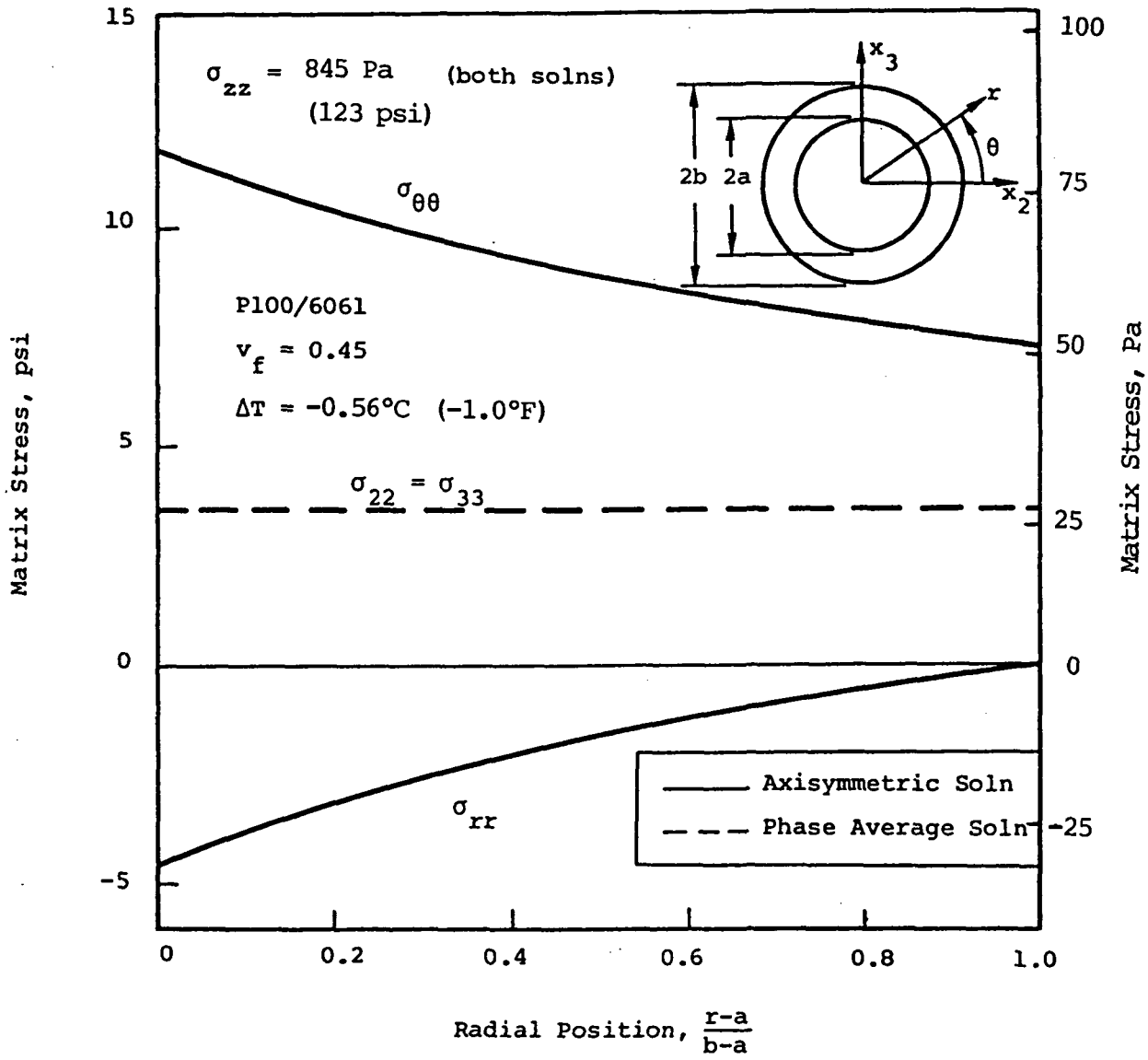

Figure A-16. Comparison of Elastic Matrix Stresses Computed for a P100/6061 Unidirectional Composite Due to a Change in Temperature.

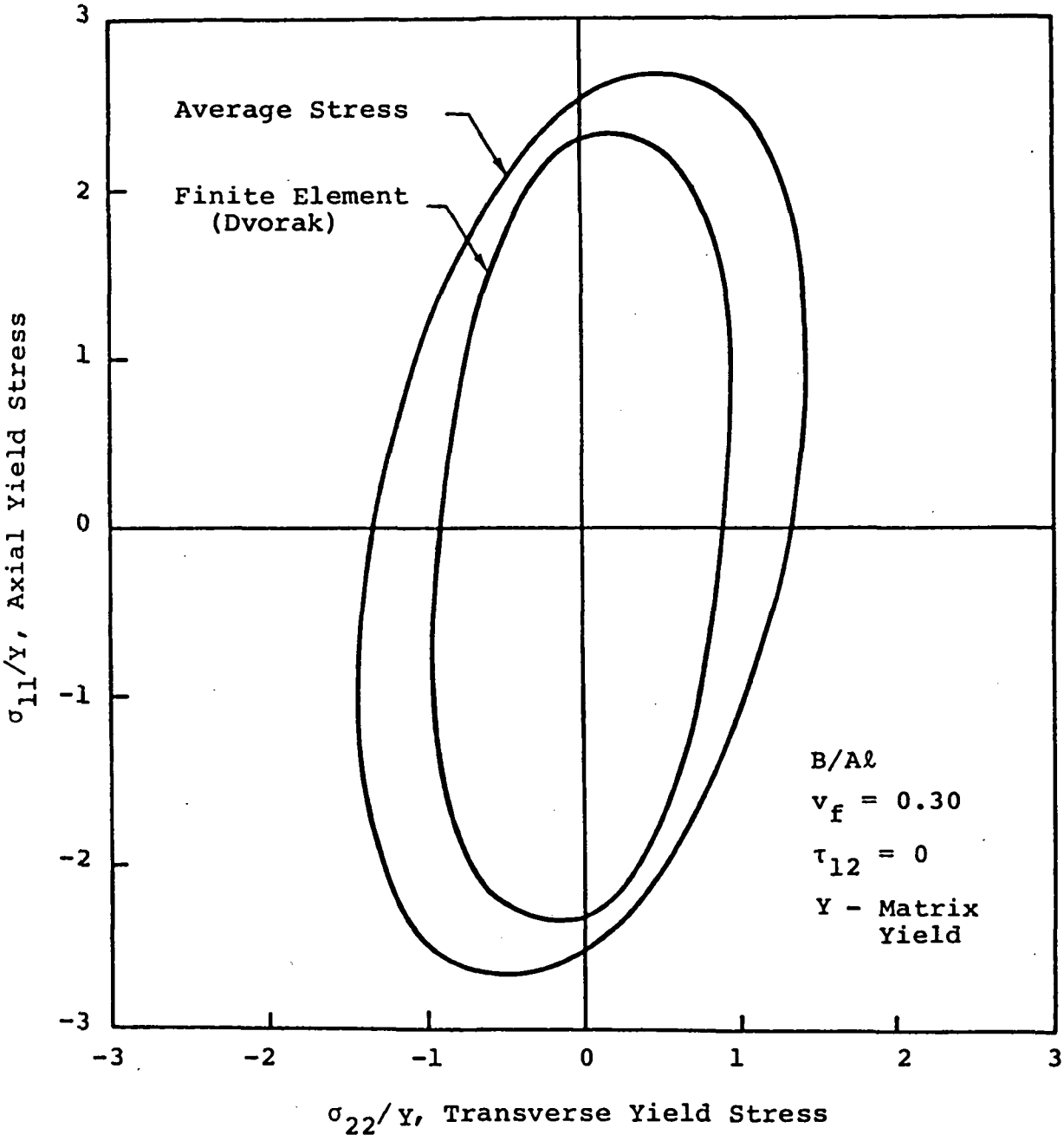

Figure A-17. Comparison of Composite Yield Surfaces Computed Using Average Stresses or Finite Element Solution

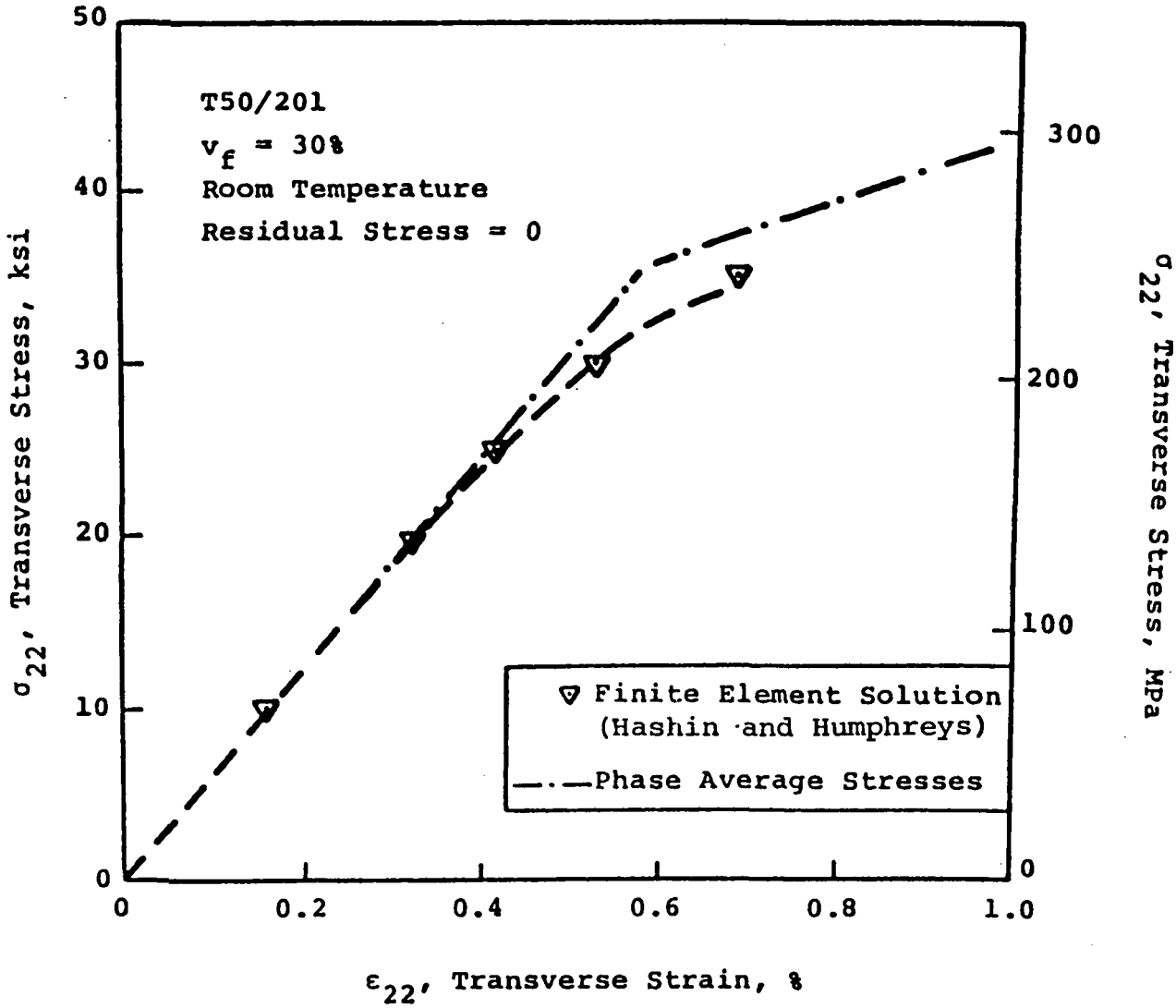

Figure A-18. Comparison of Composite Transverse Stress-Strain Curves Computed Using Average Stresses or Finite Elements

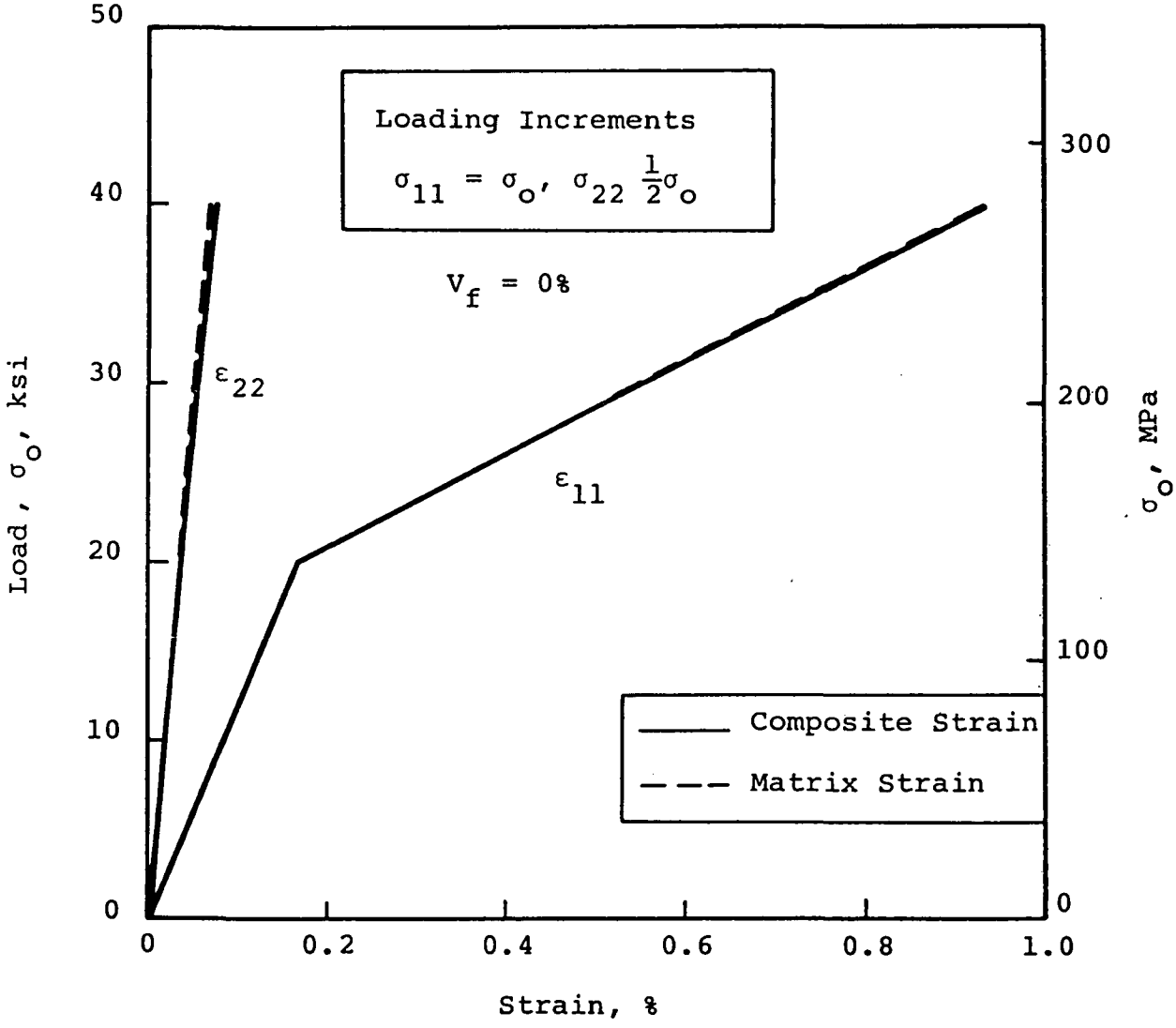

Figure A-19. Comparison of Strains Computed Using Phase Average Stress Model for Composite With No Fibers Under General Load Conditions. The comparison shows that since the composite must treat the matrix as transversely isotropic a small error may be induced in the plastic strain calculations.

Standard Bibliographic Page

1. Report No.	2. Government Accession No.	3. Recipient's Catalog No.
NASA CR-4016		

4. Title and Subtitle	5. Report Date
Temperature Dependent Nonlinear Metal Matrix Laminate Behavior	September 1986
	6. Performing Organization Code
7. Author(s)	8. Performing Organization Report No.
David J. Barrett and Kent W. Buesking	MSC TFR 1607/0211
9. Performing Organization Name and Address	10. Work Unit No.
Materials Sciences Corporation Gwynedd Plaza II, Bethlehem Pike Spring House, PA 19477	11. Contract or Grant No. NAS1-17822
12. Sponsoring Agency Name and Address	13. Type of Report and Period Covered
National Aeronautics and Space Administration Washington, DC 20546-0001	Technical Final Report Dec. 1984 - Nov. 1985
	14. Sponsoring Agency Code

15. Supplementary Notes

Langley Technical Monitor: Stephen S. Tompkins

16. Abstract

An analytical method is described for computing the nonlinear thermal and mechanical response of laminated plates. The material model focuses upon the behavior of metal matrix materials by relating the nonlinear composite response to plasticity effects in the matrix. The foundation of the analysis is the unidirectional material model which is used to compute the instantaneous properties of the lamina based upon the properties of the fibers and matrix. The unidirectional model assumes that the fibers properties are constant with temperature and assumes that the matrix can be modelled as a temperature dependent, bilinear, kinematically hardening material. An incremental approach is used to compute average stresses in the fibers and matrix caused by arbitrary mechanical and thermal loads. The layer model is incorporated in an incremental laminated plate theory to compute the nonlinear response of laminated metal matrix composites of general orientation and stacking sequence. The report includes comparisons of the method with other analytical approaches and compares theoretical calculations with measured experimental material behavior. A section is included which describes the limitations of the material model.

17. Key Words (Suggested by Authors(s))	18. Distribution Statement
Metal Matrix Composites Nonlinear Behavior Laminate Analysis Thermal Hysteresis Temperature Dependent Plasticity Phase Average Stresses	Unclassified - Unlimited Subject Category 24

19. Security Classif.(of this report)	20. Security Classif.(of this page)	21. No. of Pages	22. Price
Unclassified	Unclassified	124	A06

For sale by the National Technical Information Service, Springfield, Virginia 22161

NASA-Langley, 1986

National Aeronautics and
Space Administration
Code NIT-4

Washington, D.C.
20546-0001